PhD degree in Molecular Medicine (curriculum in Molecular Oncology)

European School of Molecular Medicine (SEMM),

University of Milan and University of Naples "Federico II"

Settore disciplinare: BIO/11

Spatial regulation of signalling by the endocytic protein NUMB

Martina Mariarosaria Zobel

IFOM, Milan

Matricola n. R10326

Supervisor: Prof. Pier Paolo Di Fiore

IFOM, Milan

Added Supervisor: Dr. Andrea Disanza

IFOM, Milan

Anno accademico 2015-2016

TABLE OF CONTENTS

ABBREVIATION LIST

3D: three-dimensional

aa: amino acid

AAK1: adaptor-associate kinase 1

ACD: asymmetric cell division

aPKC: atypical protein kinase C

ARF: ADP-rybosilation factor

ARF6: ADP ribosylation factor-6

ARH: autosomal recessive hypercholesterolemia protein

BFA brefeldin A

ccRCC: clear cell Renal Cell Carcinoma

CDR: Circular dorsal ruffles

CHO: Chinese Hamster Ovary

CME: Clathrin Mediated Endocytosis

CNS: central nervous system

Co-A: co-activators

Co-R: co-repressors

CSC: cancer stem cell

CSL: CBF1/Suppressor of Hairless/LAG-1

d-NUMB: *Drosophila* NUMB

DAB-2: Disabled-2

Dhh: Desert hedgehog

ECM: extracellular matrix

EE: early sorting endosome

EEA1: early endosome antigen-1

EEC: endo-/exocytic cycles

EGFR: Epidermal growth factor receptor

EH: Eps15 homology

EHD: EH-domain

EMT: epithelial to mesenchymal transition

Eps15: epidermal growth factor substrate 15

Eps15L1: epidermal growth factor substrate 15-like 1

ERC: endocytic recycling compartment

GAP: GTPase-activating protein

GCPs: cerebellar granule cell progenitors

GEF: guanine nucleotide exchange factor

GPCR: G protein-coupled receptors

GPI: glycosylphosphatidylinositol

HDM2: Human double minute 2

HGF: hepatocyte growth factor

Hh: Hedgehog

Hs: Homo sapiens

IB: immunoblotting

Ihh: Indian hedgehog

JIP4: JNK-interacting protein 4

LAMP-1: lysosomal-associated membrane proteins-1

LDL6: low-density receptor-related protein 6

LDLR: low-density lipoprotein receptor

LE: late endosome

m-NUMB-L: mouse NUMB-Like

m-NUMB: mouse NUMB

MAML: Mastermind/Lag-3

MDCK: Mandin Darby Canine cells

MDM2: Mouse double minute 2

MEF: Mouse Embryonic Fibroblast

MHC class I: major histocompatibility complex class I protein

Mm: Mus musculus

MMP: Matrix Metallo Protease

MMP2: Matrix Metallo Protease 2

MVBs: multi vesicular bodies

MW: molecular weight

NCME: Non Clathrin Mediated Endocytosis

NECD: NOTCH extracellular domain

NEXT: NOTCH extracellular truncated domain

NICD: NOTCH intracellular domain

gNSCLC: non-small cell lung carcinomas

NUM-1A: the nematode NUMB homolog

Nβ: short peptide released after cleavage at site 4

PD: phosphatidic acid

PDGFR: Platelet-derived growth factor receptor Epidermal growth factor receptor

$PI(4,5)P_2$: phosphatidylinositol 4,5-bisphosphate

PI3K: Phosphatidylinositol-4,5-bisphosphate 3-kinase

PIP5K: phosphatidylinositol-4-phosphate-5-kinase

PKC: protein kinase C

PL: Peripheral lamellipodia

PLD: phospholipase D

PM: Plasma Membrane

PMP22: the peripheral myelin-membrane protein

PR: peripheral ruffle

PRR: proline reach region

PRR1: proline reach region 1

PRR2: proline reach region 2

PTB: phosphotyrosine binding domain

RT: room temperature

RTK: Receptor Tyrosine Kinase

SC: stem cell

SH3: src homology domain binding site

Shh: Sonic hedgehog

SOP: sensor organ precursor

TCTP: Translationally Controlled Tumor Protein

TfR: TfR Receptor

TJ: tight junction

TNBC: Triple Negative Breast Cancer

FIGURES AND TABLES INDEX

1 ABSTRACT

NUMB was originally identified as a cell fate determinant that controls signaling outputs during asymmetric cell division. NUMB is a tumor suppressor protein that regulates NOTCH and p53 signaling pathways. Loss of NUMB occurs in 50% of all breast tumors and in 30% of lung cancers, and correlates with an increased aggressiveness and poor prognosis.

NUMB has been also characterized for its role in trafficking, acting as an adaptor protein and regulating signaling emanating from various plasma membrane receptors, including NOTCH, Receptor Tyrosine Kinases (RTKs), such as EGFR and c-MET, and integrins. Consistent with this latter notion, NUMB interacts with key players of the Clathrin-mediated endocytosis, regulating the internalization of various receptors. However, its action cannot be restricted to the initial steps of internalization at the level of the cell surface, as it also localizes, in *C. Elegans* and *D. Melanogaster*, in recycling endosomes and regulates the delivery of cargos back to the plasma membrane. Similarly, in mammalian cells, NUMB and EH (Eps15- Homology)-domain containing proteins co-localize in ARF6-associated recycling vesicles, and NUMB regulates post-endocytic sorting of NOTCH1.

The combination of endocytic/recycling trafficking and actin related dynamics is one of the major mechanisms through which spatial restriction of signaling is achieved. Indeed, the correct recycling of active RAC via ARF6 to the plasma membrane is required for the formation of migratory protrusions induced upon RTK stimulation, such as Circular Dorsal Ruffles (CDRs).

To identify novel endocytic/trafficking proteins involved in actin dynamics and directional cell migration, we performed an RNAi screening using Peripheral Ruffles (PRs) and CDRs as readout markers. We found that the endocytic adaptor NUMB is as a negative regulator of CDR formation without affecting PR formation.

In this thesis, we have characterized NUMB as a negative regulator of CDR formation downstream of c-MET and PDGFR. This function of NUMB is accompanied by an increased mesenchymal mode of motility and cell invasion. In agreement with the notion that spatial recycling of active RAC to the plasma membrane mediated by ARF6 is required for the formation of CDRs, we found that NUMB is enriched in ARF6 recycling compartments and inhibits MHC I and RAC recycling. These evidences suggest that NUMB might act as a negative regulator of ARF6-dependent recycling. Since GEFs are the primary regulatory targets of small GTP-ase, we focused our attention on ARF6 GEFs, which are reported to control actin remodeling, in particular on the EFA6A-D and Cytohesin family members. Among these GEFs, only EFA6B contains an NPxF motif in its N-terminal domain and directly binds the NUMB PTB domain. Functionally, the removal of EFA6B by itself does not alter CDR formation, but it inhibits the increase of CDR formation that is brought about by NUMB down-regulation. Whether NUMB affects EFA6B GEF activity and, as a consequence, ARF6 activation, is currently under investigation.

Our data suggest that NUMB may regulate the ARF6-dependent recycling pathway, which is required for migration and invasion of tumor cells, by interacting with and possibly modulating its GEF EFA6B. Of note, up-regulation of this pathway in the absence of NUMB may even account for the aggressiveness of NUMB-negative tumors.

2 INTRODUCTION

This thesis describes the molecular mechanism through which the endocytic protein NUMB regulates spatially and temporally defined signaling. The introduction is divided into three main topics that cover my work: endocytosis and spatial restriction of signaling, the endocytic adaptor NUMB, and the small GTP-ase ADP-ribysilation factor (ARF) protein family. First, I will provide an overview of how endocytosis and spatial restriction of cell signaling are connected. In section 2.1, I will briefly describe endocytic mechanisms and how the mode of internalization affects signaling output and endosome-mediate signaling (section 2.1.1 and 2.1.2). Then, I will describe the crosstalk between endocytosis and recycling in the light of regulated signaling in space and time (section 2.1.3). In the second part of the introduction, instead, I will describe the NUMB protein family (section 2.2.1): NUMB biological function (section 2.2.2), NUMB regulated pathways (section 2.2.3), and NUMB alterations and their implication in cancer. Finally, in the last part of the introduction, I will describe the ARF protein, focusing on ARF6, its family of guanine nucleotide exchange factors (GEFs), and on the PSD (EFA6) family (section 2.3).

2.1 Endocytosis and spatial restriction of cell signaling

By definition, endocytosis is the process by which eukaryotic cells actively transport molecules from the extracellular environment across the cell membrane. In this way cells can intake not only fluids and soluble molecules (like nutrients, ligands, lipids), but also internalize portions of plasma membrane (PM) and surface receptors(Doherty and McMahon 2009; Scita G 2010).

Cell surface receptors can internalize via two main pathways of endocytosis: Clathrin-mediated endocytosis (CME) and Non-clathrin-mediated endocytosis (NCME)(Doherty and McMahon 2009; Conner SD 2003) (Fig. 1).

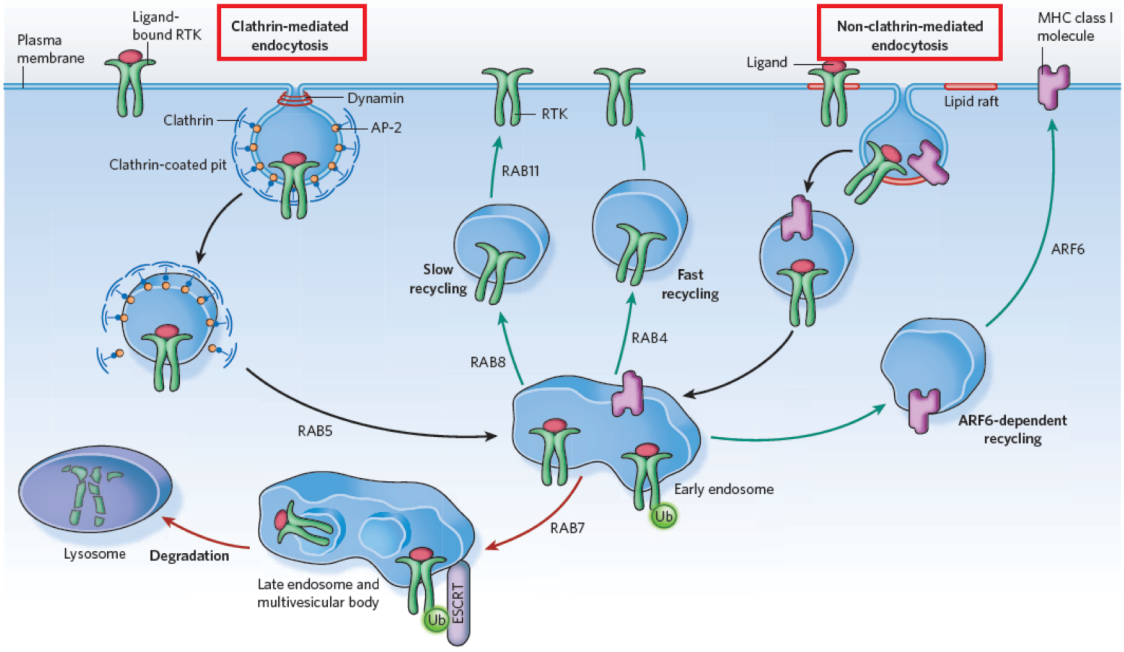

Figure 1. Endocytic pathways of signaling receptors.
The figure describes CME and NCME trafficking routes. During CME (left), upon binding of a soluble ligand, RTK receptors are internalized into clathrin-coated vesicles by adapting proteins, like AP-2 and dynamin. Many forms of NCME (right) exist and one of this occurs in the area of the PM that is enriched in particular lipids (lipids raft). After internalization, either through CME or NCME, cargos are delivered to early endosomes. From the early endosomes, receptors can be recycled back to the PM either through a fast or a slow recycling route, or through the ARF6-dependent pathway. From the early endosomes, ubiquitilated proteins are transported to late endosomes and multivesicular bodies, and finally to the lysosome to be degraded.
Modified from(Scita G 2010).

In CME, ligand binding to the receptor is followed by the recognition of cytoplasmic domains of PM proteins by specific adaptor proteins (such as AP-2 and the GTPase

dynamin), which pack them into clathrin-coated vesicles that are then delivered into the cells. The iron-bound transferrin receptors (TfRs) and low-density lipoprotein receptors (LDLRs) are two examples of receptors that are internalized into the cytosol via the CME(Conner SD 2003; Doherty and McMahon 2009). NCME exists in many forms; for example, macropinocytosis and phagocytosis are actin driven(Mayor and Pagano 2007; Sandvig K 2008), and lipid rafts are lipid microdomains enriched in sphingomyelin and cholesterol(Simons and Ikonen 1997). Lipid rafts contain caveolin-1, a protein that associates with cholesterol and sphingomyelin, and form particular structures called caveolae.

Despite the route used to enter the cells, all cargos are delivered to early endosomes (EE). Trafficking to the endosomal compartment is regulated by small GTP–binding proteins of the RAB and ARF families(H 2009). From EE, cargos can be recycled back to the PM by a fast RAB4-dependent recycling pathway or by a slow RAB8- and RAB11-dependent recycling pathway(H 2009). Moreover, proteins internalized through the NCME, like MHC class I, can be recycled to the PM via ARF6(JG 2005). From EE, ubiquitilated proteins are transported via RAB7 to late endosomes (LE) and multivesicular bodies (MVBs), and then to the lysosome(H 2009) (Fig. 1).

Endocytosis is recognized as a way to regulate signal transduction from Receptor Tyrosine Kinases (RTKs) and G protein-coupled receptors (GPCRs)(Conner SD 2003). In fact, by controlling the number of receptors on the cell surface, either by using a trafficking route that leads to degradation or by regulating the activation of downstream effectors, cells are able to generate different and specific responses to extracellular cues. Eukaryotic cells have the ability to sense spatial information by modifying their cytoskeleton and their membrane composition. More importantly, cells organize their signaling machinery in a way in which molecules are asymmetrically distributed and the output signal is spatially restricted(Disanza et al. 2009).

Cells not only arrange the signal into endosomal platforms, but also use different way to reach different compartments(Sorkin A 2009). Upon internalization, proteins are often recycled back to the PM to replace unbound receptors for a new round of signaling and transport. Moreover, the recycling can also be seen as a mean to direct signaling molecules to specific areas of the PM, like the apical and basal membrane of polarized epithelial monolayer(Lecuit T 2003), or as a mean to maintain polarized molecules, like the small GTPase CDC42 during the generation of buds in yeast(Marco E 2007).

Endocytosis of molecules is also followed by internalization and recycling of the PM, generating constant membrane flow. This flow of membrane is required to generate forces that sustain the formation of migratory protrusions(Bretscher MS 1998) or to promote the backward movement of molecules during the formation of protrusions in cell migration(Bretscher MS 1998).

CME has been shown to control cell shape in different migratory cells(Palamidessi et al. 2008), supporting the existence of a link between membrane dynamics, cell shape changing and polarized signaling. All these evidences support a role for endocytosis in spatial restriction of signaling outputs.

2.1.1 Signaling outputs are affected by the internalization route

Generally, receptors are kept off from the cell surface upon ligand binding. This event is critical to allow receptor activation and the assembly of macromolecular complexes required to transmit and amplify the signaling. Once activated, the receptors are immediately internalized and either delivered to degradative compartments to decrease the continuous signaling or recycled back to the PM(Disanza et al. 2009). However, signal transduction is not limited to the surface but can also occur while the receptor is internalized. Downregulation of cell surface receptors occurs mainly though the CME but different receptors are also internalized by NCME(Disanza et al. 2009). For example, platelet-derived growth factor receptors (PDGFRs) and epidermal growth factor receptors

(EGFRs) are sequestered by caveolae that immobilize the receptors and prevent their over-activation(Matveev and Smart 2002). Sequestration of molecules into lipid microdomains is also true for non-receptor tyrosine kinases, for example c-src, which is confined and inactivated into microdomains that are unable to give rise to signal transduction and transformation(Oneyama et al. 2008; Veracini et al. 2008). Biological outcome, extent, duration and localization of the signaling are strictly dependent on the mode of internalization(Sadowski, Pilecka, and Miaczynska 2009) (Fig. 2). For example, the TGFB and EGF receptors can be internalized either via CME or NCME. When these receptors are internalized via CME, they are efficiently recycled back to the PM to amplify and spatially restrict the signal, especially in the case of directional migration and chemotaxis(Le Roy and Wrana 2005) (Fig. 2A). On the other end, NCME mainly directs the receptors to degradation by targeting them with ubiquitin(Di Guglielmo et al. 2003; Sorkin A 2009), suggesting that this posttranslational modification maybe fundamental to receptor fate (Fig. 2A). Recently, it has been shown that other cargos, like the WNT3A and the low-density receptor-related protein 6 (LDL6) receptors, use the endocytic pathway in an opposite manner(Kikuchi, Yamamoto, and Kishida 2007; Yamamoto et al. 2008) (Fig. 2B).

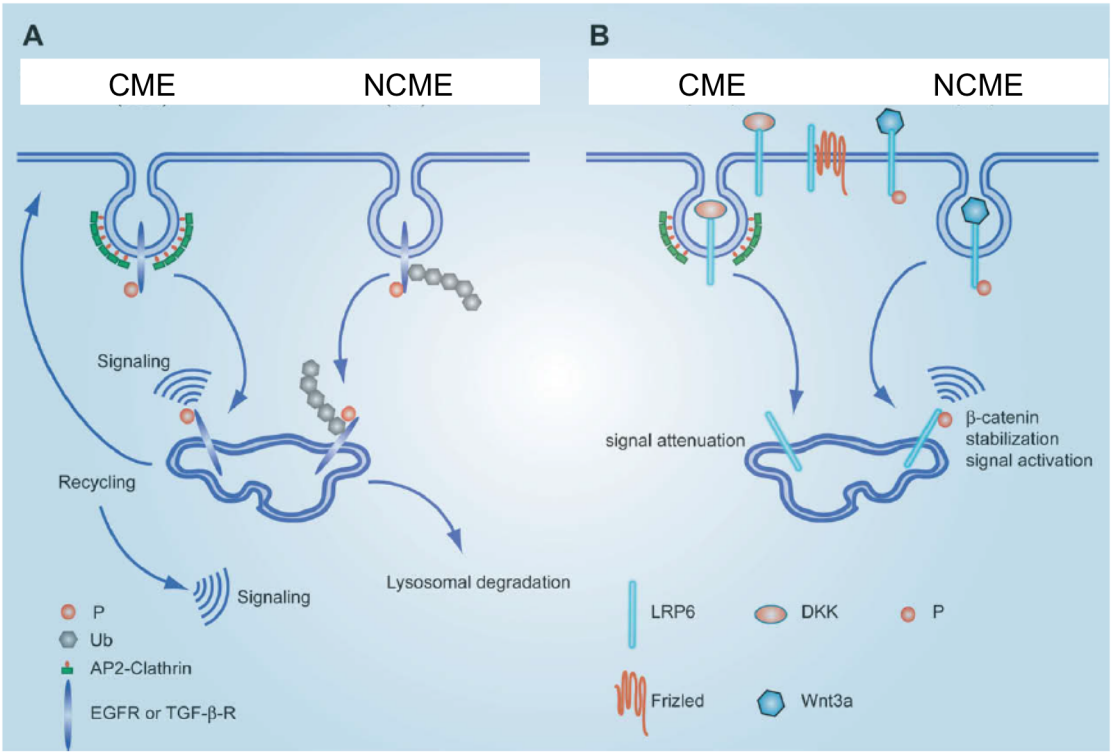

Figure 2. Signaling outputs are affected by the way in which receptors are internalized.
A. EGFR and TGF-ß-R, when internalized via CME, are efficiently recycled back to the PM to sustain cell signaling. When internalized via NCME, instead, receptors are delivered to degradation compartments to attenuate signaling.
B. Wnt3a binds to the LPR6 receptor and is internalized via NCME to promote signal transduction. DKK-LPR6 complex enters the cell via CME to decrease the signaling.
Modified from(Disanza et al. 2009)**.**

A peculiarity of the EGFR internalization is that the choice between CME and NCME depends on the ligand concentration and on the number of receptors on the cell surface(Sigismund et al. 2005; Sorkin A 2009). In fact, low doses of EGF promote internalization exclusively via CME(Sigismund et al. 2005), while high doses of EGF promote a mixture of CME and NCME. Under this condition the receptors are ubiquitinated and routed to multi-vesicular bodies for degradation(Sigismund et al. 2005; Sigismund et al. 2008). Ligand concentration not only modulates the duration and the intensity of the response but also the specificity. For example, low doses of PDGF induce changes in the actin cytoskeleton and the formation of migratory protrusions, which are CME dependent. On the contrary, high doses of PDGF induce mitogenesis and cell proliferation, which rely on the presence of NCME pathways(De Donatis et al. 2008). Ligand concentration is also important in a physiological contest. During morphogenesis,

some RTKs and GPCRs acts as motogenic sensors, which respond to chemotactic gradients that guide the migratory cells to their destination. This phenomenon occurs for example during the migration of primordial germ cells in the zebrafish gonad development(Raz 2004). Thus, CME and NCME are differentially linked to signal activation or downregulation, depending on the types of cargo, different ligands and the concentration of the ligands.

2.1.2 Endosomes function as a signaling compartment

Upon internalized, either through CME or NCME, sorted cargos are direct to EEs, which are the first sorting station in the internalization process. This compartment is marked by the presence of the small GTPase RAB5 and the early endosome antigen-1 (EEA1), and is characterized by precise protein and lipid composition(Zerial and McBride 2001). The pH in the EEs is about 6. From this compartment, cargos can either be routed to MBVs or recycled back to the PM. In the last years, the concept that EEs are specialized compartments where signals are originated and maintained in order to generate spatially and temporally restricted outputs has emerged.

The “signaling endosome hypothesis” was initially formulated in neurons to sustain long-range transmission of signaling(Howe and Mobley 2005). During the years, the “signaling endosome hypothesis” has also been extended to others cell types, thanks to the big increase in the development of signaling biosensors and new cell imaging live techniques. In fact, activated RTKs, like EGFR, and their targets, such as H-Ras, have been found to signal from EEs by imaging specific biosensors in the cell(Jiang and Sorkin 2002; Baass et al. 1995). The same tool allowed the visualization of EGF associated with its receptors in EEs, from which the RAS/ERK signaling takes place(Baass et al. 1995).

Spatial regulation of signaling relies also on the variety of endocytic compartments. For instance, endosomes marked by the presence of the RAB5 effectors APPL1 and APPL2

are different from those marked by EEA1 and are linked to mitogenic signaling(Miaczynska et al. 2004).

An example is provided by the endosomes that mediate signal transmission between the PM and the nucleus, like in the case of c-MET receptor and STAT3(Kermorgant and Parker 2008). Upon hepatocyte growth factor (HGF) binding, c-MET receptor may activate either ERK1/2 or STAT3. Activation of the former occurs when the receptor localizes in EEs but not in the perinuclear area; activation of the latter requires translocation of the active receptor to the perinuclear area via microtubules and protein kinase C (PKC)-α(Kermorgant and Parker 2008).

Passing through the LE compartment or MVBs, cargos finally reach the lysosomal degradative compartment. MVBs are characterized by the presence of the lysosome-associated membrane protein-1 (LAMP-1) and RAB7(Hurley 2008). Generally, this compartment is considered a place where signals are weekend(Hurley 2008), however, there are few exceptions. For example, as a consequence of the presence of specific adaptors, MVBs contain activated receptors and promote ERK activation. This is the case of the late endosomal adaptors p14 and MP1, which form a complex and recruit MEK1 to the PM and activate ERK(Teis, Wunderlich, and Huber 2002).

All these examples support the concept that endosomes are intracellular, spatially confined platforms, and an additional step in the control of biological response to extracellular cues.

2.1.3 Endocytosis/recycling cross-talk spatially restricts the signals controlling proliferation and cell fate determination, actin-based cell migration and cell adhesion

Upon being internalized, receptors that are not routed to degradative compartments are recycled back to their sites of origin. The endosomal recycling pathway is composed of different types of endosomes: the early sorting endosome (EE), the endocytic recycling

compartment (ERC), and the ADP ribosylation factor-6 (ARF6) dependent recycling compartment, which include integral membrane proteins that are internalized via NCME(Donaldson and Honda 2005). The ERC is also characterized by many regulatory components, including RABs, which control several steps in the intracellular membrane trafficking(Zerial and McBride 2001).

A growing number of evidences suggests that the endocytosis/recycling of membrane bound proteins is strictly connected to signaling, controlling its intensity and specificity. Of course, spatial restriction of signaling is required to carry out a number of fundamental cellular functions that are defined by an "asymmetric and polarized" distribution of molecules and functional activities.

In the following section I will describe examples of how endocytosis/recycling controls localized intracellular responses to different stimuli, resulting in spatial restriction of polarized signals.

2.1.3.1 Recycling re-sensitize desensitized receptors by endocytosis

The endocytic recycling pathway controls the levels and the activity of GPCRs(Hanyaloglu and von Zastrow 2008). Several studies demonstrate that the rapid desensitization is mediated by the coupling of receptor phosphorylation and internalization. In agreement with this notion, agonist-bound receptors initiate signaling by the activation of G proteins at the PM, and quickly undergo phosphorylation by GPCR kinases that phosphorylate agonist-activated receptors(Hanyaloglu and von Zastrow 2008). Once phosphorylated, the receptors bind the adaptor proteins ß-arrestin-1 and ß-arrestin-2 to prevent the interaction of the receptor with G-protein, and terminate, thus, G-protein mediated signaling(Hanyaloglu and von Zastrow 2008). Arrestins can also bind to clathrin, thereby promoting CME of arrestin-bound receptors, contributing to their desensitization. Delivery of internalized receptors into a recycling pathway promotes the return of intact receptors to the PM and effectively re-sensitize cells to respond again to extracellular ligands. This

cycle of desensitization/re-sensitization(Disanza et al. 2009) has important implication also in the specification of the nature of the resulting signaling(Disanza et al. 2009).

2.1.3.2 Endocytosis/recycling in asymmetric cell division

The endocytic recycling is also fundamental in the determination of cell fate and control of asymmetric division. Studies in the developing sensory organ of *Drosophila*(Coumailleau and Gonzalez-Gaitan 2008), as well as in other model organism(Gonczy 2008) and in mammalian cells(Furthauer and Gonzalez-Gaitan 2009), show that a general mechanism for creating asymmetric signals, in order to specify fate determination, is the polarization of endocytic recycling pathways(Coumailleau and Gonzalez-Gaitan 2008). Several players of asymmetric cell division (ACD) have been characterized(Furthauer and Gonzalez-Gaitan 2009). In *Drosophila*, the endocytic protein NUMB is asymmetrically partitioned at the division of sensor organ precursor cells (SOP), conferring different destinies to the two daughter cells(Furthauer and Gonzalez-Gaitan 2009). This function of NUMB will be further discussed in section 2.2.2.1.

2.1.3.3 Endocytosis and recycling in directed cell motility

Cell motility depends on localization of signaling molecules and their signaling. During locomotion, cells polarize PM proteins according to their migratory direction, which allows cells to orchestrate membrane trafficking, adhesion to the substrate, actin remodeling, and to generate propulsive forces that are required for active motility at the leading edge(Disanza et al. 2009).

One mechanism that has been proposed to coordinate protrusion in directional migration of cells is the polarization of motogenic factors and their effectors by a flow of endocytic internalization of membranes, followed by re-translocation of vesicles and cargos to the cell front(Bretscher and Aguado-Velasco 1998b). This concept originates from the observation that vesicles containing recycling cargos, like LDLR and TfR, are concentrated towards the periphery of the cells(Bretscher 1983).

The endocytic/recycling pathways are critical for directional cell migration in response to chemotactic gradient. Studies in *Drosophila* demonstrated that the migration of border cells is controlled by the gradient of motogenic factors like EGF and PV (PDGF/VEGF), towards which cells move directionally(McDonald et al. 2006). In *Drosophila*, the migration of border cells depends on CBL, an E3 ubiquitin ligase, and on Spirt, an homologue of RAB5 GEF Rin1, indicating that endocytic pathways are required to guarantee spatial resolution of chemotactic signaling emanating from different RTKs, thus regulating actin-based polarized protrusion activity and motility(Jekely et al. 2005). Numerous studies support the role of endosomal recycling also in mammalian cells during migration. Indeed, in human KB cells (derivatives of HeLa cells)(Bretscher and Aguado-Velasco 1998a), surface ruffles have been shown to depend on exocytosis of recycled membrane derived from endosomes(Bretscher and Aguado-Velasco 1998a). Other evidence in mammalian epithelial cells suggests that interference with RAB11-dependent recycling increases random motility and impaired directional and persistent migration, as a consequence of delocalized formation of lamellipodia(Prigozhina and Waterman-Storer 2006). Polarized endosomal recycling is hence required for the establishment of cell migration polarity and perturbation of this pathway leads to disorganized cell motility.

2.1.3.4 Spatial restriction of signaling is controlled by endocytosis/recycling during migration in a 3D environment

Migratory protrusions, such as peripheral lamellipodia (PL) and circular dorsal ruffles (CDRs), generated by RTKs stimulation(Buccione, Orth, and McNiven 2004) are required for migration in three-dimensional (3D) matrices(Suetsugu et al. 2003) (Fig. 3). The formation of these protrusions needs endocytic proteins and actin regulatory proteins, such as Dynamin and cortactin, suggesting that CDRs are sites where actin dynamics and endocytosis are integrated(Krueger et al. 2003; Orth and McNiven 2003).

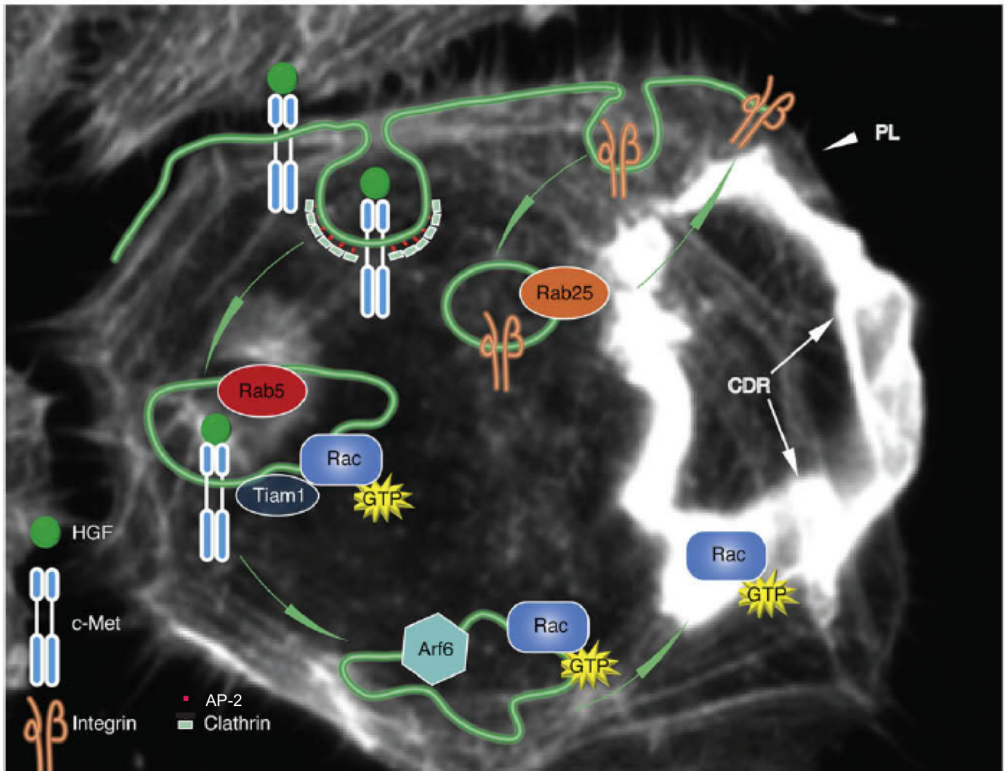

Figure 3. Endocytic trafficking of RAC is required for spatial restriction of signaling in the control of migratory programs.
Upon binding of HGF to C-Met, the receptor is internalized via CME in EEs that contain the small GTPase RAB5. In this compartment, the small GTPase RAC is activated by TIAM1, a nucleotide exchange factor, and is recycled back to specific regions of the PM via ARF6, where CDR and PL are formed. The integrin α5ß1 can associate with the small GTPase RAB25 and traffic bidirectionally between intracellular RAB25 vesicles and the PM within the confines of the pseudopodial tips.
Modified from(Disanza et al. 2009).

Moreover, a tripartite signaling cascade originating from RAB5, Phosphatidylinositol-4,5-bisphosphate 3-kinase (PI3K) and RAC must function at the same time to allow CDR formation(Lanzetti et al. 2004). Conversely, a linear pathway connecting RAS, PI3K and RAC to actin remodeling is sufficient to generate lamellipodia protrusions in response to RTKs(Lanzetti et al. 2004). The endocytic/recycling trafficking of RAC is necessary for the generation of CDRs(Palamidessi et al. 2008). Consistently, in Hela cells, RAB5-dependent RAC activation and CDR formation relies on clathrin and dynamin, thus, on endocytosis. Additionally, RAC trafficking from the PM to endocytic vesicles, containing RAB5 and TIAM1, is necessary for spatially confined RAC activation. Inhibition of recycling blocks CDR formation through RAB5 activation and HGF stimulation, indicating that the recycling step is required as well. Vesicles are targeted to the PM by the small GTPase ARF6, but not by RAB4 or RAB11(Palamidessi et al. 2008), which were

previously implicated in RAC trafficking(Radhakrishna et al. 1999). Moreover, ARF6 controls also the trafficking of ß1 integrins to the PM(D'Souza-Schorey and Chavrier 2006), suggesting that these vesicles are sites where different types of cargo are sorted and delivered to guarantee spatial restriction of signaling for polarized motility(Disanza et al. 2009). From a mechanistic point of view, a question to address is how molecules are recycled to specific regions of the PM to generate spatially restricted signals. For example, upon the activation of CME(Palamidessi et al. 2008), RAC is delivered to membrane binding sites in lipid rafts(del Pozo et al. 2004; del Pozo et al. 2005) where its internalization is blocked by integrin signaling. In this context, ARF6-dependent recycling plays a fundamental role in delivering RAC, integrins and lipid rafts back to the PM, thus coordinating RAC signaling and directional migration with cell adhesion(Balasubramanian et al. 2007). The importance of spatial restriction of RAC signaling in the control of migratory protrusions is highlighted by the discovery of the correlation of CDR formation with the ability of the cells to acquire a mesenchymal mode of motility and migration in 3D(Suetsugu et al. 2003), properties that are features of metastatic invading cancer cells. RAC signaling has also been shown to be involved in mesenchymal migration(Sanz-Moreno et al. 2008), suggesting that endocytic/recycling pathways, by ensuring RAC spatial restriction and polarization, may also control the amoeboid-to-mesenchymal transition. For example, the ectopic expression of RAB5 in melanoma cells, a model for amoeboid motility, induces a switch to a mesenchymal-like mode of motility. On the contrary, inhibition of RAB5 in colon carcinoma cells, a model for mesenchymal motility, induces a switch to an amoeboid-like mode of motility(Palamidessi et al. 2008). Of note, RAB5 was shown to be critical for normal germ cell migration during zebrafish development(Palamidessi et al. 2008). All these examples indicate that spatial regulation and trafficking of signaling molecules, like RAC, is evolutionary conserved to organize actin dynamics, polarized protrusion, and directional cell migration, finally affecting the mode of motility of normal and cancer cells.

2.1.3.5 Migratory and invasive programs are regulated by the trafficking of adhesion receptors

Endocytic trafficking of adhesion receptors directly contributes to invasive migration(Ramsay, Marshall, and Hart 2007). Evidence that recycling pathways control the capacity of integrin-mediated migration into fibronectin-containing 3D-extracellular matrix has been provided that α5β1 associates with RAB25 and is involved in vesicle recycling(Caswell et al. 2007). RAB25 sustains the formation of long pseudopodial extensions when cells migrate in 3D contexts, and both RAB25 and α5β1 integrin co-localize in intracellular vesicular compartments within the distal tip of pseudopods(Caswell et al. 2007). Moreover, RAB25 promotes spatial restriction confinement of α5β1within the tip region of pseudopods cancer cells that move forward through a 3D matrix(Caswell et al. 2007). The picture that is emerging from these studies is that there is an intense trafficking of vesicles and molecules when cells become motile and that a fine regulation of this trafficking is required to ensure a migratory response both in 2D and 3D environments.

2.1.3.6 Endocytosis/recycling controls epithelial cell polarity

Recent studies have shown that endocytosis and recycling of adhesion molecules are essential during developmental processes. For example, the endoytic/recycling route of E-chaderin, a component of adherent juctions in epithelial cells, is emerging as an important mechanism in the assembly and disassembly of epithelial tissues(Yap, Crampton, and Hardin 2007). The localization of E-cadherin to adherent junctions is maintained by the redirection of the protein to the PM through a recycling pathway instead of preventing its endocytosis. The recycling of E-cadherin has been studied in mammalian cells(Paterson et al. 2003) and in *Drosophila*(Langevin et al. 2005), and appears to be controlled by the small GTPase RAB11 and by the exocyst complex(Wu et al. 2005). In *Drosophila*, exocyst activity is important for the transportation of E-cadherin from the recycling compartment

to the PM(Beronja et al. 2005) or specifically to epithelial cell junctions(Langevin et al. 2005; Blankenship, Fuller, and Zallen 2007). Thus, the constant turnover of junctional material is required for epithelial cells to rapidly adjust polarity and cell-cell contact in responce to extracellular cues.

2.2 NUMB

2.2.1 NUMB family proteins

NUMB was originally identified in *Drosophila* (d-NUMB) as a cell fate determinant(Uemura et al. 1989). During ACD of SOP cells in *Drosophila*, NUMB is inherited only by one daughter cell, the pIIb, which acquires a different destiny from the pIIa cell(Uemura et al. 1989). In particular, loss of d-NUMB results in defective neuronal differentiation, while its ectopic expression causes an increase in neuron differentiation to disadvantage of other differentiated cell types(Uemura et al. 1989; Spana and Doe 1996; Spana et al. 1995; Rhyu, Jan, and Jan 1994).

The NUMB protein is conserved throughout the evolution and its mammalian homologues are encoded by two genes, *numb* and *numb-like*, that were first discovered in mice(Verdi et al. 1996; Zhong et al. 1996; Zhong et al. 1997). Both mouse NUMB (m-NUMB) and d-NUMB show strong sequence similarity with the N-terminal portion of mouse NUMB-Like (m-NUMB-L) (amino acid 42 to 331), with 76% and 63.7% identity, respectively (Fig. 4). The similarity between m-NUMB and m-NUMB-L is present throughout the protein, while the similarity between m-NUMB and d-NUMB is restricted to the N-terminal portion of the protein(Zhong et al. 1997).

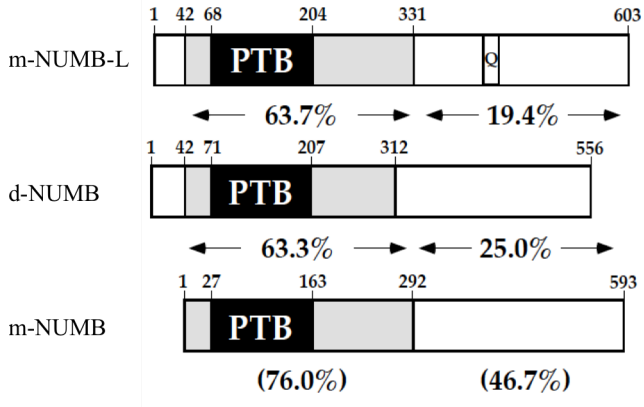

Figure 4. Schematic representation of m-NUMB-Like, d-NUMB and m-NUMB.
Amino acid similarity between adjacent proteins is shown as percentage and written between the diagrams; homology between m-NUMB-L and m-NUMB is quantified as percentage and is written in parentheses. PTB indicates a putative phosphotyrosin binding domain and Q is a poly-glutamine stretch. Adopted from(Zhong et al. 1997).

NUMB functions are conserved between vertebrates and invertebrates and this concept is based on two evidences: first, when expressed in *Drosophila*, m-NUMB shares cellular functions with d-NUMB(Zhong et al. 1996; Zhong et al. 1997); second, the chicken NUMB homologue is able to antagonize-NOTCH-mediated inhibition of differentiation in neuroepithelial cells(Wakamatsu et al. 1999).

From a structural point of view, NUMB has a modular architecture; it contains an amino terminal phosphotyrosin binding (PTB) domain (Bork and Margolis 1995), followed by a C-terminal proline reach region (PRR) composed of several putative Src homology (SH3) domain-binding sites (Verdi et al. 1996). The PRR region contains two DPF motives that are consensus binding sites for the clathrin adaptor α-adaptin, and one NPF motif, which associates with proteins containing Eps15 homology (EH) domains (Salcini et al. 1997). Both motifs are conserved in all vertebrate NUMB isoforms in the related mammalian protein NUMB-Like and in the *Drosophila* homologue (Salcini et al. 1997).

The mammalian *numb* gene encodes for four proteins that derive by alternative splicing of two exons: the first exon is located in the PTB domain and the second is located in the PRR region(Verdi et al. 1999; Dho et al. 1999). An 11-amino acid (aa) insert in the PTB domain (PTB^{L} long) distinguishes NUMB-1 and NUMB-2 from the NUMB-3 and NUMB-4 (PTB^{S} short). Moreover, the NUMB isoforms 1 and 3 contain an insert of 48 aa in the

PRR (also called PRR^L long), which is missing in the NUMB isoforms 2 and 4 (PRR^S short)(Dho et al. 1999; Verdi et al. 1999) (Fig. 5).

Studies conducted in immortalized mouse neuronal crest cell lines and in primary cultures of rat neuronal crest stem cells with overexpressed h-NUMB isoforms showed that PRR^S containing h-NUMB isoforms promote neuronal differentiation, while the and PRR^L h-NUMB is involved in neuronal proliferation(Verdi et al. 1999). The PTB domain has also been reported to control NUMB localization(Dho et al. 1999). The two isoforms containing the PTB^L are associated with the PM, while the two isoforms containing the PTB^S are mainly cytoplasmic(Dho et al. 1999). Thus, multiple functions of mammalian NUMB could be in part due to the different isoforms and the diversity of interacting proteins(Verdi et al. 1996; Verdi et al. 1999; Dho et al. 1999; Karaczyn et al. 2010).

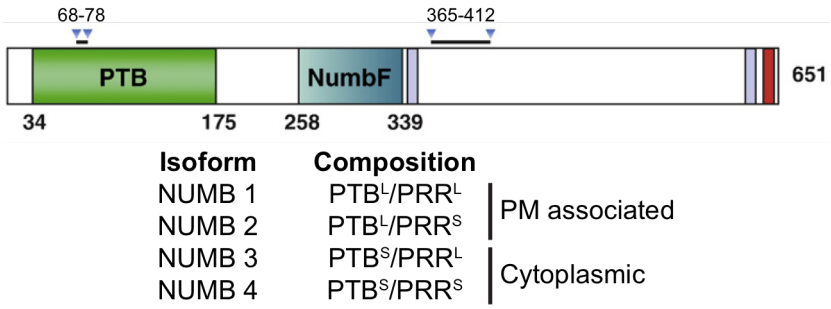

Figure 5. Schematic representation of the four mammalian NUMB isoforms.
Mammalian Numb gene is transcribed in four different splicing variants, due to the alternate skipping of two exons. Arrowheads indicate the boundaries of the protein sequences encoded by the two alternative exons**.** In the upper part, the modular structure of the longest human Numb isoform is shown. The PTB domain and the NumbF domain (domain found in the Numb family of proteins adjacent to the PTB domain) are indicated. The position of the DPF and NPF motifs are indicated as gray and red boxes respectively. In the lower part, a schematic diagram shows the structures of the four Numb isoforms which contain either short (S) or long (L) PTB and PRR domains. NUMB 1 and NUMB 2 isoforms are associated with PM while NUMB 3 and NUMB 4 isoforms are mainly cytoplasmic.
Figure modified from (Pece et al. 2011).

2.2.2 NUMB functions: a biological point of view

2.2.2.1 Asymmetric cell division

NUMB owes its name to the fact that its loss of function in *Drosophila* mutants causes a dramatic loss of sensory neurons, causing flies to became "numb"(Pece et al. 2011).

NUMB appeared in the scientific scene more than twenty years ago when it was shown that an intrinsic cellular player participates in cell fate specification during ACD in the

fly(Uemura et al. 1989). Indeed, during interphase of SOP, NUMB is equally distributed at the PM and is then concentrated at one of the two spindle poles during mitotic division. As a consequence of NUMB asymmetric distribution during cytokinesis, the daughter cell that inherits NUMB, the pIIb, will have a different destiny from the pIIa cell(Rhyu, Jan, and Jan 1994) (Fig 6).

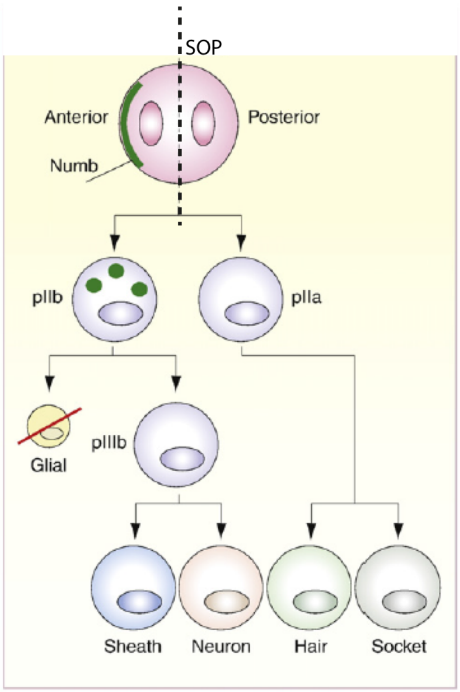

Figure 6. NUMB in ACD of SOP cells of *Drosophila.*
The figure describes the ACD in *Drosophila* SOP. The plane of division with orientation is indicated. NUMB is indicated in green as crescent in SOP and as spheres in pIIb cell. For simplicity, only the first ACD is represented in detail. However, all the other divisions of pIIb are asymmetric and involve asymmetric partitioning of NUMB.
Modified from(Pece et al. 2011).

From a molecular point of view, NUMB acts by inhibiting Notch function(Guo, Jan, and Jan 1996): the evidence that lead to this conclusion came from experiments performed in the SOP system, where gain of function NOTCH mutations phenocopied NUMB loss-of-function(Guo, Jan, and Jan 1996). Finally, NUMB and NOTCH were shown to directly interact(Guo, Jan, and Jan 1996). Of note, the role of NUMB as a cell fate determinant was confirmed also in the central nervous system (CNS) in *Drosophila*(Spana and Doe 1996; Spana et al. 1995) and in mammals(Zhong et al. 1996). In particular, NUMB knock-out

mice showed severe alterations during the development of the CNS(Zhong et al. 2000), linking the NUMB-NOTCH axis to ACD in a true SC compartment.

Asymmetric NUMB localization and segregation in SOP cells and CNS in *Drosophila* is achieved by the PAR polarity complex machinery, which is evolutionary conserved and composed of three proteins: Bazooka (Par3 in mammals)-Par6-aPKC (atypical protein kinase C)(Rhyu, Jan, and Jan 1994; Knoblich, Jan, and Jan 1995). In mammals, there are direct and indirect evidences suggesting that the PAR polarity complex controls NUMB asymmetrical distribution during ACD: mammalian NUMB binds to aPKC and Par3(Nishimura and Kaibuchi 2007; Wang et al. 2009) and is phosphorylated by aPKC(Nishimura and Kaibuchi 2007; Smith et al. 2007). NUMB asymmetric cellular distribution may promote distinct fates in stem/progenitor cells by interacting with components of signaling pathways triggered by specific micro environmental cues(Pece et al. 2011). The identity and function of the micro-environmental key factors that crosstalk with NUMB to trigger the cell fate choice are not fully understood as yet. Nevertheless, a number of pathways that control stem/progenitor cell development have been described to interact with NUMB. For instance, NOTCH or Hedgehog (Hh) activation and loss-of-function of p53 promote SC maintenance and expansion.

2.2.2.2 Endocytosis

The molecular mechanisms by which NUMB functions remained unveiled for a long time. Initially, hypotheses and interpretation of data describing NUMB-NOTCH antagonism focused mainly on the NOTCH signaling pathway(Guo, Jan, and Jan 1996). Later, it became increasingly clear that NUMB is expressed in almost all cells, and in the vast majority of these, cell division and the subsequent NUMB segregation at mitosis is symmetric. In some settings, however, the asymmetric distribution of NUMB, and consequently cell fate specification, leads to biochemical asymmetry, suggesting that NUMB is involved in the regulation of basic cellular functions.

The first data that showed how NUMB could work derived from the study of protein-protein interaction in the endocytic network(Salcini et al. 1997; Di Fiore, Pelicci, and Sorkin 1997; Paoluzi et al. 1998; Santolini et al. 1999), in which h-NUMB was found to interact with the EH domain of two endocytic proteins, epidermal growth factor substrate 15 (EPS15) and epidermal growth factor substrate 15-like 1 (EPS15L1)(Coda et al. 1998; Confalonieri et al. 2000; Fazioli et al. 1993), suggesting a putative role for NUMB in endocytosis(Salcini et al. 1997; Confalonieri and Di Fiore 2002). Subsequentially, NUMB was defined as an endocytic protein(Santolini et al. 2000) based on its subcellular localization in endocytic organelles, its co-trafficking with internalizing receptors, its interaction with the α-adaptin subunit of the major clathrin adaptor AP2, and the ability of dominant negative NUMB mutants to block constitutive and ligand-induced endocytosis(Santolini et al. 2000). In the following years, a number of studies established the involvement of NUMB in internalization and recycling, consolidating the role of NUMB in endocytosis.

2.2.2.3 Internalization

The first link between NUMB and internalization could be directly coupled to NUMB function as a cell-fate determinant in the SOP system (Berdnik et al. 2002). In a genetic screen for mutations affecting bristle morphology in the fly, it was found that α-adaptin phenocopies loss-of-function NUMB mutants(Berdnik et al. 2002). Of note, all isolated α-adaptin mutants are characterized by a mutation in the ear domain, the very same domain with which NUMB interacts. Genetic analysis showed that, in the SOP linage, α-adaptin acts downstream of NUMB and upstream of NOTCH. α-adaptin partitions asymmetrically in pIIb cells through a NUMB-dependent manner(Berdnik et al. 2002). These results show that the NUMB-α-adaptin axis couples endocytosis with cell-fate specification and further suggest that the mechanism of NUMB-NOTCH counteraction could be due to unequal NOTCH endocytosis in the pIIb cell vs. the pIIa cell, resulting in biochemical and

signaling asymmetry. Subsequent work in *Drosophila* and mammals reinforced the concept that NUMB plays a role in the internalization step of endocytosis (Fig. 7).

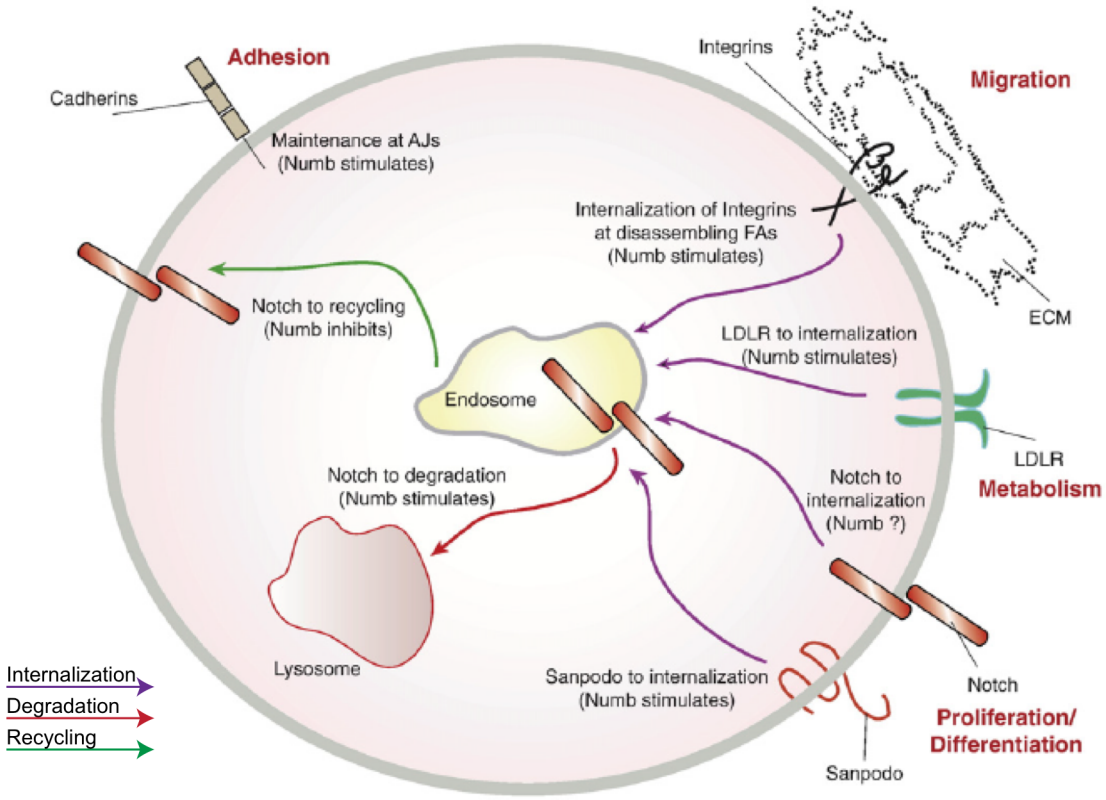

Figure 7. NUMB functions in endocytosis and recycling.
The figure describes NUMB functions in the intracellular trafficking. Cellular activities controlled by the endocytic functions of Numb (migration, adhesion, metabolism, proliferation/differentiation) are indicated in red. Violet, red and green arrows indicate internalization, degradative and recycling routes, respectively. ECM, extracellular matrix; LDLR, low-density lipoprotein receptor; FAs, focal adhesions; AJs, adherens junctions.
Modified from(Pece et al. 2011).

In the SOP system, NUMB was shown to be necessary for the endocytosis of Sanpodo, a membrane protein required for NOTCH signaling(Hutterer and Knoblich 2005; Roegiers, Jan, and Jan 2005). In mammals, NUMB was found to regulate endocytosis of the neuronal cell adhesion molecules L1(Nishimura et al. 2003), integrin ß-1 and integrin ß3(Nishimura and Kaibuchi 2007). In another study, NUMB removal increased the surface levels of α1, α5 and ß1 integrins, a result compatible with the role of NUMB in their endocytosis(Teckchandani et al. 2009).

The role of NUMB as a cargo-selective adaptor is conflicting. Teckchandani and colleagues showed that NUMB is not required for the internalization of the

TfR(Teckchandani et al. 2009), while Sorensen and colleagues published that NUMB is involved in TfR internalization upon phosphorylation by a key endocytic kinase, adaptor-associate kinase 1 (AAK1)(Sorensen and Conner 2008). The expression of a NUMB mutated in the phosphorylation site from AAK1 impairs the uptake of TfR and LDLR but not that of EGFR(Sorensen and Conner 2008), reminding of the principle of cargo selectivity. Although some differences could be due to the experimental settings, NUMB may be seen as a cargo-selective adaptor. In fact, NUMB is structurally related to cargo-selective endocytic adaptors, such as Disabled-2 (DAB-2) and the autosomal recessive hypercholesterolemia protein (ARH). In particular, the PTB domains of these protein are highly related and share some features, like the ability to bind to acid phosphoinositides that mediated the interaction with the PM(Dho et al. 1999; Mishra et al. 2002; Mishra, Watkins, and Traub 2002). Both DAB2 and ARH are cargo-selective adaptors(Mishra et al. 2002; Mishra, Watkins, and Traub 2002; Teckchandani et al. 2009), supporting the idea that NUMB may belong to the same functional family of endocytic adaptors.

2.2.2.4 Recycling

The idea that NUMB is more than an adaptor protein in the internalization step came from studies conducted in Dr. Jane McGlade's laboratory (Fig. 7). They found that NUMB interacts and co-localizes *in vivo* with the EHD (EH-domain) protein family, which function in recycling of PM receptors internalized both by CME and NCME regulated by ARF6. Moreover, both NUMB and EHD proteins were found to be localized in vesicles containing the small GTPase ARF6, which represent the recycling endosomes(Smith et al. 2004). Genetic analysis in the nematode *C. Elegans* proved the role of NUMB in recycling. In this system, overexpression of NUM-1A (the nematode NUMB homolog) phenocopies the loss of function of rme-1, the nematode homolog of EHD(Nilsson et al. 2008). These results indicated that NUM-1A negatively regulates recycling, a finding consistent with the fact that loss of NUM-1A bypasses the requirement for RME(Nilsson et al. 2008). Later

on, the same group further characterized the molecular mechanism and proposed that NUM-1A inhibits recycling by preventing the ability of TAT-1 to translocate phosphatidylserine synthetize in the recycling endosome(Nilsson, Jonsson, and Tuck 2011). The role of NUMB as a negative regulator of recycling could also be extended to mammals. In C2C12 myoblastic cells, overexpression of NUMB promotes sorting of NOTCH through the late endosomes for degradation, while its depletion promotes NOTCH recycling(McGill et al. 2009). In the last few years, a role for NUMB as a negative regulator of recycling has emerged, and the molecular mechanisms through which NUMB affects recycling are only now being addressed. Recently, two complementary works described a "recycling inhibition model" in which NUMB negatively regulates the recycling of Sanpodo in the *Drosophila* SOP system(Couturier, Mazouni, and Schweisguth 2013; Cotton, Benhra, and Le Borgne 2013). Collectively, they showed that Sanpodo is a positive regulator of NOTCH turnover and that NUMB inhibits the recycling of internalized NOTCH-Sanpodo via its interaction with Sanpodo in sorting endosome(Cotton, Benhra, and Le Borgne 2013; Couturier, Mazouni, and Schweisguth 2013). The authors proposed that the AP-2- and AP-1-dependent trafficking, regulated by NUMB, is required for Sanpodo localization(Cotton, Benhra, and Le Borgne 2013; Couturier, Mazouni, and Schweisguth 2013). Although the molecular mechanism is still not clear, this scenario is in line with the proposed role for NUMB in *C. Elegans*(Nilsson et al. 2008) and in mammals(McGill et al. 2009). The recycling inhibition model can be applied also to fish, where it has been shown that the OPO protein (a transmembrane protein similar to Sanpodo) interacts with NUMB via a conserved NPAF motif and antagonizes NUMB in the control of integrin trafficking(Bogdanovic et al. 2012).

2.2.2.5 Cell adhesion, migration and epithelial-mesenchymal transition

Given its role in endosomal trafficking of transmembrane receptors, NUMB could be involved in the control of cells adhesion. Indeed, NUMB has been reported to localize in

RAB11-positive recycling endosomes containing cadherin. NUMB interacts via its PTB domain and C-terminal(Rasin et al. 2007) domain with the cadherin-catenin complex, which in other words is the association of E-cadherins, alpha cathenins and beta-catenins with the actin cytoskeleton. The cadherin/cathenin complex regulates PM dynamics, cell migration and cell shape(Pollard and Borisy 2003). Continuous internalization of cadherins and recycling to and from the cell surface via the endocytic machinery is necessary for the maintenance of adherence junctions(Nishimura and Kaibuchi 2007; Rasin et al. 2007). Moreover, cadherins and integrins have been identified as binding partners for NUMB(Casanova 2007a). In fact, NUMB binds to integrin-ßs(Nishimura and Kaibuchi 2007), leading to integrin endocytosis and directional cell migration towards integrin substrates. NUMB is also involved in the directional integrin trafficking in migrating cells, in which NUMB localizes in clathrin-containing structures at the leading edge and around focal adhesions(Nishimura and Kaibuchi 2007). Depletion of NUMB induces a decrease in endocytosis and in integrin-stimulated cell migration(Nishimura and Kaibuchi 2007).

NUMB is also required for epithelial polarity and cell-cell adhesion in epithelial-mesenchymal transition (EMT). The EMT is a critical process in development and plays an important role in many physiological processes. In addition, cancer cells can re-activate EMT in order to execute migratory programs associated with metastasis(Thiery and Sleeman 2006). In epithelial cells, under physiological condition, NUMB binds to E-cadherin or to the PAR complex via PAR3(Wang et al. 2009). Removal of NUMB in Mandin Darby Canine (MDCK) cells leads to lateral mislocalization of PAR3 and a-PKC, a decrease in cell adhesion, apical translocation of E-cadherin and ß-catenin, an increase in cell migration and proliferation, and to active F-actin polymerization. These data suggest that NUMB plays a role in the regulation of cell polarity, cell adhesion and cell migration during EMT.

2.2.3 NUMB regulates different signaling pathways

2.2.3.1 The NOTCH pathway

NUMB was originally identified as an inhibitor of NOTCH signaling in *Drosophila*(Uemura et al. 1989; Skeath and Doe 1998). NOTCH is activated by engagement with ligands of the DLS protein family (Fig.8). Upon binding to its ligands, NOTCH undergoes a series of proteolytic cleavages. As a consequence, the NOTCH intracellular domain (NICD) is translocated from the cytosol to the nucleus, where it converts CSL proteins (CFB1, RBPjk, Suppressor of Hairless, Lag1) from transcriptional repressors to transcriptional activators, thereby turning on the expression of target genes(De Strooper et al. 1999; Jarriault et al. 1995; Mumm et al. 2000; Struhl and Greenwald 1999).

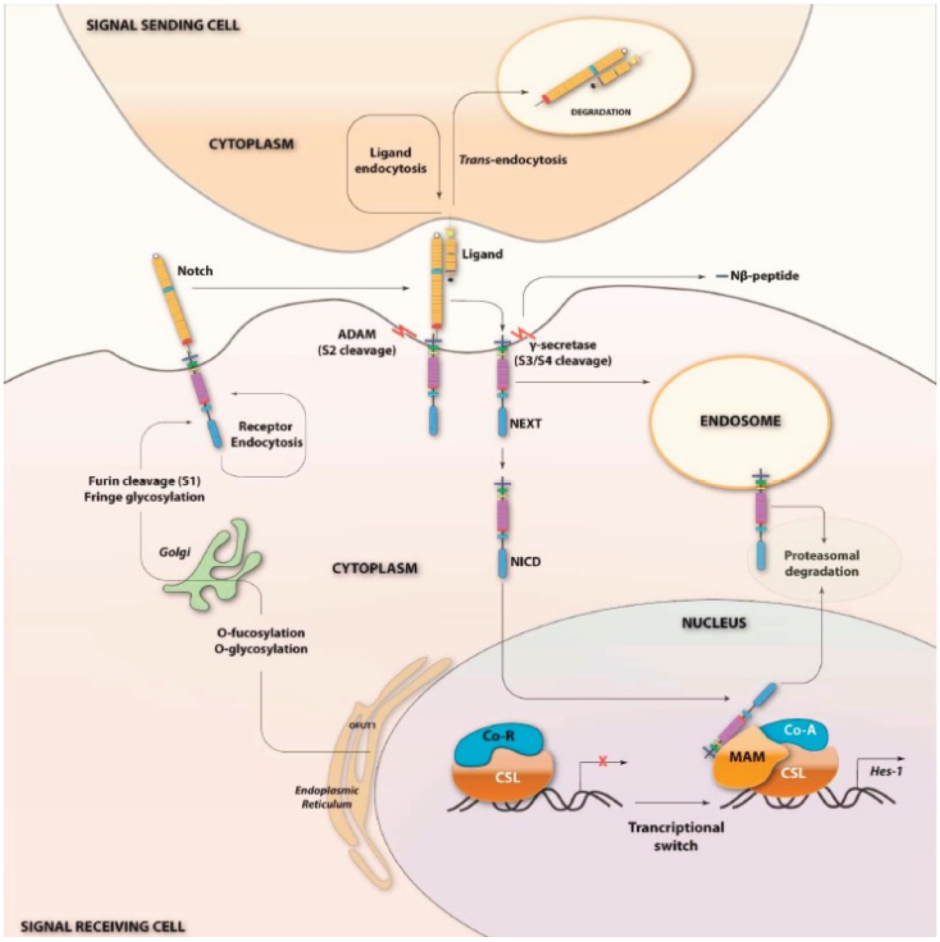

Figure 8. Notch signaling pathway.
The figure describes the NOTCH signaling pathway. The signaling sending cell express the NOTCH ligand on its surface. The ligand binds to the receptor, expressed by the signaling receiving cell and the

receptor undergoes to a series of proteolytic cleavages releasing the NICD. Then the NICD enters into the nucleus where it activates transcription. NECD: NOTCH extracellular domain; NICD: NOTCH intracellular domain; NEXT: NOTCH extracellular truncated domain; CSL: CBF1/Suppressor of Hairless/LAG-1; MAML: Mastermind/Lag-3; Co-A: co-activators; Co-R: co-repressors; Nβ: short peptide released after cleavage at site 4.
Modified from (Yavropoulou and Yovos 2014)

One theory of how NUMB regulates NOTCH is that NUMB acts as an adaptor between NOTCH and its E3-ubiquitin ligase Itch(Qiu et al. 2000), causing poly-ubiquitination and degradation of cytoplasmic NICD but not of the membrane bound form of NOTCH(McGill and McGlade 2003). NUMB has been shown to interact with Itch in the same region in witch NOTCH binds Itch, and co-expression of NUMB and Itch further enhances the ubiquitination of the NICD(McGill and McGlade 2003). In addition, to facilitating NOTCH ubiquitination, NUMB controls the intracellular trafficking of NOTCH, thereby suppressing its function (see section 2.2.4). These data indicate that, in mammals, NUMB regulates post-endocytic sorting of NOTCH, leading to its degradation(McGill et al. 2009).

2.2.3.2 The Hedgehog pathway

Another pathway that is regulated by NUMB is the Hedgehog (Hh) signaling pathway(Di Marcotullio et al. 2006). The Hh signaling pathway is fundamental during development of multicellular organisms, including humans(Teglund and Toftgard 2010; Varjosalo and Taipale 2008). Initially, Hh was discovered as a "segment-polarity" gene that controls Drosophila embryonic cuticle pattern(Nusslein-Volhard and Wieschaus 1980). Hh is a secreted molecule and is subject to an autocatalytic cleavage, resulting in an N-terminal activated fragment(Porter et al. 1995), which is modified by the addition of a cholesterol moiety at the C-terminus(Porter et al. 1996). Only one Hh gene is present in the fly. In vertebrates, instead, three homologues have been described: Sonic (Shh), Desert (Dhh) and Indian (Ihh)(Echelard et al. 1993; Marigo et al. 1996; Stone et al. 1996), and all three are responsible for the activation of the pathway upon binding to their related receptor, Patched. The most widely studied vertebrate Hh gene is Shh, which is expressed throughout the developing CNS, lungs, limbs, gut, hair follicles, and teeth(Bellusci et al.

1997; Goodrich et al. 1996; St-Jacques et al. 1998). The pathway terminates with the activation of three transcription factors; Gli1, Gli2 and Gli3(Dai et al. 1999; Sasaki et al. 1999). Besides tissue development, the Hg pathway has been implicated in numerous cellular processes ranging from cell proliferation and differentiation, to migration, and to DNA repair. It is also involved in tissue repair/regeneration and in SC self-renewal(Varjosalo and Taipale 2008; Teglund and Toftgard 2010; Jiang and Hui 2008). Alteration of the Hg pathway have been implicated in a variety of developmental abnormalities and in different types of cancer(Jiang and Hui 2008; Teglund and Toftgard 2010; Varjosalo and Taipale 2008; Mullor, Sanchez, and Ruiz i Altaba 2002).

Studies conducted in mouse cerebellar granule cell progenitors (GCPs) have shown that Hh expression maintains GCPs proliferating and undifferentiated, while its inhibition leads to GCPs differentiation(Di Marcotullio et al. 2006). Importantly, this transition correlates with the expression of NUMB in developing GCPs and to the association of NUMB with Gli1 and the recruitment of the E3-ubiquitin ligase Itch, causing, thus, Gli1 proteasome-dependent degradation(Di Marcotullio et al. 2006). As a consequence, Hg signaling is suppressed and GCPs begin to differentiate(Di Marcotullio et al. 2006).

2.2.3.3 The p53 pathway

A recent work from our group has described a new role for NUMB in the regulation of the tumor suppressor protein TP53 (p53)(Colaluca et al. 2008). p53 is a transcription factor that activates different downstream genes(Farmer et al. 1992) and their related pathways, such as apoptosis(Shaw et al. 1992), DNA repair , growth arrest(Yonish-Rouach et al. 1991), and cell cycle arrest(el-Deiry et al. 1992). p53 protein levels and its activity are regulated by different stress-induced signaling, like DNA damage or UV radiation(Kastan et al. 1991; Maltzman and Czyzyk 1984), preventing thus genome instability and tumorigenesis(Vogelstein, Lane, and Levine 2000; Lane 1992). p53 is a tumor suppressor in cancer because 50% of all human cancers have been show to contain mutations in both

alleles of the p53 gene. Many tumors express high levels of p53 but in tumors in which p53 is mutated, its function is lost despite the high expression levels(Bartek, Bartkova, et al. 1990; Bartek, Iggo, et al. 1990; Iggo et al. 1990). One mechanism of p53 inactivation occurs through the activation of the oncogene E3 ubiquitin ligase Mouse double minute 2 (MDM2; HDM2 in human), which is responsible for p53 ubiquitination and subsequent proteasomal degradation(Haupt et al. 1997; Kubbutat, Jones, and Vousden 1997). MDM2 expression is a transcriptional target of p53, which causes increased MDM2 levels but lower p53 levels(Wu et al. 1993). NUMB binds and blocks MDM2, preventing the ubiquitination and degradation of p53 in the normal mammary epithelial cell line, MCF10A(Colaluca et al. 2008). Notably, the downregulation function of NUMB over MDM2 occurs in the contest of NUMB/p53/MDM2 tri-complex(Colaluca et al. 2008), which results in increased p53 levels and activity, and p53-dependent phenotypes. On the contrary, NUMB removal decreases p53 levels and activity, and is accompanied by DNA-damage, deregulated apoptosis, and cell cycle checkpoint activation response(Colaluca et al. 2008).

2.2.3.4 The TCTP pathway

Translationally controlled tumor protein (TCTP) was initially identified as a factor implicated in cell growth(Thomas, Thomas, and Luther 1981; Yenofsky, Bergmann, and Brawerman 1982). TCTP is ubiquitously expressed, suggesting an important role for this protein in normal physiological function(Chen SH1 2007). This protein also plays a role in a number of cellular events related to cancer progression(Cans et al. 2003; Jung et al. 2004; Yoon et al. 2000; Liu, Urbe, and Clague 2012) and is directly involved in malignant transformation(Tuynder et al. 2004; Tuynder et al. 2002; Arcuri et al. 2004). In line with these functions, TCTP-dependent transformation has been coupled to TCTP regulation of p53 and *vice versa*. As described above, NUMB enters in a complex with p53 and prevents p53 degradation(Colaluca et al. 2008); in this contest, TCTP competes with NUMB for

MDM2 binding, promoting p53 ubiquitination and degradation(Amson et al. 2012). In addition, TCTP increases the MDM2-mediated ubiquitination of p53(Amson et al. 2012).

2.2.4 Deregulation of NUMB and cancer

2.2.4.1 NUMB acts as a tumor suppressor in human cancers

Considering its critical role in many cellular processes, subversion of NUMB has been linked to important human pathologies(Pece et al. 2010), including neurodegeneration(Kyriazis et al. 2008; Merdes et al. 2004; Roncarati et al. 2002) and cancer(Pece et al. 2004; Wang et al. 2015; Westhoff et al. 2009; Wu et al. 2014; Xie et al. 2015). Initial evidences that highlighted NUMB as a potential tumor suppressor came from *Drosophila*(Rhyu, Jan, and Jan 1994; Guo, Jan, and Jan 1996; Wang et al. 2009), where it was described as a negative regulator of NOTCH signaling through its direct interaction with NOTCH via its PTB(Guo, Jan, and Jan 1996; Rhyu, Jan, and Jan 1994). Remarkably, NUMB was also identified as a tumor suppressor in an *in vivo* RNA screening in a mouse model of lymphomagenesis, whose loss can accelerate the onset of lymphomas(Bric et al. 2009).

Loss of NUMB occurs in 50% of all breast cancers(Pece et al. 2004) and correlates with poor prognosis(Colaluca et al. 2008), a less-differentiated phenotype, compered to NUMB expressing tumors(Colaluca et al. 2008; Pece et al. 2004; Rennstam et al. 2010), and the expression of cancer stem cell (CSC) markers(Rennstam et al. 2010); this latter is interesting as recent findings show that poorly differentiated breast tumors harbor a higher CSC-content than well-differentiated tumors(Pece et al. 2010). Loss of NUMB in breast tumors leads to the alteration of two distinct pathways: the hyper-activation of the NOTCH-driven oncogenic pathway and the downregulation of the p-53-induced tumor suppressor pathway(Colaluca et al. 2008; Pece et al. 2004), thus, inducing tumor transformation(Colaluca et al. 2008; Pece et al. 2004). These evidences directly correlate with human breast cancer. Indeed, the ectopic re-expression of NUMB in NUMB deficient

(but not NUMB-proficient) tumors inhibits proliferation and reverts NOTCH signaling to basal levels (Pece et al. 2004). Moreover, restoration of NUMB levels in human primary breast tumors cells rescues p53 expression and sensitizes cells to chemotherapeutic treatment, while NUMB ablation in NUMB-proficient tumor cells confers chemoresistance(Colaluca et al. 2008).

The expression of NUMB is lost in about 30% of all non-small cell lung carcinomas (NSCLCs)(Westhoff et al. 2009), with concomitant activation of the NOTCH pathway and addiction to high NOTCH levels. In 10% of these tumors, gain-of-function mutations in the NOTCH gene lead to NOTCH activation in a NUMB-independent manner and correlates with a poor clinical outcome in NSCLC patients that do not present p53 mutations(Westhoff et al. 2009). In both breast cancer and NSCLCs, loss of NUMB is due to a massive ubiquitination and degradation; in fact, NUMB protein levels can be restored by proteasomal inhibition and the restoration event is coupled with hyper-ubiquitination in NUMB-deficient, but not NUMB-proficient, tumors(Pece et al. 2004; Westhoff et al. 2009). Loss of NUMB occurs in the absence of genetic lesions to the *NUMB* locus and in the presence of normal RNA levels(Pece et al. 2004; Westhoff et al. 2009). It is possible that NUMB alterations are caused by the components of the ubiquitination/deubiquitination system.

Reduced NUMB levels also correlate with poor prognosis in salivary gland carcinoma(Maiorano et al. 2007), in clear cell renal cell carcinoma (ccRCC)(Sima et al. 2015) and in hepatocellular carcinoma(Sima et al. 2015; Xie et al. 2015), although no additional mechanisms are currently known for these tumors.

2.2.4.2 NUMB controls stem cell fate and differentiation in cancer

The tumor suppressor role of NUMB in cancer could be related to its ability to control stem/progenitor fate. It has been known for many years that only a small portion of human tumor cells can give rise to tumors when transplanted in immunocompromised

mice(Gupta, Vyas, and Enver 2009; Reya et al. 2001). These cells are defined as cancer stem cells (CSCs) and it is hypothesized that only these are capable of self-renewal. Therefore, it is understandable that NUMB is the target of transformation in the stem cell compartment. Indeed, our group has demonstrated that in the mammary gland compartment NUMB plays a dual role(Tosoni et al. 2015). In the stem cell (SC) compartment, NUMB establishes an asymmetric mode of division and is retained in the cell that maintains the SC identity by sustaining high p53 activity. At progenitor level, loss of NUMB correlates with EMT and results in differentiation defects and reacquisition of stemness features (Tosoni et al. 2015). NUMB removal in the mouse mammary gland results in an expansion of the SC compartment, morphological alteration and tumorigenicity due to low p53 levels(Tosoni et al. 2015). These latter phenotypes could be rescued by restoration of p53 levels or activity, which could be a potential SC-targeted treatment(Tosoni et al. 2015).

2.2.4.3 How NUMB acts in cancer: the circuitry level

From a biochemical and molecular point of view, the tumor suppressor function of NUMB are connected with growth promoting and growth suppressing circuitries (Fig. 9). For example, in the absence of NUMB, both NOTCH and Hh signaling are increased and result in pro-proliferative and anti-differentiative effects, while the signaling of the tumor suppressor p53 is attenuated. Moreover, subversion of NUMB is predicted to have a major impact on the entire homeostasis of endocytosis, itself proposed as a tumor suppressor mechanism(Lanzetti and Di Fiore 2008; Polo, Pece, and Di Fiore 2004).

Lastly, the alteration of many polarity function, connected with the PAR polarity complex(Aranda, Nolan, and Muthuswamy 2008; Goldstein and Macara 2007; Sancho, Batlle, and Clevers 2004), could contribute to transformation events, such as deregulation of PAR complex activity as a key factor for initiation of transformation(Wang et al. 2009), established or sustained by loss-of-NUMB. In this scenario, the implication of NUMB in

the control of EMT is interesting: loss of NUMB causes phenotypes characteristic of EMT, which is a strategy used by tumor cells to acquire invasive ability and resistance to cell death, senescence, immunosurveillance, immunotherapy and chemotherapy(Singh and Settleman 2010; Thiery et al. 2009), thereby confirming the involvement of NUMB in tumor-related phenotypes.

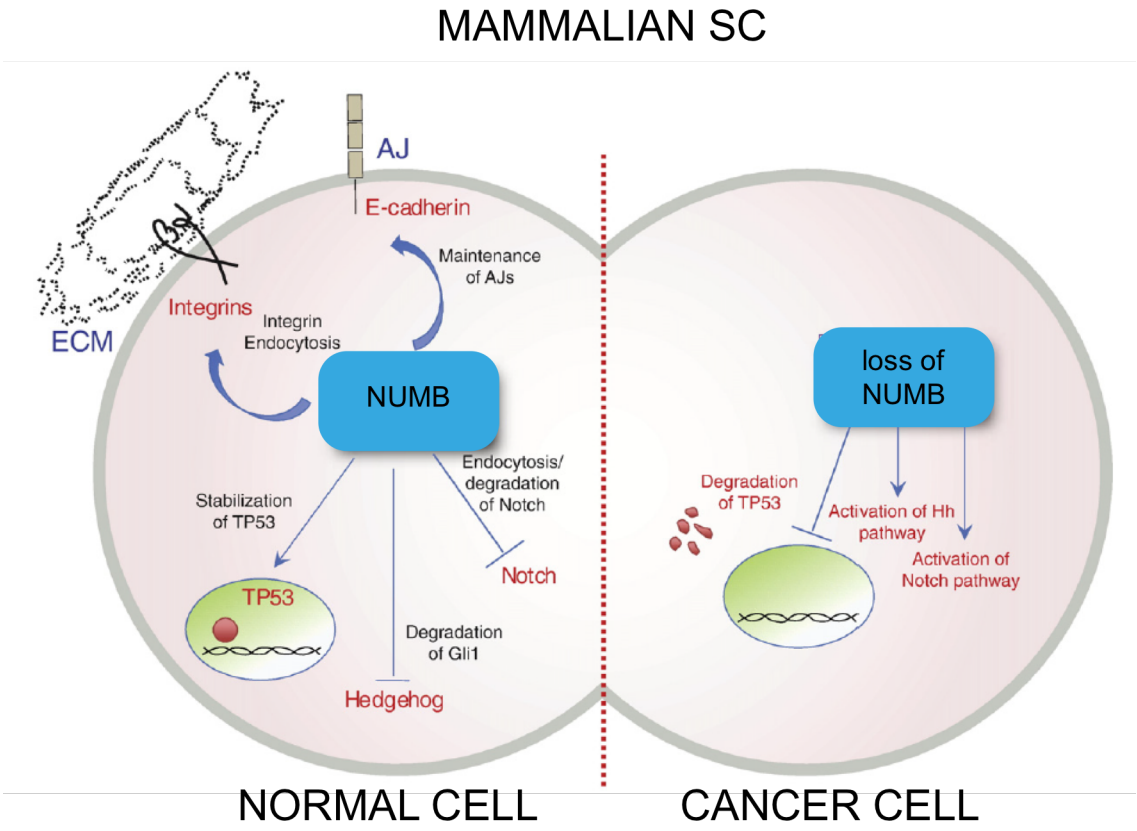

Figure 9. NUMB in cancer.
The figures describe a "hypothetical division" of mammalian SC, in which NUMB segregates only in one daughter cell. The pathways that would be inherited in the daughter cell that receives NUMB (left), and in the daughter cell that does not receive it (right), are depicted. The figure also shows a simplified view of the difference between a normal cell and a cancer cell, in which the expression of NUMB is lost.
Modified from(Pece et al. 2011).

2.3 ARF proteins

The ARF protein family belongs to the Ras Superfamily of small GTPases(D'Souza-Schorey and Chavrier 2006; Donaldson and Jackson 2011a). The ARFs have been shown to participate in many cellular processes, like control of membrane trafficking, activation of enzymes and regulation of actin remodeling(D'Souza-Schorey and Chavrier 2006; Donaldson and Jackson 2011a). The mammalian ARF protein family is composed of 6 members that are grouped in three classes based on sequences homology: Class I (ARF1, ARF2, ARF3), Class II (ARF4 and ARF5) and Class III (ARF6)(D'Souza-Schorey and Chavrier 2006; Donaldson and Jackson 2011a). While the function of class II ARF proteins is still unclear(D'Souza-Schorey and Chavrier 2006), Class I ARF proteins have been shown to regulate the assembly of different types of coated complexes in the secretory pathway(Bonifacino and Glick 2004) and ARF6, the only member of Class III, controls mainly the endosomal membrane trafficking and the structural organization at the cell surface(D'Souza-Schorey et al. 1995; Peters et al. 1995). Like others small GTPases of the Ras Superfamily, ARF proteins cycle between an active GTP-bound status and an inactive GDP bound status(D'Souza-Schorey and Chavrier 2006; Donaldson and Jackson 2011a). The on-off status is controlled by guanine nucleotide exchange factors (GEFs) and GTPase-activating proteins (GAPs), which are activators and inactivators, respectively (Fig. 10). GAPs catalyze the hydrolysis of bound GTP and are important because ARFs have low intrinsic GTP-hydrolysis activity. GEFs, through a conserved SEC7 domain, catalyze the release of GDP from the ARF substrate (Fig. 11)(D'Souza-Schorey and Chavrier 2006; Donaldson and Jackson 2011a). All ARF proteins are anchored to the PM by myristoylation, lipid modification, at the second Gly residue of the N-terminus(Amor et al. 1994).

The functions of the ARFs are mainly dependent on the unique cellular distribution of each ARF and on their binding partners. So far, crystallography studies reveled that while the switch regions of ARF1 and ARF6 assumes different conformations in the GDP-bound

state, the GTP bound structures are very similar(Pasqualato et al. 2001). This raises the issue of the specificity of downstream interactors and protein functions of activated ARF. Indeed, the majority of ARF effector molecules that have been identified can interact with more than one ARF protein *in vitro*(Shin, Couvillon, and Exton 2001; Shin and Exton 2001; Kawasaki, Nakayama, and Wakatsuki 2005; Brown et al. 1993; Cockcroft et al. 1994). However, in cells, ARF proteins have different localization, which allows each member of the family to perform a specific function(Peters et al. 1995). Probably, different interactors and effectors establish a specific interaction with active ARF outside the switch region(Al-Awar et al. 2000).

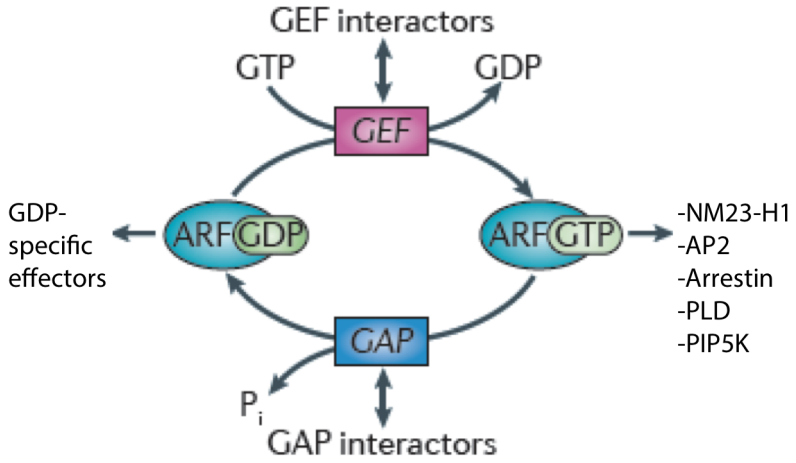

Figure 10. The GDP/GTP cycle of ARF protein.
The ARF family of G proteins undergoes a cycle of GTP binding and hydrolysis of GEFs and GAPs, respectively. The GTP-bound form acts through interaction with 'classical effectors', including vesicle coat proteins and enzymes that can change membrane lipid composition. GDP-specific effectors are less known.
Modified from(Donaldson and Jackson 2011a).

Although ARF1 and ARF6 have unique cellular localization, it is now emerging that ARF6 plays a role at the cell surface, similar to the one of ARF1 at the Golgi apparatus, in which ARF1 controls the assembly of clathrin and non-clathrin coats and organelle structure(D'Souza-Schorey and Chavrier 2006).

As the aim of this PhD project was to functionally characterize the relationship between NUMB, ARF6 and its GEFs EFA6B, I will now give a brief description of ARF6 function in endosomal recycling and actin remodeling, followed by a description of its GEFs and

their function, with a special focus on the EFA6 family.

2.3.1 ARF6

ARF6 is the least-conserved member of the ARF protein family(D'Souza-Schorey and Chavrier 2006). It localize to the PM and to the endosomal compartment, where it regulates endocytic membrane trafficking and actin remodeling(D'Souza-Schorey and Chavrier 2006). The GTP-GDP cycles facilitate ligand internalization and trafficking along the endocytic pathway upon internalization, endosomal recycling and the fusion of an endosomal membrane with the PM(Schweitzer, Sedgwick, and D'Souza-Schorey 2011). On the cell surface, ARF6 facilitates receptor internalization and its activation is required for membrane recycling back to the cell surface(Schweitzer, Sedgwick, and D'Souza-Schorey 2011).

ARF6 regulates the entry of cargos, either via CME or NCME, by changing the lipid composition of the PM (Fig. 11). Indeed, ARF6-GTP activates phosphatidylinositol-4-phosphate-5-kinase (PIP5K)(Honda et al. 1999; Krauss et al. 2003) and phospholipase D (PLD)(Brown et al. 1993; Cockcroft et al. 1994), which results in the production of phosphatidylinositol 4,5-bisphosphate ($PI(4,5)P_2$) and phosphatidic acid (PD). In the presence of these lipids, active ARF6 recruits NM23-H1(Palacios et al. 2002) and the clathrin adaptor AP2(Krauss et al. 2003) to promote CME. ARF6 is also able to interact with arrestins to facilitate GPCRs internalization(Claing et al. 2001) and with AP2(Paleotti et al. 2005) and clathrin during GPCR-mediated cell signaling(Poupart et al. 2007) (Fig. 11). A recent work has demonstrated that ARF6 is internalized in clathrin-coated vesicle to facilitate the fast recycling route of the TfR back to the PM through interaction with the microtubule motor adaptor protein JNK-interacting protein 4 (JIP4) after clathrin uncoating(Montagnac et al. 2011). ARF6 promotes also internalization via NCME and caveolae(Donaldson 2003). Ligands that are internalized via this pathway include the major histocompatibility complex class I protein (MHC class I), M2 acetylcholine

receptors, ß1 integrins and the peripheral myelin-membrane protein (PMP22)(Donaldson 2003).

As discussed above, upon internalization either via CME or via NCME, macromolecules reach the EE(Maxfield and McGraw 2004). For example, internalized ß1 integrin in HeLa cells is recycled to the cell surface in an ARF6-dependent manner and co-localizes with internalized TfR, the small GTP-binding protein Rab11, and MHC class I molecules in recycling endosome(Powelka et al. 2004).

The first evidence that ARF6 is required for endosomal recycling derived from experiments in Chinese Hamster Ovary (CHO) cells in which the expression of dominant negative ARF6 mutants blocked the recycling of endosomal ligands(D'Souza-Schorey et al. 1995; Stearns et al. 1990). Recycling to the PM may occur directly from the EE or through a pericentriolar-recycling endosomal compartment(Maxfield and McGraw 2004). Experiments in HeLa cells showed that ARF6 activity affects the recycling of integral PM proteins that lack cytoplasmic AP2 and a clathrin sorting sequence, including the IL-2 receptor α-subunit, the MHC class I and the glycosylphosphatidylinositol (GPI)-anchored protein(Naslavsky, Weigert, and Donaldson 2003; Radhakrishna and Donaldson 1997). ARF6-positive tubules in these cells slightly overlap with EEs and diffuse from the perinuclear region to the cell periphery.

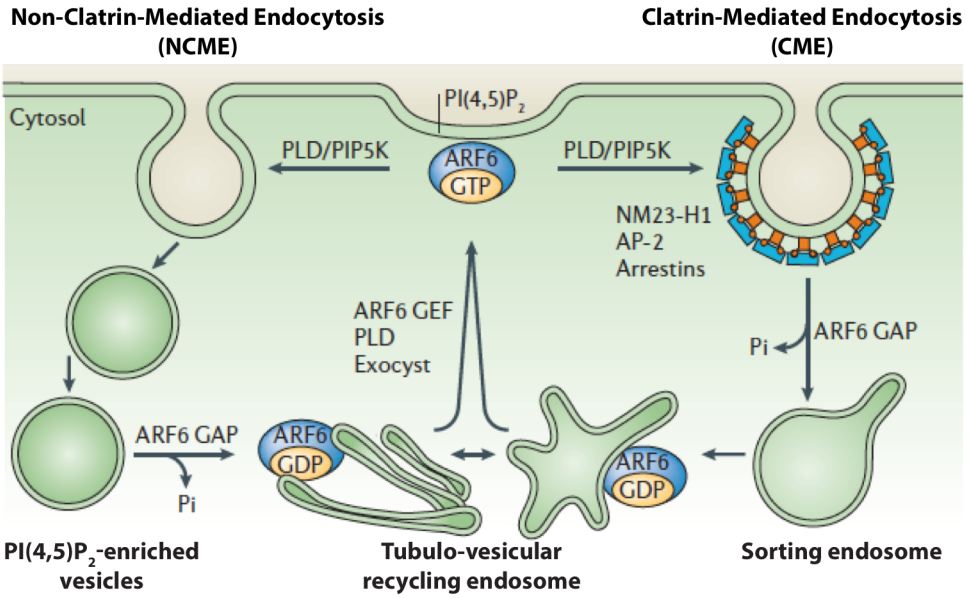

Figure 11. ARF6 regulates the CME and the NCME pathways.
ARF6-GTP mediates its effects on CME and NCME through PIP5K and PLD, and through the production of $PI(4,5)P_2$. ARF6-regulated recruitment of NM23-H1 and/or the adaptor protein AP-2 facilitates CME ARF6 activation is also required for the dissociation of arrestin molecules to facilitate receptor internalization. ARF6–GTP hydrolysis through specific GAPs is required for further trafficking along each pathway, whereas the activation of ARF6 through specific GEFs promotes the recycling and subsequent fusion of an endosomal membrane with the PM. ARF6-regulated membrane recycling is dependent in part on the vesicle-tethering exocyst complex and PLD.
Modified from(D'Souza-Schorey and Chavrier 2006).

In addition to its role in endosomal membrane trafficking, ARF6 is required for actin remodeling at the cell periphery and for events that require a rapid change in cell-surface shape(D'Souza-Schorey and Chavrier 2006). ARF6-dependent actin remodeling is necessary for the formation of pseudopods and membrane ruffles(D'Souza-Schorey et al. 1997; Radhakrishna, Klausner, and Donaldson 1996), neuritis outgrowth and cell spreading(Albertinazzi et al. 2003; Hernandez-Deviez et al. 2004), cell migration(Palacios et al. 2001; Riley et al. 2003; Santy and Casanova 2001) and phagocytosis(Balana et al. 2005; Niedergang et al. 2003; Wong and Isberg 2003; Zhang et al. 1998). ARF6 activity induces alteration in the actin cytoskeleton by its influence on RAC1, RAC1 effectors and phospholipid modulation(D'Souza-Schorey and Chavrier 2006). It has been proved that ARF6 facilitates the re-localization of endosomes containing RAC1 to the cell surface(Radhakrishna et al. 1999; Boshans et al. 2000). Moreover, ARF6 can induce the trafficking of RAC1 to the PM and regulate the activation of RAC1 via its activation of ERK, thereby impacting on RAC-mediated rearrangement of the actin cytoskeleton(Tushir and D'Souza-Schorey 2007). The migratory ability of cells is also modulated by the integrin engagement with the extracellular matrix and requires ARF6-mediated activation of RAC1 for the formation of migratory structures(Schweitzer, Sedgwick, and D'Souza-Schorey 2011).

Since ARF6 plays numerous roles in remodeling of the actin cytoskeleton, it is not unexpected that its activity affects several cellular events that require a rapid change in cell surface morphology. For example, ARF6 has been reported to be an important factor in the regulation of cell-cell(D'Souza-Schorey 2005) and cell- extracellular matrix (ECM) adhesion. In epithelial cells, activated ARF6 favors the internalization of E-cadherin from

cell-cell contact sites to EEs, which causes the disruption of adherens junctions. On the contrary, the expression of a dominant-negative ARF6 mutant blocks HGF-induced internalization of E-cadherin(D'Souza-Schorey 2005). ARF6 is also involved in the control of adhesion to the ECM by acting directly on the distribution of ß1 integrin receptors(D'Souza-Schorey 2005). ARF6 has also been shown to be involved in the regulation of syndecan recycling, a heparan sulfate proteoglycan ECM molecule, by interacting with syntenin, a PDZ domain-containing adaptors, and $PI(4,5)P_2$, on recycling endosomes(Zimmermann et al. 2005).

Invadopodia are actin-rich structures that are required for the degradation of the ECM(Buccione, Orth, and McNiven 2004). *In vitro* cell invasion assays, using breast cancer and melanoma cell lines, have demonstrated that the removal of ARF6 or the expression of its dominant negative mutant inhibits cell invasion, proving, thus, that ARF6 activity can impinge on the invasive potential of tumor cells(Hashimoto et al. 2004; Tague, Muralidharan, and D'Souza-Schorey 2004).

All examples described until now point to the fact that the ARF6-dependent endosomal trafficking impinges on different cellular activities like cell migration, disassembly of cell-cell contact, change in cell shape, and degradation of ECM. Finally, other cellular functions regulated by ARF6-mediated endosomal trafficking are cytokinesis, by promoting the complete abscission, and the cholesterol homeostasis, by facilitating normal cholesterol efflux and preventing cholesterol accumulation(Schweitzer, Sedgwick, and D'Souza-Schorey 2011).

2.3.2 The ARFs family GEFs

ARFs proteins are converted into their GTP-bound form by GEFs, which are able to displace the GDP and allow the binding of GTP(Gillingham and Munro 2007; Casanova 2007b). GEFs are fundamental in the precise control of spatial and temporal activation of ARFs proteins(Donaldson and Jackson 2011a). Thus, they determine the amount and the

localization of active ARFs. All ARFs GEFs share a conserved central domain of a 200 amino acid sequence named SEC7 that catalyze the nucleotide exchange(Chardin et al. 1996). The structure of SEC7, either isolated or in complex with ARF1, has been solved and shows that an invariant glutamate residue is critical for the catalysis(Goldberg 1998; Mossessova, Corpina, and Goldberg 2003; Renault, Guibert, and Cherfils 2003). Most GEFs that contain the SEC7 domain are sensible to the fungal metabolite brefeldin A (BFA)(Misumi et al. 1986), a drug that blocks secretion of proteins by inhibiting ARF1 activation and preventing the assembly of coat protein components onto donor membranes. The effect of BFA is due to the inhibition of ARF nucleotide exchange by sequestering the GEF in an abortive reaction intermediate(Donaldson, Finazzi, and Klausner 1992; Peyroche et al. 1999). Indeed, BFA acts through the stabilization and abortion of ARF-GTP-Sec7 by interacting with residues both on the ARF and on the GEFs(Peyroche et al. 1999; Robert et al. 2004).

Based on the presence of the SEC7 domain, mammals have 15 ARFs GEFs that can be grouped into six evolutionary conserved families: GBF1, BIG, PSD (PH and SEC7 domain), IQSEC, Cytohesin and FBXO8 (Table 1)(Gillingham and Munro 2007; Donaldson and Jackson 2011a; Casanova 2007b).

Name	Aliases and orthologues	Substrate	Location	Motifs and domains	Interactors
ARF GEFs					
GBF1	Gea1,2 (*Sc*), GARZ (*Dm*), GNL1 (*At*)	ARF1,3,5	ERGIC, Golgi	DCB	p115 tether, Rab1, γCOP, Drs2 (with Gea2)
BIG1	p200 ARF GEP, Sec7 (*Sc*)	ARF1,3	TGN, endosome, nucleus	DCB, AKAP	Myosin IXb, Exo70
BIG2	BIG5 (BEN1, AtMIN7) (*At*)	ARF1,3	TGN, endosome	DCB, AKAP	GABA receptor
Cytohesin 1	PSCD1, Steppke (*Dm*)	ARF1,6	PM, endosome	CC, PH, Polybasic	ARFRP1, CASP, ARL4, CNK1
Cytohesin 2	ARNO, PSCD2, Steppke (*Dm*)	ARF1,3,6	PM, endosome	CC, PH, Polybasic	CASP, GRASP (tamalin), IPCEF, A2AR, β-arrestin, V-ATPase, ARL4, ARF6, CNK1, ERBB receptor
Cytohesin 3	GRP1, ARNO3, PSCD3, Steppke (*Dm*)	ARF1,6	PM, endosome	CC, PH, Polybasic	CASP, GRASP (tamalin), THR, ARL4, ARF6, CNK1
Cytohesin 4	PSCD4	ARF1,5	–	CC, PH, Polybasic	–
EFA6A–D	PSD1–4, Yel1 (*Sc*), Syt1 (*Sc*), EFA6 (*Dm*)	ARF6	PM, endosome	PH, CC, pro	TWIK1 K^+ channel
BRAG1	IQSEC2, IQARFGEF, Loner (*Dm*), Schizo (*Dm*)	ARF6	PSD	PH, CC, IQ	IRSp53
BRAG2	GEP100, IQSEC1, Loner (*Dm*), Schizo (*Dm*)	ARF6	PM, endosome, nucleus	PH, CC, IQ	AMPA receptor
BRAG3	IQSEC3, SYNARFGEF, Loner (*Dm*), Schizo (*Dm*)	ARF6	PSD	PH, CC, IQ	PSD95, Homer, utrophin (dystrophin), S-SCAM

Table 1. The ARF GTPases family GEFs.
Modified from(Donaldson and Jackson 2011a).

2.3.2.1 The PSD (EFA6) family

The PSD, or EFA6 (Exchange Factor for ARF6) family was first identified by Franco and colleagues by screening of protein databases for proteins containing the SEC7 domain(Franco et al. 1999). This family is composed of four members (Fig. 12): PSD (EFA6A) and PSD2 (EFA6C), which are expressed predominantly in the brain(Derrien et al. 2002; Matsuya et al. 2005), and PSD3 (EFA6D) and PSD4 (EFA6B), which are expressed ubiquitously(Derrien et al. 2002; Sakagami et al. 2006). Each member of the EFA6 family is encoded by a different gene but in the case of EFA6A(Sironi et al. 2009), EFA6C(Matsuya et al. 2005) and possibly EFA6B(Derrien et al. 2002; Luton et al. 2004), additional isoforms are generated by alternative splicing. Structurally, each member contains a variable N-terminal domain, followed by a central SEC7 domain paired with the PH domain, and a C-terminal domain containing a coiled-coil motif (Fig. 11)(Derrien et al. 2002).

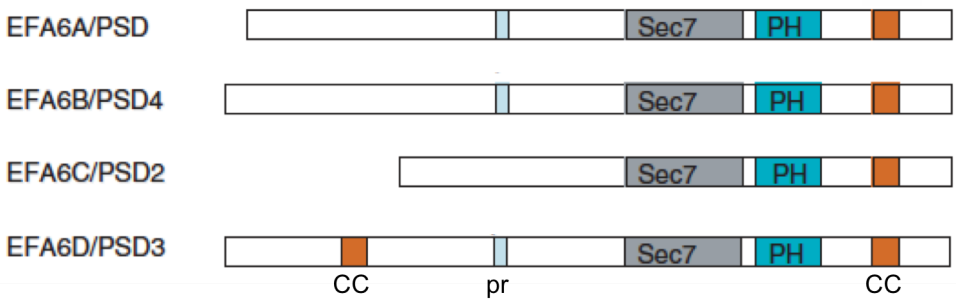

Figure 12. Domain organization of the EFA6 family GEFs
The Sec7 domain, the PH domain, the coiled-coil (CC) domain and the prolin region (pr) are depicted in grey, blu, orange and light blu, respectively.
Modified from(Casanova 2007b).

In vitro, the EFA6 family catalyzes guanine nucleotide exchange preferentially on ARF6 rather than on ARF1(Padovani et al. 2014). EFA6 proteins localize to the PM through the PH domain(Franco et al. 1999), which directly binds with high affinity to $PI(4,5)P_2$(Macia et al. 2008). This interaction is critical for PM localization and for an efficient exchange

factor activity(Macia et al. 2008). The PH domain binds also directly to filamentous actin, targeting EFA6 to F-actin-enriched structures at the PM(Macia et al. 2008). The interaction with F-actin does not influence nucleotide exchange activity of EFA6(Macia et al. 2008). The expression of EFA6 induces rearrangements in the actin cytoskeleton and the formation of membrane ruffles by catalyzing GDP/GTP exchange on ARF6 and by activating RAC, respectively(Franco et al. 1999). EFA6 has been involved in the regulation of endocytic/recycling transport of different PM proteins like the TfR(Franco et al. 1999; Boulakirba et al. 2014), the ß2 adrenergic receptor(Macia et al. 2012) and the K^+ channel Twik1(Decressac et al. 2004). Recently, EFA6B and EFA6D have been shown to be involved in the regulation of ß1 integrin recycling. Indeed, their removal blocks the HGF-induced ß1 integrin recycling in endothelial cells, similar to ARF6 knockdown(Hongu et al. 2015).

EFA6 function has been linked to development and maintenance of cell polarity in epithelial cells by the Luton group(Luton et al. 2004; Klein et al. 2008; Theard et al. 2010): they showed that the expression of EFA6A in MDCK cells accelerates the de-novo formation of actin cytoskeleton and a functional tight junction (TJ)(Luton et al. 2004). Molecularly, EFA6 is recruited by E-cadherin and participates to the establishment of cell polarity by stabilizing the apical actin ring, which becomes the platform where TJ molecules are anchored(Luton et al. 2004). EFA6 effects depend on both its exchange activity by the SEC7 domain and its actin remodeling activity of the C-terminal domain. Also, active ARF6 participates in this process through the C-terminal domain of EFA6(Klein et al. 2008). Simultaneous expression of a constitutively active ARF6 mutant and the C-terminal of EFA6 mimic the modification induced by EFA6 full length during TJ assembly(Klein et al. 2008). The same group has also characterized a novel regulatory pathway for TJ formation involving EFA6 and its stabilization by the deubiquitinase USP9X(Theard et al. 2010): they found that, in MDCK cells, EFA6B levels are critical for the rate of TJ formation. In fact, EFA6 protein levels are maintained at steady state by its

constitutive ubiquitination and are augmented before TJ formation due to deubiquitination by USP9X. Moreover, USP9X is transiently localized at early cell-cell contact sites to allow the spatially and temporally regulated increase of EFA6B levels.

The mechanisms that regulate EFA6 activity are different from those that regulate cytohesin activity, whose PH domain is autoinhibitory and supports a positive feedback loop(Padovani et al. 2014). Recently, it has been demonstrated that the PH domain of EFA6 is not autoinhibitory but supports a negative feedback loop, which is regulated by the interaction of ARF6 GTP with the PH- and the C-terminal domains of EFA6(Padovani et al. 2014). Although previous studies found that EFA6 is not able to activate ARF1 *in vitro*, it was found to efficiently activate ARF1 in the presence of liposomes(Padovani et al. 2014).

More recent findings have highlighted a role for EFA6 GEFs in breast cancer(Zangari et al. 2014) and in clear cell renal cell carcinoma ccRCC(Hashimoto et al. 2016). In breast cancer, EFA6B has been shown to act as an antagonist at an early stage of development by preventing TJ disassembly and loss of epithelial polarity(Zangari et al. 2014). *In vivo* breast cancer analysis revealed that loss of EFA6B correlates with poor prognosis and associates with Triple Negative Breast Cancer (TNBC) and Claudin-low subtypes(Zangari et al. 2014). *In vitro*, EFA6B antagonizes TGFß-induced EMT and maintains the epithelial apico-basal polarity of mammary acini. Thus, EFA6B appears to be a potential tumor antagonist whose down-regulation may promote breast cancer progression(Zangari et al. 2014). In ccRCCs, LPA activates, through its GPCRs, ARF6 and EFA6 to sustain mesenchymal-type of invasion, metastasis and drug resistance. In this situation, all members of the EFA6 family, except for EFA6D, appear to be potential activators of ARF6 upon LPA stimulation to promote cell invasion. This function of EFA6 is mediated by interaction with the GTP-Gα12, a GPCR(Hashimoto et al. 2016).

3 AIM OF THE STUDY

Cells are able to respond to spatial information by adopting their cytoskeleton architecture and maintaining asymmetric and polarized distribution of molecules whose signaling outputs are spatially restricted. Thus, spatial restriction of signaling is a fundamental tool for the cell to perform a variety of processes, including directional cell migration, cell-fate decision, epithelia-cell polarization, growth cone movement, tissue morphogenesis during development, and tumor/cancer cell invasion into the surrounding tissues and metastasis (Disanza et al. 2009).

Endocytosis/recycling of membrane and membrane-bound proteins is a process strictly connected with signaling, controlling its intensity and its specificity by spatially confining signaling outputs where these occur.

During directional migration, polarized recycling of endosomes is required for the maintenance of cell polarity during cell migration. A similar mechanism is also required for the generation of different kinds of migratory protrusions induced upon receptor tyrosine kinase RTK stimulation, such as Peripheral Ruffles (PRs) and CDRs(Buccione, Orth, and McNiven 2004). To find out novel endocytic/trafficking proteins involved in directional cell migration, we performed an RNAi screening using PRs and CDRs as readout markers. We found that the endocytic adaptor protein NUMB is as a negative regulator of CDR formation but does not affect PR formation.

The protein NUMB is a cell fate determinant and acts as a tumor suppressor. Indeed, loss of NUMB occurs in about 50% of all breast tumors(Pece et al. 2004) and in 30% of all lung cancers(Westhoff et al. 2009), and correlates with a decreased activity of p53, and/or an increased activation of NOTCH(Pece et al. 2004; Westhoff et al. 2009). As an endocytic adaptor protein, NUMB interacts with key players of the CME via its NPF and DPF motives, which mediate the association with EHD containing proteins, such as Eps15, and α adaptin, a subunit of the AP2 complex, respectively(Santolini et al. 2000). NUMB also

localizes in recycling endosomes where it controls the delivery of cargos back to the PM in various organisms(Smith et al. 2004; Nilsson et al. 2008; Nilsson, Jonsson, and Tuck 2011; McGill et al. 2009; Rasin et al. 2007). Consistently, the *C. Elegans* and *Drosophila* NUMB homologs are negative regulators of membrane recycling(Nilsson et al. 2008; Nilsson, Jonsson, and Tuck 2011; Cotton, Benhra, and Le Borgne 2013; Couturier, Mazouni, and Schweisguth 2013). In mammalian cells, NUMB was shown to regulate post-endocytic sorting of NOTCH-1(McGill et al. 2009). Finally, NUMB and EHD-containing proteins are physically localized in recycling vesicles containing the ARF6 GTPase(Smith et al. 2004). The molecular mechanism by which NUMB acts in the recycling pathway has not been clarified yet.

Based on results from our laboratory that demonstrate that NUMB is a negative regulator of CDRs (unpublished data), whose formation requires endocytic trafficking of RAC via ARF6(Palamidessi et al. 2008), and that NUMB functions in the recycling compartment are ill-defined, the main aim of this thesis was to further characterize the molecular mechanism beyond this novel NUMB function.

Since CDRs are sites of fluid phase endocytosis and necessary for cell migration within a 3D matrix(Buccione, Orth, and McNiven 2004), we aimed to clarify the link between the endocytic functions of NUMB and its tumor suppressor role using a mechanistic approach. Indeed, NUMB may control recycling of key cargos, the fate of which may regulate cell signaling, leading to the acquisition of migratory and invasive phenotypes of tumor cells. Our approach will, thus, allow us to understand how NUMB is involved in growth factor-dependent mesenchymal cell motility and how this affects the tumor suppressive role of NUMB. Our studies have shed light on how loss of NUMB contributes to the combined disruption of pathways that regulate both stem cell homeostasis and cell motility, favoring, thus, the generation of tumors with an aggressive phenotype.

4 RESULTS

4.1 NUMB is a negative regulator of CDR formation downstream growth factor activation

Growth factor-induced CDRs represent a surrogate marker preceding the acquisition of mesenchymal mode of cell migration(Palamidessi et al. 2008). CDRs structures are an "easy-to-follow read out" that can be detected through low-magnification phase-contrast time-lapse microscopy(Palamidessi et al. 2008). It has been demonstrated that a tripartite signaling cascade, originating from RAB5, PI3K, and RAC, must simultaneously operate to allow the formation of CDRs(Lanzetti et al. 2004). In epithelial cells, the ectopic expression of RAB5 activates RAC in a Dynamin-dependent manner and induces CDRs. Additionally, inhibition of CME and interference with recycling abrogates HGF-, and RAB5-induced CDRs formation(Palamidessi et al. 2008). Collectively, these results demonstrate that RAB5, by controlling the endo-/exocytic cycles (EEC) of RAC, spatially restricts RAC signaling, generating the formation of polarized, migratory protrusions(Palamidessi et al. 2008).

In order to assess the impact of endocytic/trafficking proteins on mesenchymal mode of motility in a 2D environment, an RNAi screening was set up and CDRs and PRs were used as read-out markers. First, we confirm that blocking of CME by clathrin and dynamin RNAi blocks CDRs formation(Palamidessi et al. 2008; Frittoli et al. 2014) (Tab. 2). As previously demonstrated, in absence of RAB5, RAC and TIAM neither CDRs nor PRs are formed (Tab. 2)(Frittoli et al. 2014; Palamidessi et al. 2008). Among all the candidates, we noticed the removal of the endocytic adaptor NUMB, Caveolin-1 and the F-BAR containing proteins Toca1/FBP1/CIP4 increase CDRs formation, while does not impairs PRs formation (Tab. 2). Since NUMB is one of the main focus of our research group, we decided to further investigate this novel function of NUMB. To begin, we confirmed that

NUMB is a negative regulator of CDR formation downstream of C-Met activation in HeLa cells by its transient silencing with four independent oligos (Fig. 13).

RNAi gene	Circular dorsal ruffles (CDRs)	Peripheral ruffles (PR)
Dynamin	Inhibited	Inhibited
Clathrin	Inhibited	Inhibited
Caveolin-1	Increased	Unchanged
Eps15/Eps15r	Unchanged	Unchanged
AP-2	Inhibited	Inhibited
Rab5	Inhibited	Inhibited
Numb	Increased	Unchanged
Toca1/FBP1/CIP4	Increased	Unchanged
Arf6	Inhibited	Inhibited
Rab35	Inhibited	Inhibited
Rab4	Unchanged	Unchanged
Rab11	Unchanged	Unchanged
Rab43	Unchanged	Unchanged
Rab30	Unchanged	Unchanged
Exo70	Unchanged	Unchanged
Tiam-1	Inhibited	Inhibited
Sos-1	Inhibited	Unchanged
Rac	Inhibited	Inhibited
Cdc42	Inhibited	Unchanged
Abi-1	Inhibited	Inhibited
WAVE2	Inhibited	Inhibited
N-WASP	Unchanged	Unchanged
Eps8	Unchanged	Unchanged
IRSp53	Reduced	Unchanged
ß1	Unchanged	Unchanged

Table 2. RNAi screening of endocytic/trafficking proteins affecting RTK-induced CDRs and PRs. Analysis of CDR and PR formation upon stimulation with motogenic factors (such as HGF and/or EGF) of HeLa cells. (See Materials and Methods for a detailed description of the experimental settings.)

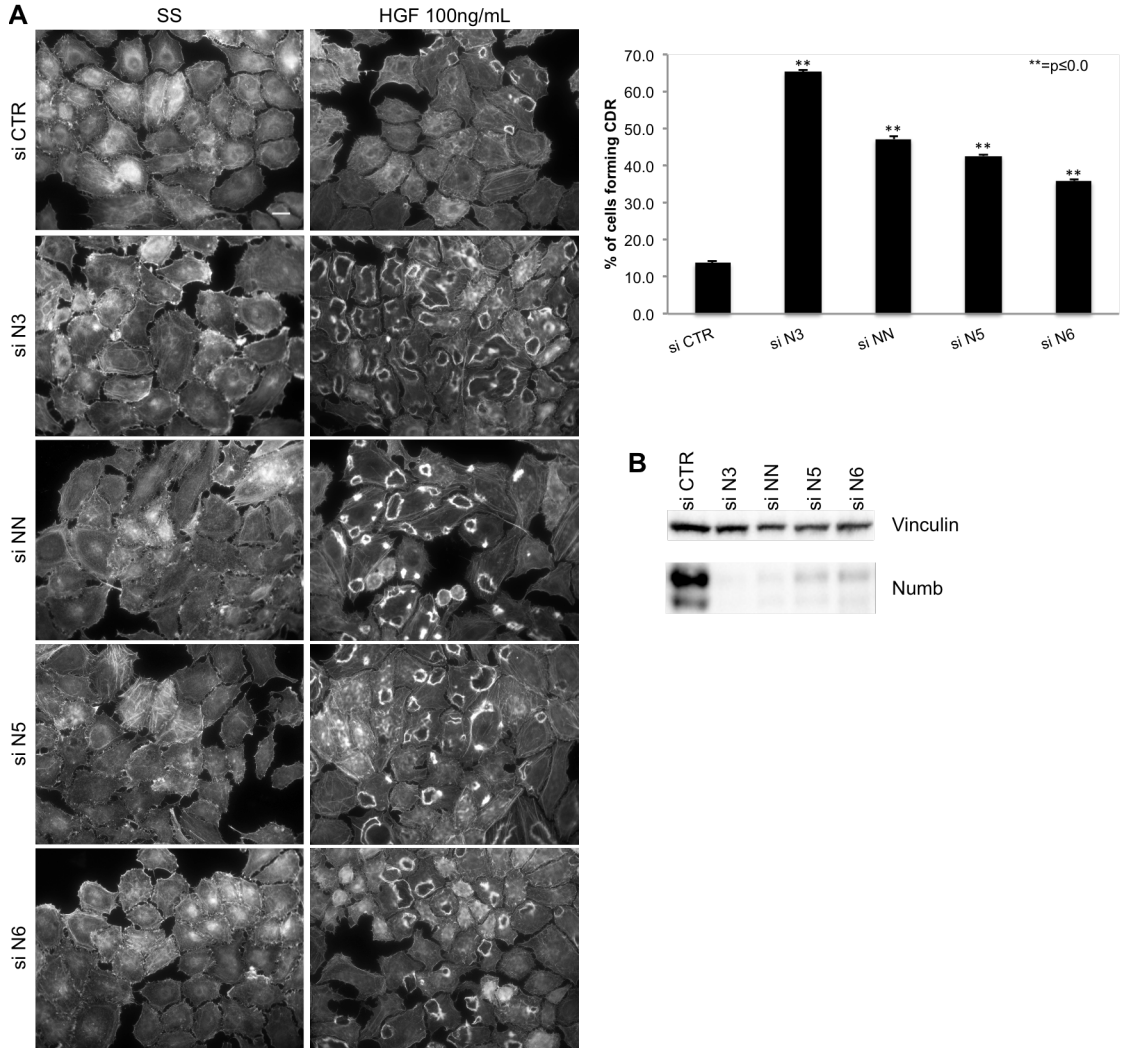

Figure 13. Silencing of NUMB increases HGF-induced CDR formation.
A. HeLa cells transfected with four different siRNA (N3, NN, N5, N6) against NUMB or scramble oligo (si CTR) as control were seeded on matrigel-coated coverslips. After 48 hours, cells were serum starved (SS) for 2 hours stimulated with 100 ng/mL HGF for 4 minutes, fixed and stained with F-actin antibody. Scale bar: 20 µm. Right panel: the number of cells forming CDR over the total number of cells per field. At least 20 fields were analyzed in each condition and three independent experiments were performed. Representative images are shown. The data are presented as the mean ± SEM (Standard Error of the Mean).
B. The expression levels of NUMB and vinculin were analyzed by immunoblotting (IB). Molecular Weight (MW) markers are shown on the left of the blots.

To strengthen the notion that NUMB acts downstream the activation of an RTKs, such as C-Met, and negatively regulates CDR formation, Mouse Embryonic Fibroblasts (MEFs), a very well characterized system for CDR formation upon PDGF receptor activation(Buccione, Orth, and McNiven 2004), were employed. NUMB ablation by transient RNAi in this cellular system increases the number of cells forming CDRs upon PDGF stimulation (Fig. 14). These results confirm that NUMB is indeed a negative regulator of CDR formation downstream C-Met and PDGFR activation.

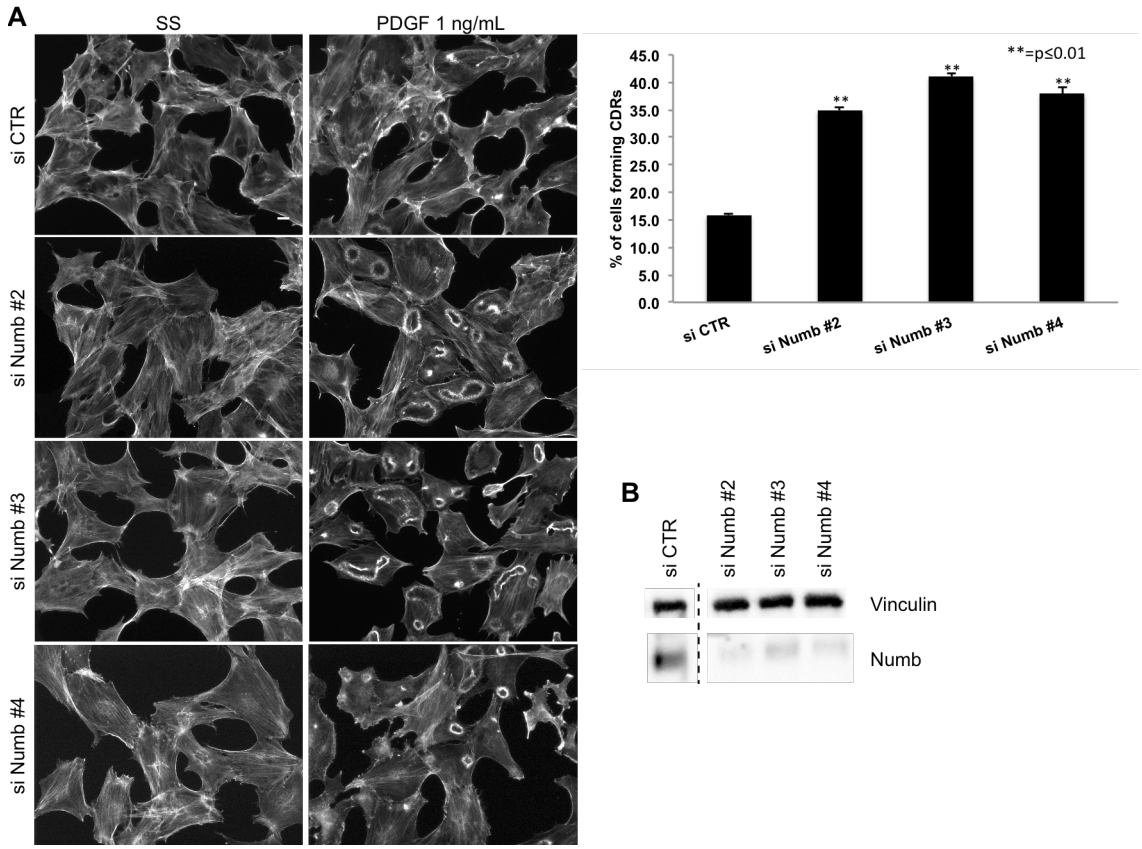

Figure 14. Silencing of NUMB increases PDGF-induced CDR formation.
A. MEF cells transfected with three different siRNA (Numb #2, Numb #3, Numb #4) against NUMB or scramble oligo (si CTR) as control were seeded on gelatin-coated coverslips. After 24 hours, cells were serum starved (SS) for 2 hours, stimulated with 1 ng/mL PDGF for 8 minutes, fixed and stained with F-actin antibody. Scale bar: 20 µm. Right panel: the number of cells forming CDR over the total number of cells per field. At least 20 fields were in analyzed in each condition and three independent experiments were performed. Representative images are shown. The data are the mean ± SEM.
B. The expression level of NUMB and vinculin were analyzed by IB. MW markers are shown on the left of the blots.

4.2 Re-expression of NUMB in MEF cells rescues CDR formation

The mammalian *Numb* gene is transcribed in 4 different splicing variants due to the alternate splicing of two exons, one in the PTB domain and another in the C-terminal region(Verdi et al. 1999) (see section 2.2.1).

All isoforms were silenced by RNAi with the oligos described above (Fig. 13 and 14). To investigate whether all four isoforms share the same function on CDR formation, MEFs interfered for NUMB were transfected either with GFP empty vector (control) or with the four GFP-fused human NUMB isoforms. Our results showed that all four NUMB human isoforms, when expressed, were able to revert the increase in CDR formation due to

endogenous NUMB ablation (Fig. 15), once again confirming that NUMB is a negative regulator of these migratory protrusions.

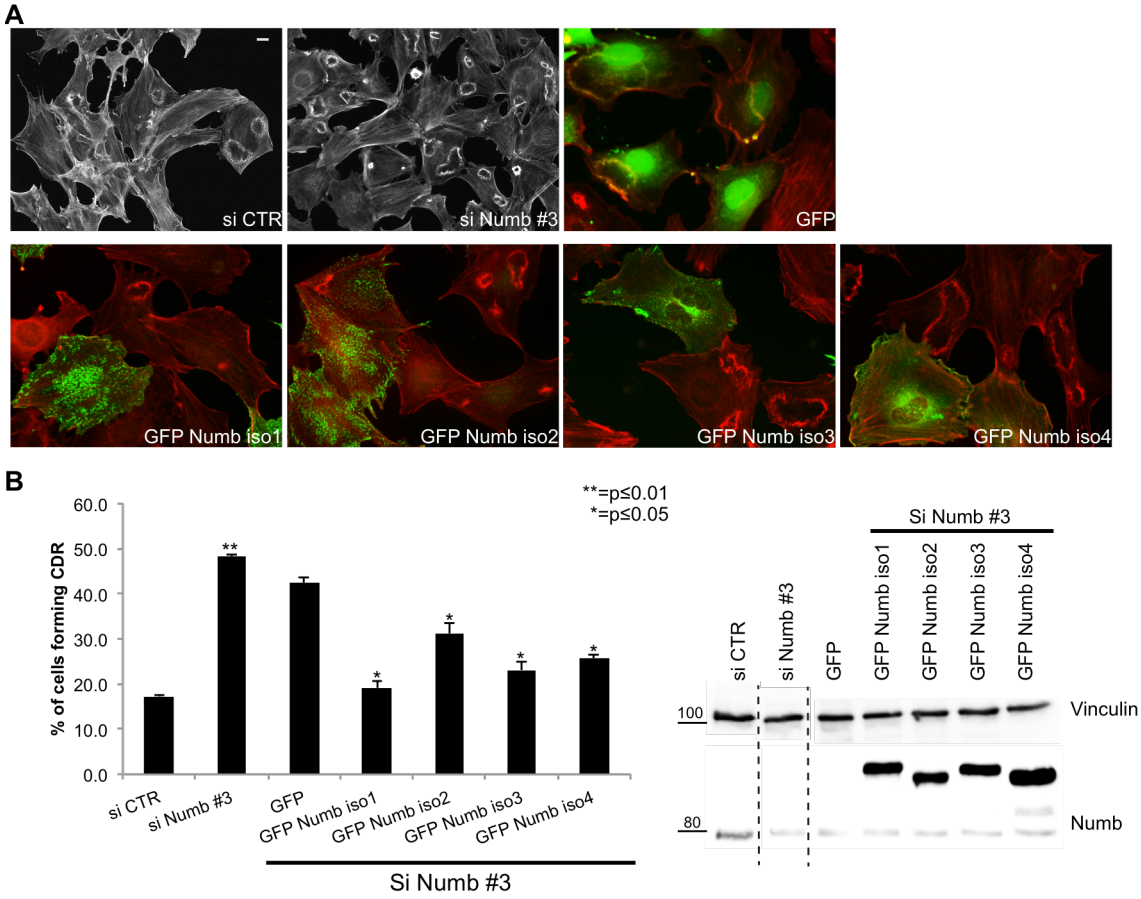

Figure 15. Re-expression of NUMB in MEF cells rescues CDR formation.
A. MEF cells interfered with a scramble oligo (siCTR) as control, or with siRNA against NUMB (Numb #3, upper panels), or interfered with siRNA against NUMB (Numb #3) and transfected with GFP empty vector or GFP-NUMB isoform 1, 2, 3 and 4 (upper-lower panels) were seeded on gelatin-coated coverslips. After 24 hours, cells were serum starved (ss) for 2 hours, and stimulated with 1 ng/mL PDGF for 8 minutes, fixed and processed for epifluorescence to visualize GFP or GFP–NMB (green, where indicated) and stained with F-actin antibody (red). Scale bar: 20 µm (10 µm in GFP or GFP-NUMB panels).
B. Left panel. The percentage of cells forming CDR over the total number of cells per field was counted. At least 20 fields were analyzed in each condition and three independent experiments were performed. Representative images are shown. The data are presented as the mean ± SEM. Right panel. The expression levels of NUMB and vinculin were analyzed by IB. MW markers are shown on the left of the blots.

4.3 NUMB is a negative regulator of HGF-induced cell migration and invasion

CDR formation correlates with mesenchymal migration(Palamidessi et al. 2008). We investigated whether NUMB could have an impact on cell migration in 2D and 3D cell cultures upon growth factor-induced stimulation of RTKs, for assessment of cell migration and invasion, respectively. NUMB RNAi resulted in an increased cell elongation index (a

ratio between the major axis and the minor axis), which directly correlates with mesenchymal cell locomotion(Palamidessi et al. 2008), and was accompanied by a concomitant increase in the migration and in the velocity of NUMB depleted cells compared to control cells (Fig. 16).

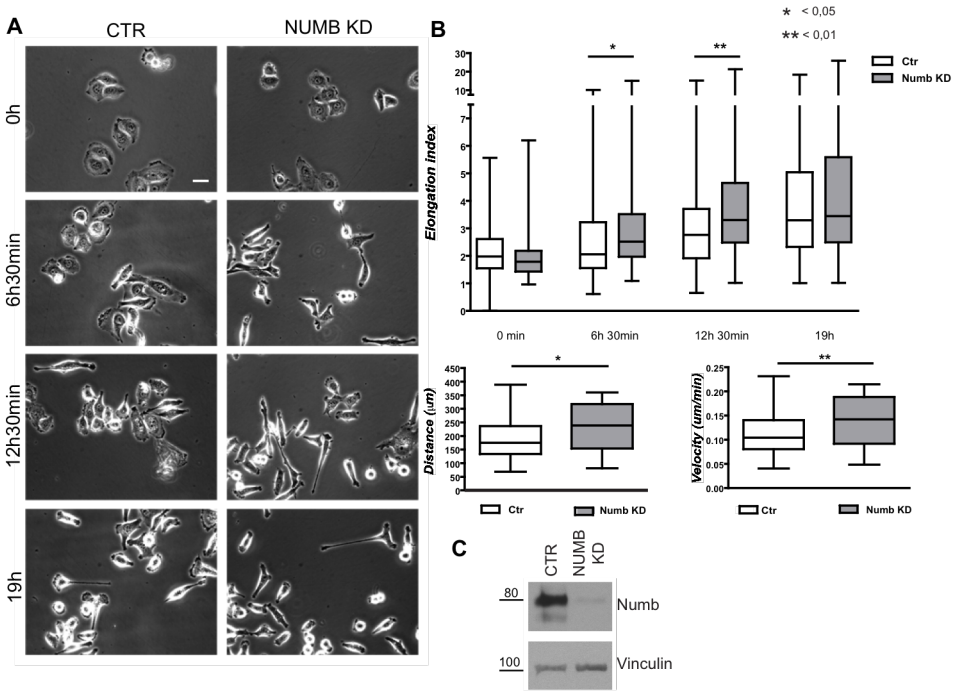

Figure 16. Silencing of NUMB promotes HGF induced cell migration.
A. HeLa cells were transfected with a siRNA against NUMB (Numb KD) or scramble oligo (si CTR) as control. After 48 hours, cells were serum starved (ss) for 2 hours, stimulated with 100 ng/mL HGF and analyzed by time-lapse microscopy for 19 hours. Representative images for each condition at specific time points (0h, 6h30min, 12h30min, 19h) are shown. Scale bar: 20 µm
B. Upper panel. Elongation index (ratio between the major and the minor axis) was quantified for each condition at the indicated time points. Lower panels. Total distance accumulated by cells (left graph) and mean velocity (right panel) were measured. The analysis was conducted on at least 30 single cells/experiment of three independent experiments. The data are presented as the mean ± SEM.
C. The expression levels of NUMB and vinculin were analyzed by IB. MW markers are shown on the left of the blots.

We next investigated the role of NUMB in cell motility in a 3D matrix. Matrigel-coated boyden chambers were employed and HGF was used as chemoattractant. We found that removal of NUMB by siRNA promoted cell invasion (Fig. 17). Collectively, these observations support the notion that NUMB acts as a negative regulator of c-MET-induced mesenchymal motility. Accordingly, NUMB has recently been shown to control ill-defined recycling pathways, which is in turn necessary for the integrity of adherent junctions and for the acquisition of migratory properties and EMT features(Wang et al. 2009).

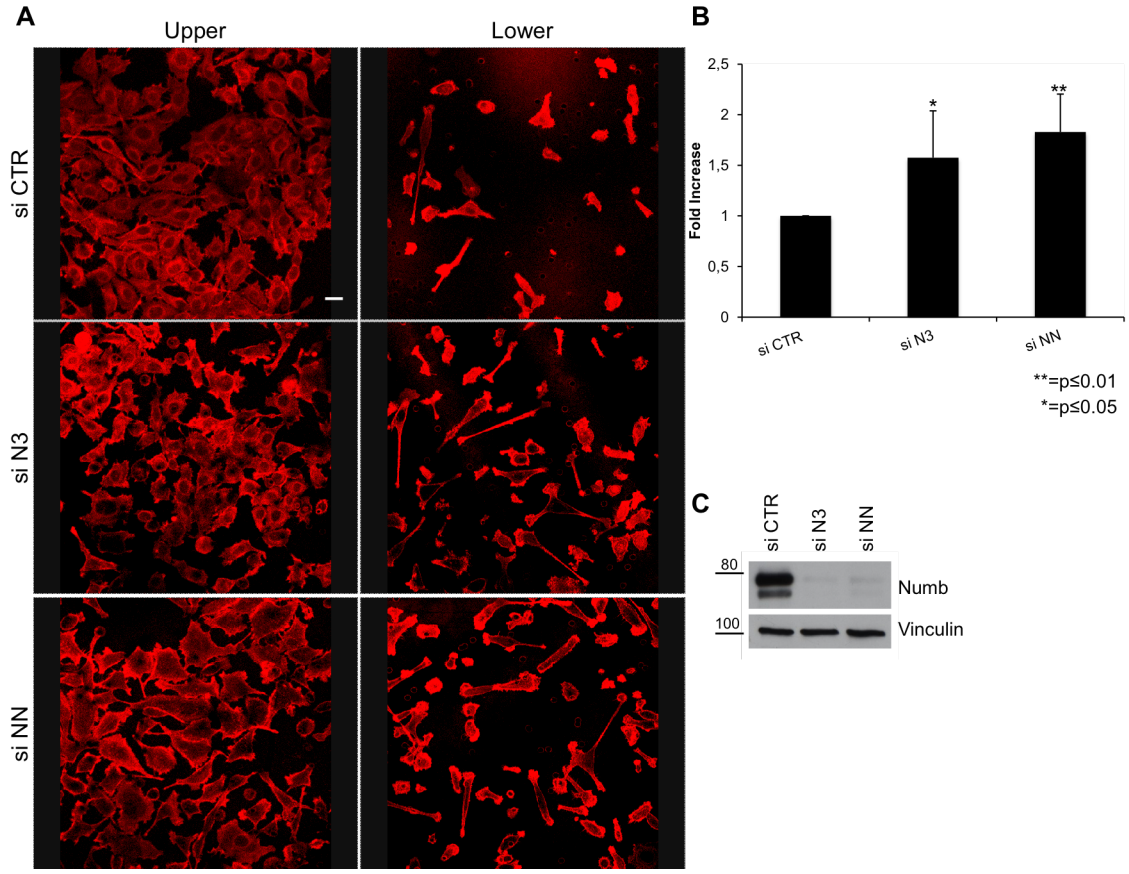

Figure 17. Silencing of NUMB promotes HGF-induced cell invasion.
A. HeLa cells transfected with siRNA against NUMB (si N3, si NN) or scramble oligo (si CTR) as control were seeded on matrigel-coated chambers. 100 ng/ml HGF was added in the lower chamber to generate a chemo-attractive gradient. After 24 hours, cells were fixed, stained with rodhamine phalloidin antibody to detect actin and analyzed by confocal microscopy. Representative images of upper, non-invasive cells (left panels) and lower, invasive cells (right panel) are shown. Scale bar: 40 μm.
B. Quantification of the number of cells passing through the semi-permeable membrane is shown as fold increase compared to control cells. At least 10 fields were analyzed for each condition. The data are presented as the mean ± SEM. from three independent experiments.
C. The expression levels of NUMB and vinculin were analyzed by IB. MW markers are shown on the left of the blots.

4.4 NUMB localized in RAB5/ARF6 induced enlarged endosomes

The small GTPase RAB5 is a key regulator of CDR formation(Lanzetti et al. 2004; Palamidessi et al. 2008). RAB5 controls endocytic/endosomal dynamics and is activated upon ligand-bound RTKs, leading to the trafficking of RAC1 and its GEF TIAM1 to early endosomal compartments via CME(Palamidessi et al. 2008). There, RAC1 undergoes activation and is recycled back to specific region of the PM, via ARF6, where it promotes CDR formation(Palamidessi et al. 2008). Since NUMB, as an endocytic protein, localizes in the recycling compartment(Smith et al. 2004) and is emerging as a negative regulator of recycling in *C. Elegans*(Nilsson et al. 2008; Nilsson, Jonsson, and Tuck 2011) and

Drosophila(Cotton, Benhra, and Le Borgne 2013; Couturier, Mazouni, and Schweisguth 2013), one possibility is that NUMB may have an impact on the ARF6-dependent recycling pathway of RAC1 to the PM. We therefore assessed the subcellular localization of NUMB, focusing our attention on the EE and on the ARF6 recycling compartment. We found that NUMB is enriched in EE when induced by RAB5 ectopic expression (Fig. 18A), and in enlarged endosomes when induced by the expression of dominant active ARF6 (ARF6 Q67L) (Fig. 18B).

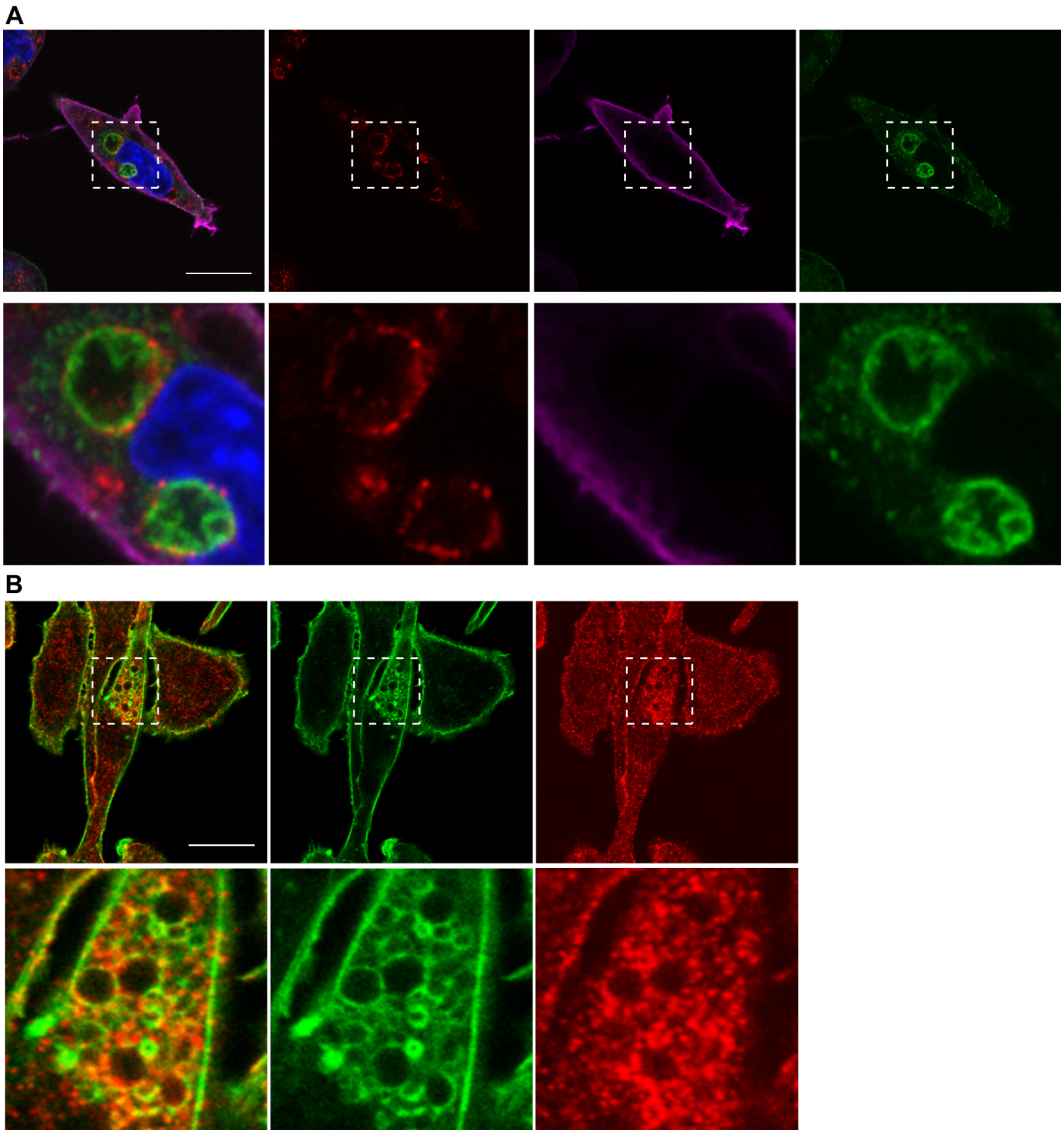

Figure 18. NUMB is enriched in RAB5/ARF6 induced enlarged endosome.
A. Upper panels: confocal analysis of HeLa cells transfected with Rab5. 24 hours after transfection, cells were fixed and stained with EEA1 (red), RAB5 (magenta) and NUMB (green) specific antibodies to visualize Rab5-induced enlarged endosomes and Numb localization. Scale bar: 20 µm
Lower panels: 4X magnification of the selected area.
B. Upper panels: confocal analysis of HeLa cells transfected with ARF6 Q67L. 24 hours after transfection, cells were fixed and stained with F-actin (green) or Numb (red) specific antibodies to visualize ARF6-induced enlarged endosomes and NUMB localization. Scale bar: 20 µm.
Lower panels: 4X magnification of the selected area.

4.5 NUMB is a negative regulator of ARF6-dependent recycling pathway

To study whether the localization of NUMB in enlarged endosomes, induced by ARF6, has a functional role, we decided to investigate if removal NUMB has an impact on the recycling of cargos routed back to the PM specifically via ARF6, like MHC class I(Schweitzer, Sedgwick, and D'Souza-Schorey 2011). We found that depletion of NUMB increases the rate of recycling of MHC class I (Fig. 19).

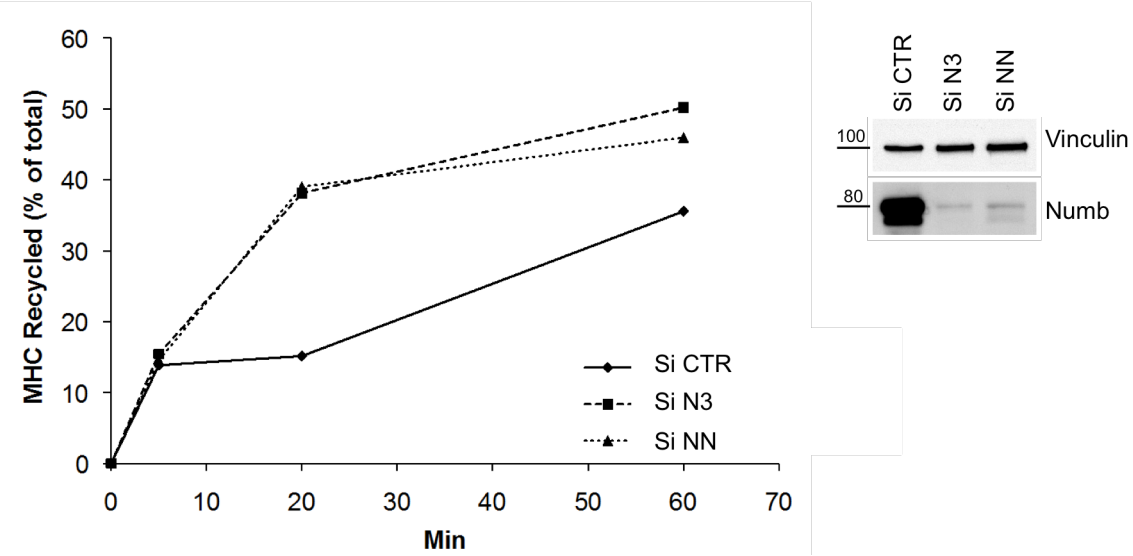

Figure 19. NUMB negatively regulates MHC I, ARF6 dependent recycling.
Left panel: FACS analysis. HeLa cells were transfected with siRNA against NUMB (si N3, si NN) or scramble oligo (si CTR). 48 hours after transfection, cells were incubated with MHC-I specific antibody for 3 hours at 16˚C to allow internalization and avoid recycling and to allow the binding of the antibody to the cell surface. Finally, cells were stripped with acid wash (pH 2,5) and analyzed directly (t=0) or released at 37˚C for 5, 20 and 60 minutes and then analyzed by FACS using MHC-I specific antibody to detect the amount of MHC-I recycled back to the cell surface. The assay was repeated three times and representative data of a single experiment are shown.
Right panel. The expression levels of NUMB and vinculin were analyzed by IB. MW markers are shown on the left of the blots.

The formation of CDRs requires the recycling of active RAC1 back to the PM via ARF6(Palamidessi et al. 2008). We therefore investigated whether NUMB has an impact on this critical step. We observed that ectopic expression of NUMB strongly decreased RAC1 recycling compared to control cells (Fig. 20). These data, together, demonstrate that NUMB is a negative regulator of ARF6-dependent recycling pathway.

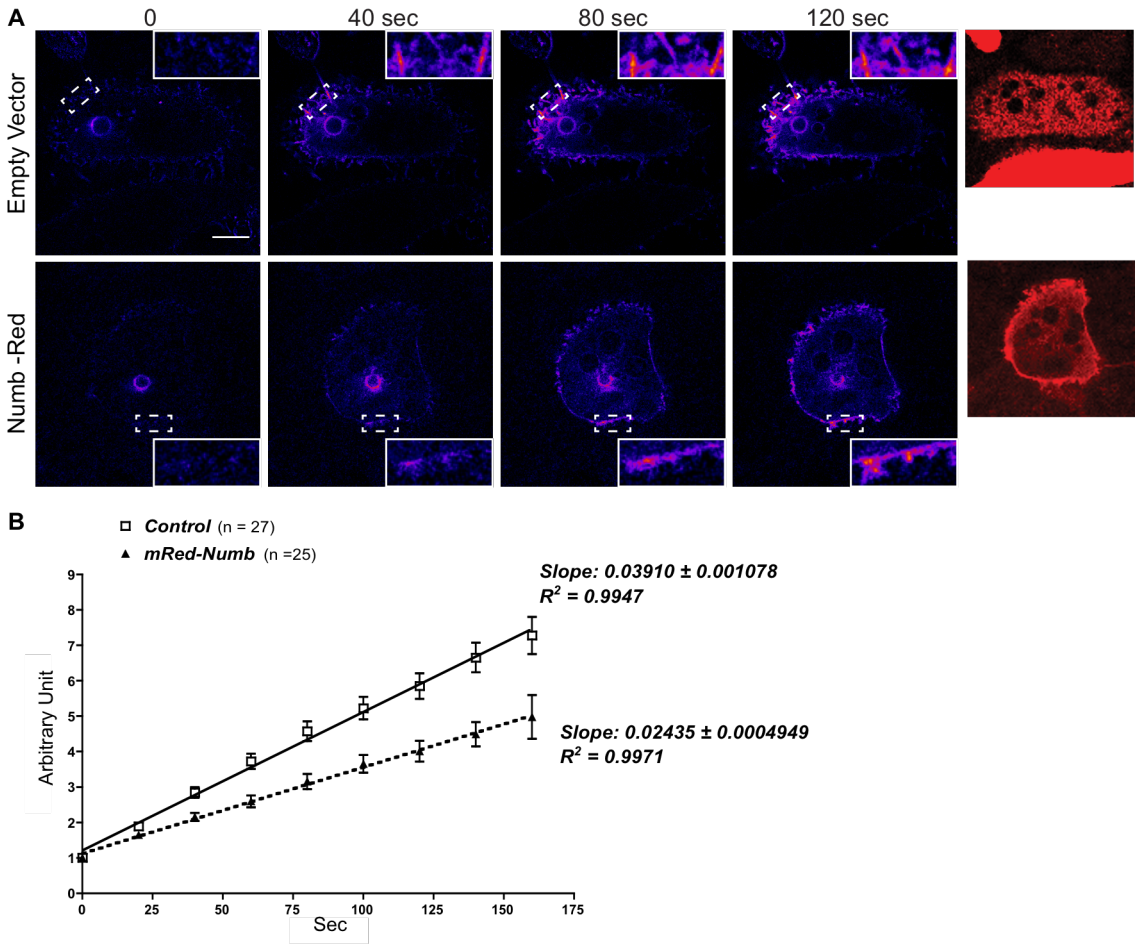

Figure 20. NUMB negatively regulates RAC-1, ARF6 dependent recycling.
A. HeLa cells were co-transfected with paGFP RAC and Numb Red or empty vector. paGFP barely absorbs 488 nm light in its native form, thereby exhibiting a weak fluorescence emission. Focal plane-restricted, multiphoton-induced photoactivation of paGFP-RAC was achieved by exciting the area corresponding to a vesicle. Images were then collected every 20 seconds (exciting fluorescence at 488 nm). Right panels: Numb Red epifluorescence images are shown. Scale bar: 10 µm.
B. The increase in fluorescence over time in a target region of the PM adjacent to the photoactivable vesicle. The data are presented as the mean ± SEM of 27 and 25 events counted for the empty vector (control) and NUMB (mRed-Numb) transfected cells, respectively.

4.6 NUMB binds to EFA6 B, a GEF for ARF6

Like all small GTPases, ARF6 cycles between its active-GTP-bound and its inactive-GDP-bound conformations(Donaldson and Jackson 2011b). Guanine nucleotide exchange factors, GEFs, activate ARF6 by mediating exchange of GTP for GDP, whereas GTPase activating proteins, GAPs, down-regulate ARF6 activity through hydrolysis of GTP to GDP(Donaldson and Jackson 2011b). Since GEFs are the primary regulatory target of small GTPases(Donaldson and Jackson 2011b), we investigated whether NUMB could interact with a GEF for ARF6. Among all GEFs for ARF6, we focused our attention on

those that have been reported to control actin remodeling (see section 2.3.2), in particular on the EFA6 A-D and Cytohesin family of GEFs. These two subfamilies have been reported to control actin remodeling(Casanova 2007b; Gillingham and Munro 2007), which is required for the formation of CDRs and cell migration(Hoon, Wong, and Koh 2012). We tested which of these GEFs are expressed in our experimental model systems (HeLa and MEF cells) by qPCR analysis. We found that all Cytohesin (ARNO) family members are present, while only EFA6B and EFA6D are expressed in our model systems (Tab. 2).

GENE	CT	GAPDH
EFA6A	34.7	18.0
EFA6C	not detectable	18.0
EFA6D	27.6	18.0
EFA6B	29.9	18.0
Cytohesin 1	26.9	19.5
Cytohesin 2	26.9	19.5
Cytohesin 3	27.8	19.5

GENE	CT	GAPDH
EFA6A	33.5	18.2
EFA6C	34.5	18.2
EFA6D	28.3	18.2
EFA6B	31.8	18.2
Cytohesin 1	28.3	18.2
Cytohesin 2	26.5	18.2
Cytohesin 3	25.5	18.2

Table 3. q-PCR Analysis of mRNA levels of EFA6 and Cytohesin family members.
Left table: HeLa cells.
Right table: MEF cells.

To test which of these GEFs may bind NUMB we performed a pull-down assay. We found that EFA6 B, but not EFA6D and ARNO, is able to bind NUMB via its PTB domain (Fig. 21).

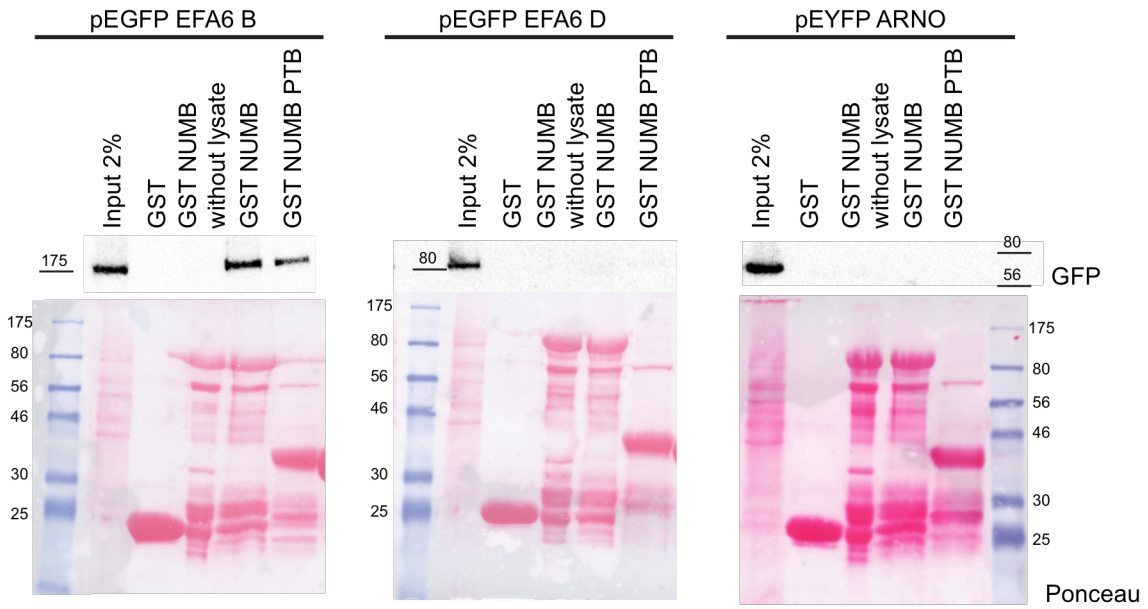

Figure 21. NUMB interacts with EFA6B.
Lysates (2.5 mg) from Phoenix cells transfected with pEGFP EFA6B, pEGFP EFA6D or pEYFP ARNO were incubated with 0.5 µM GST, GST NUMB, or GST-NUMB PTB domain immobilized on beads as indicated. Input lysates (2% of the total) and bound material were analyzed by IB with anti-GFP to visualize EFA6B, EFA6 D and ARNO or by Ponceau staining to detect the recombinant GST proteins. GST-NUMB was incubated either with cell lysate or with lysis buffer to evaluate any possible IB non-specific signal. MW markers are shown on the left of the blots.

To investigate if the NUMB C-terminal region is involved in the interaction, we then performed a pull-down assay, using two NUMB constructs that cover this region, the Proline Reach Region 1 (PRR1) and the Proline Reach Region 2 (PRR2), respectively, as a bait (Fig. 22A). Our results confirmed that only EFA6B interacts with the NUMB PTB domain (Fig 22B).

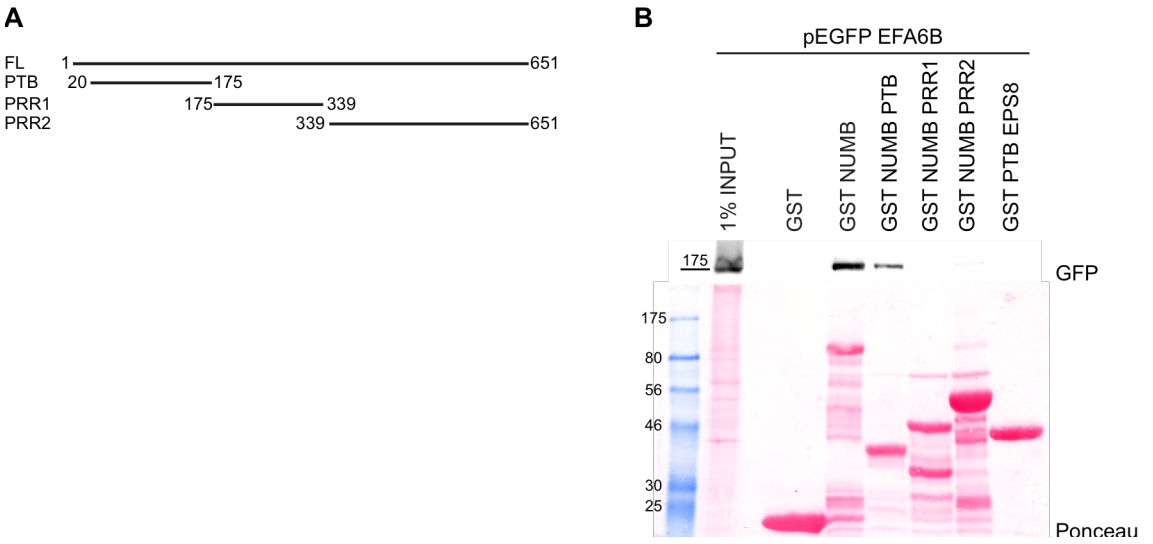

Figure 22. EFA6B interacts with NUMB PTB.
A. Schematic representation of NUMB deletion fragments.
B. Lysate (2.5 mg) from Phoenix cells transfected with pEGFP EFA6B was incubated with 0.5 µM GST, GST NUMB FL, GST NUMB PTB (20-175 aa), GST NUMB PRR1 (175-339aa), or GST NUMB PRR2 (339-651aa) immobilized on beads as indicated. Input lysates (1% of the total) and bound material were analyzed by IB with anti-GFP to visualize EFA6B, EFA6 D and ARNO or by Ponceau staining to detect the recombinant GST proteins. MW marker is shown on the left of the blot.

To detect *in situ* protein:protein interactions(Soderberg et al. 2006), HeLa cells expressing NUMB-FLAG and EFA6B-GFP or NUMB-FLAG and GFP (control) were analyzed by proximity ligation approaches (see Materials and Methods for details). We were able to score proximity ligation signal in 30% of NUMB-FLAG and EFA6B-GFP co-transfected cells, while only 3% of NUMB-FLAG and GFP control cells were positive (Fig. 23). Additional negative controls, HeLa cells expressing only NUMB-FLAG or EFA6B-GFP, or both NUMB-FLAG and EFA6B-GFP processed without primary antibodies, were analyzed by proximity ligation but did not result in any signal.

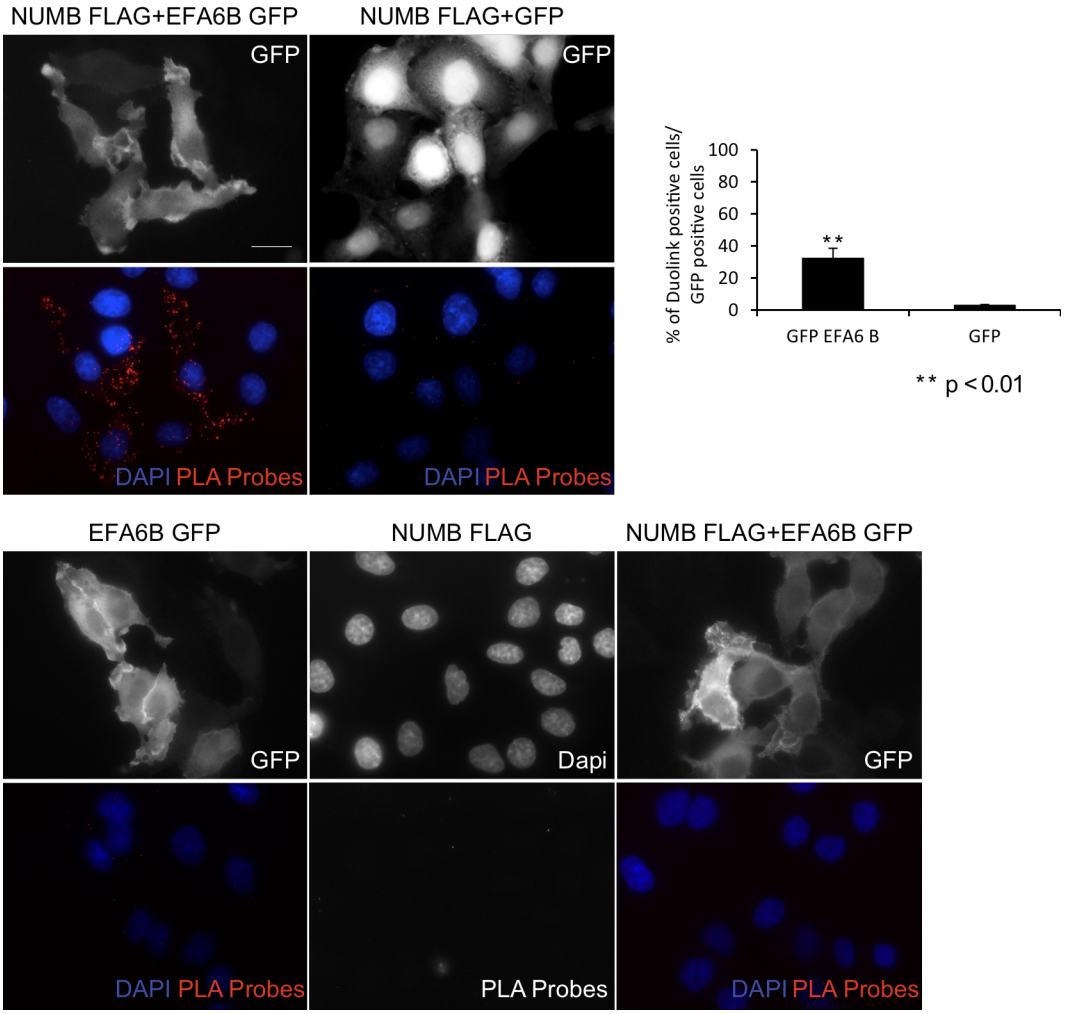

Figure 23. *In situ* protein:protein interactions between NUMB and EFA6B.
Upper, left panel: HeLa cells co-transfected with NUMB-FLAG and EFA6B-GFP or GFP alone (control) were fixed and stained with anti-FLAG monoclonal and anti-GFP polyclonal antibodies. The signals were detected by Duolink® 30 Detection Kit 613 (red), and the nuclei were counterstained with DAPI (blue). Red dots represent the detection of protein-protein interaction.
Upper, right panel: quantification of Duolink positive cells over the total number of GFP positive cells. Three independent experiments were performed and at least 100 cells were counted for each condition. The data are presented as the mean ± SEM.
Lower, left and middle panel: HeLa cells transfected with NUMB-FLAG and EFA6B were fixed and stained with anti-FLAG monoclonal and anti-GFP polyclonal antibodies. The signals were detected by Duolink® 30 Detection Kit 613 (red), and the nuclei were counterstained with DAPI (blue).
Lower, right panel: HeLa cells co-transfected with NUMB-FLAG and EFA6B-GFP were fixed and directly processed with Duolink® 30 Detection Kit 613 (red). The nuclei were counterstained with DAPI (blue). Scale bar: 20 µm.

To verify if the interaction between NUMB and EFA6B is regulated by growth factors, we performed Co-IP experiments. 293T cells were transfected with GFP-EFA6B and NUMB-FLAG or an empty vector as a control and stimulated or not with growth factors. The expression of NUMB-FLAG resulted in FLAG immunoprecipitates containing EFA6B (Fig. 24) and the interaction is not modulated by growth factors, as shown by equal level of

EFA6B with or without growth factors stimulation by IB analysis. Of note, the efficacy of growth factors stimulation was confirmed by the activation of downstream pathways.

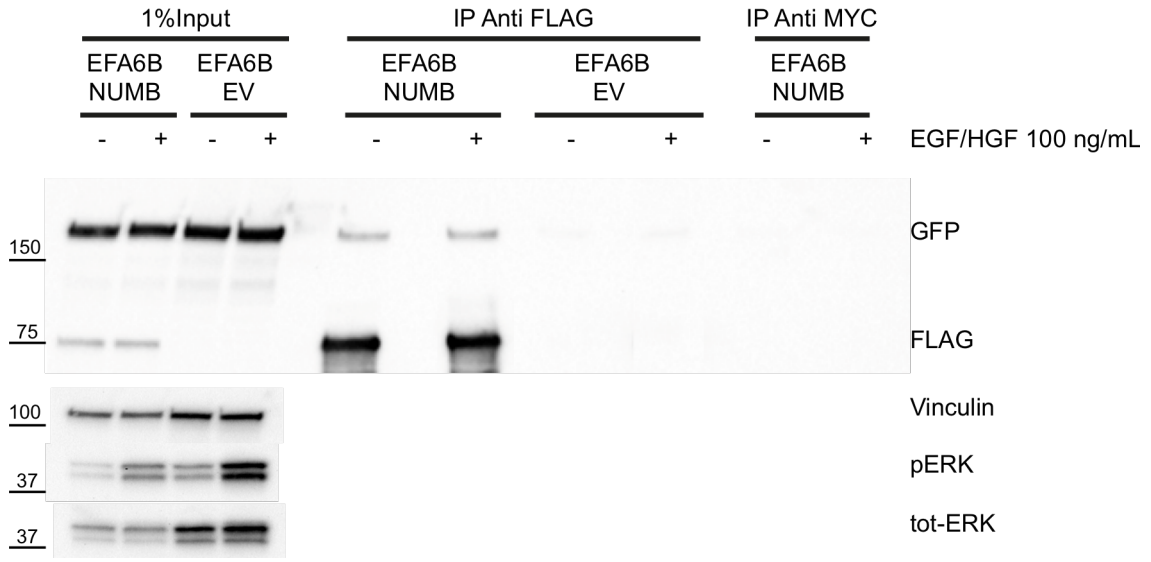

Figure 24. The interaction between NUMB and EFA6B is not modulated by growth factor stimulation.
Phoenix cells transfected with GFP-EFA6B and NUMB-FLAG or an EV-FLAG (control) were serum starved for 4 hours (-) and stimulated for 5 minutes with 100 ng/mL HGF and EGF**.** 1.5 mg of total cell lysate for each condition were immunoprecipitated with anti-FLAG M2 affinity gel (2 rounds with 15 µL) or anti-MYC as control. Inputs (1%) and immunoprecipitates were analyzed by Western blot (WB) analysis and IB with indicated antibodies. MW markers are shown on the left of the blots.

Finally, to test if the interaction between NUMB and EFA6B is direct, we performed a pull-down assay employing recombinant purified proteins. Our results indicate that EFA6B binds directly to NUMB, as shown by IB (Fig. 25). These results support the notion that NUMB may regulate ARF6-dependent recycling by binding and possibly modulating its GEF EFA6B.

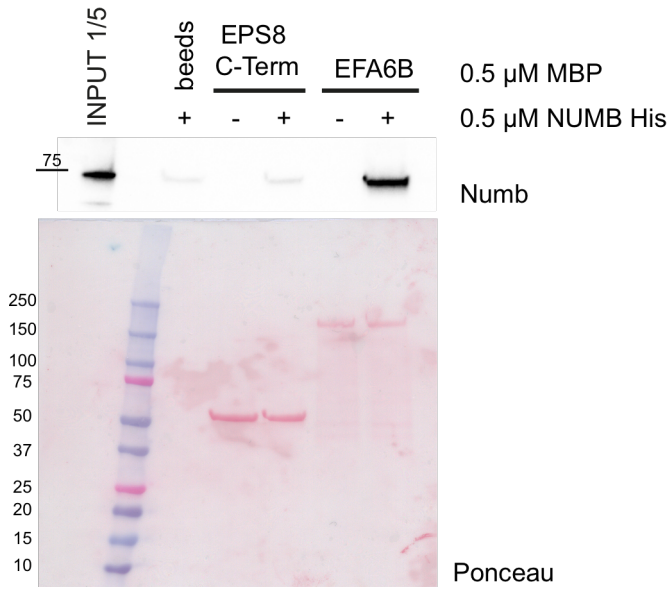

Figure 25. EFA6B binds to NUMB.
Purified NUMB-His at 0.5 µM was incubated or not with 0.5 µM MBP EPS8 C-terminal or MBP EFA6B immobilized on beads as indicated. Input (1/5) and bound material were analyzed by IB with anti-Numb to visualize NUMB or Ponceau staining to detect MBP recombinant protein. MW markers are shown on the left of the blot.

4.7 The N-terminal domain and the C-terminal domains of EFA6B are required for the interaction with NUMB

The most conserved element in the EFA6 family is the C-terminal region, which contains a SEC7 domain flanked by a PH domain, followed by a ~150 amino-acid region carrying a putative coiled-coil motif (Fig. 26A)(Derrien et al. 2002). Additionally, among the members of the EFA6 family, EFA6B contains a long N-terminal region. To identify the EFA6B regions required for the interaction with NUMB, we generated different deletion constructs (Fig. 26A) and tested them in a pull-down assay using GST-NUMB as bait or GST alone as a control. We found that the N-terminal domain of EFA6B (1-554 aa) strongly binds to NUMB, at levels comparable to the full length protein, while the C-terminal region (555-1056 aa) retains a weaker interaction. Of note, the Sec7 domain alone (555-738 aa) is not able to bind NUMB. The PH domain and the coild-coiled region (739-1056) display a weak interaction with NUMB, comparable to the entire C-terminal region (555-1056 aa) (Fig. 26B).

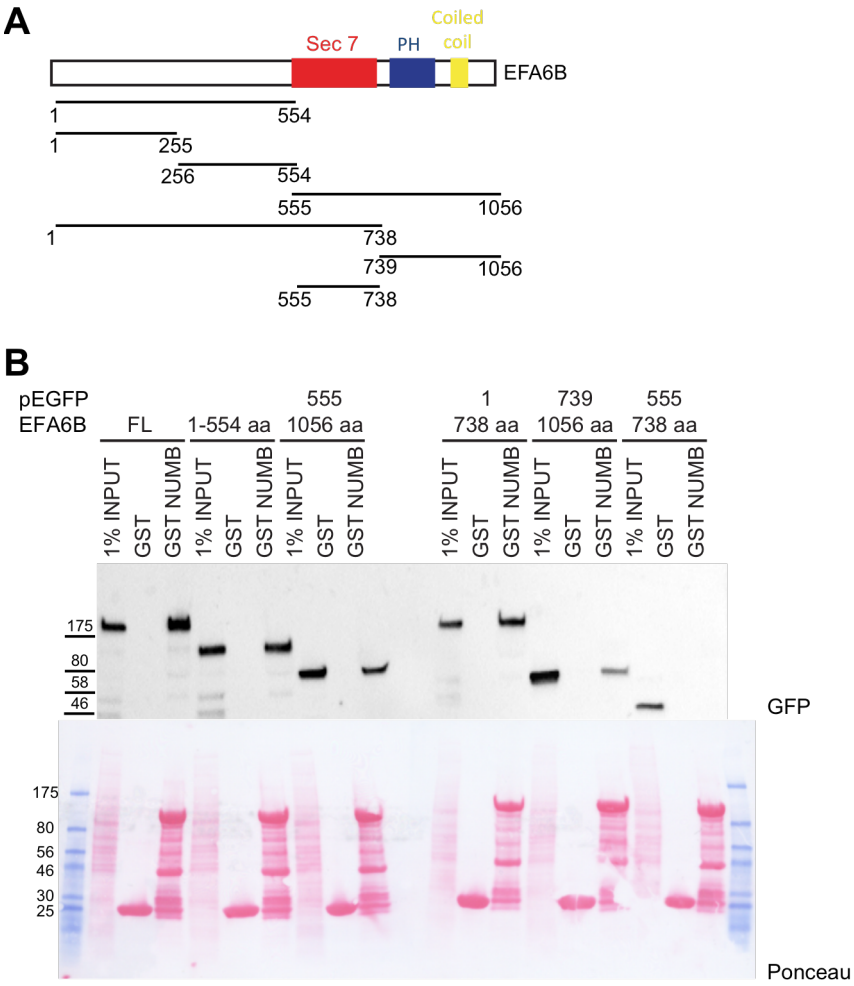

Figure 26. Identification of EFA6B surface required to bind NUMB.
A. Schematic rapresentation of EFA6B. The Sec7 domain, the PH domain and the coiled coil domain are depicted in red, blu and yellow, respectively. Deletion mutants are indicated below the schematic representation.
B. Lysates (1.5 mg) from Phoenix cells transfected with pEGFP-EFA6B FL or its deletion mutants were incubated with 0.5 µM GST or GST-NUMB immobilized on beads as indicated. Input lysates (1% of the total) and bound material were analyzed by IB with anti-GFP to visualize EFA6B and its deletion mutants or by Ponceau staining to detect the recombinant GST proteins. MW markers are shown on the left of the blots.

4.8 The NPxF domain motif in the N-terminal of EFA6B is required for the binding of NUMB via its PTB

Analysis of the amino acid sequence of EFA6B revealed the presence in the N-terminal region of an NPxF (248-251 aa) consensus motive for binding to NUMB (Qin et al. 2004; Bogdanovic et al. 2012). To check whether this consensus motif is required for the interaction, we generated two deletion mutants in the context of EFA6B N-terminal region (1-554 aa). The first mutant (1-255 aa) contains the NPxF stretch, while the second mutant (256-554 aa) does not. We found that only the 1-256 aa fragment was able to bind NUMB

as the whole N-terminal region (1-554 aa) in a pull-down assay (Fig. 27A), suggesting that this consensus motif is required for the interaction. To confirm this finding, we generated single point mutants (N248A and F251A) alone or in combination in the contest of the EFA6B N-terminal region (1-554 aa). We found that only the WT EFA6B 1-554 aa was able to bind NUMB in a pull-down assay, while the interaction with proteins carrying the single point mutations alone or in combination was strongly impaired (Fig. 27B).

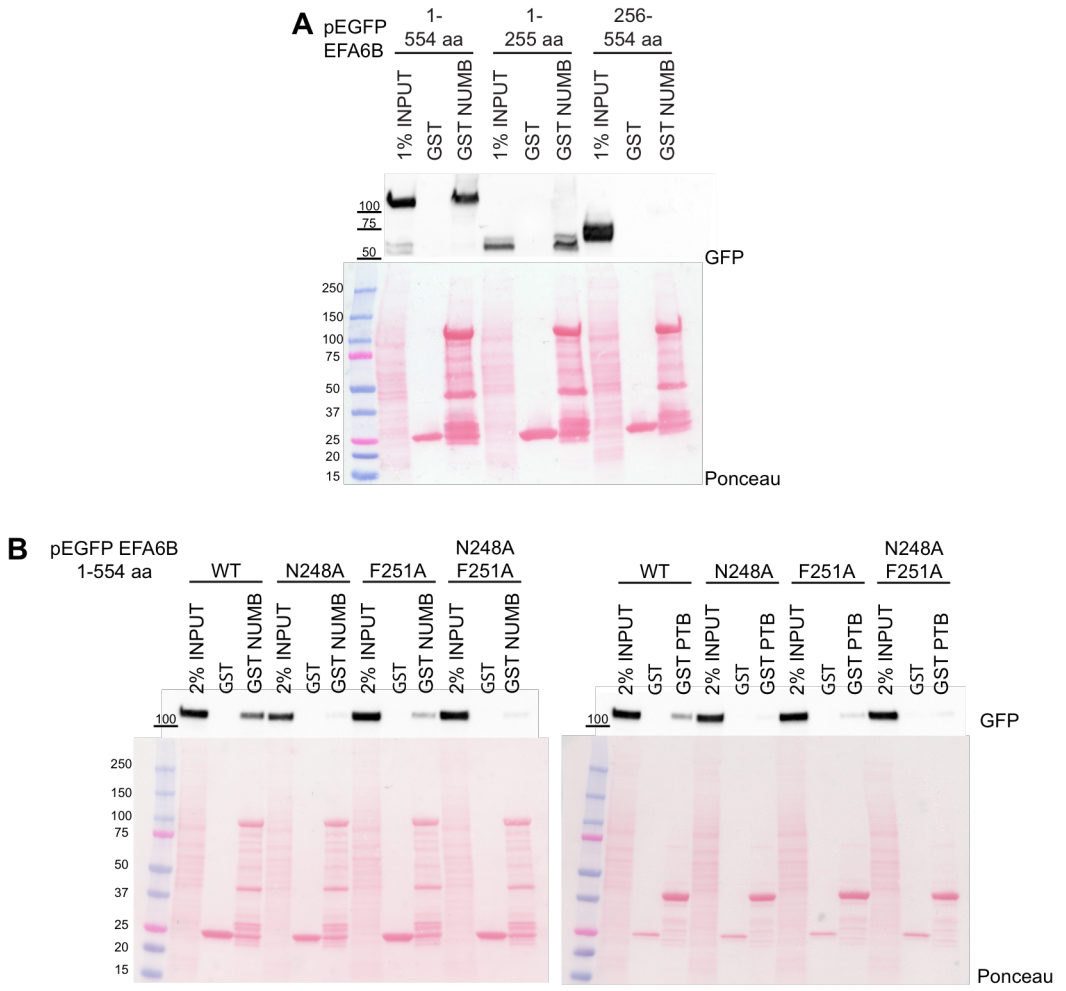

Figure 27. The NPxF domain in the N-terminus of EFA6B is required for binding to NUMB via PTB.

A. Lysates (1.5 mg) from Phoenix cells transfected with pEGFP-EFA6B 1-554, pEGFP-EFA6B 1-255 or pEGFP-EFA6B 256-554 were incubated with 0.5 µM GST or GST-NUMB immobilized on beads as indicated. Input lysates (1% of the total) and bound material were analyzed by IB with anti-GFP to visualize EFA6B and its deletion mutants or by Ponceau staining to detect the recombinant GST proteins. MW markers are shown on the left of the blots.

B. Lysates (750 µg) from Phoenix cells transfected with pEGFP-EFA6B 1-554 WT, N248A, F251A or N248A F251A were incubated with 0.5 µM GST, GST-NUMB or GST PTB immobilized on beads as indicated. Input lysates (2% of the total) and bound material were analyzed by IB with anti-GFP to visualize EFA6B and its deletion mutants or by Ponceau staining to detect the recombinant GST proteins. MW markers are shown on the left of the blots.

These findings were confirmed in a set of pull-down assays using purified proteins. A titration curve was carried out to establish the minimal amount of NUMB in solution that allows detection of the binding with GST-EFA6B (Fig. 28A). In these conditions, an EFA6B construct carrying the N248A and F251A mutations in the NPxF motif showed reduced binding to recombinant purified NUMB compared to WT GST-EFA6B (Fig. 28B). Equal results were obtained in an *in vitro* pull-down assay using purified recombinant NUMB PTB (Fig. 29).

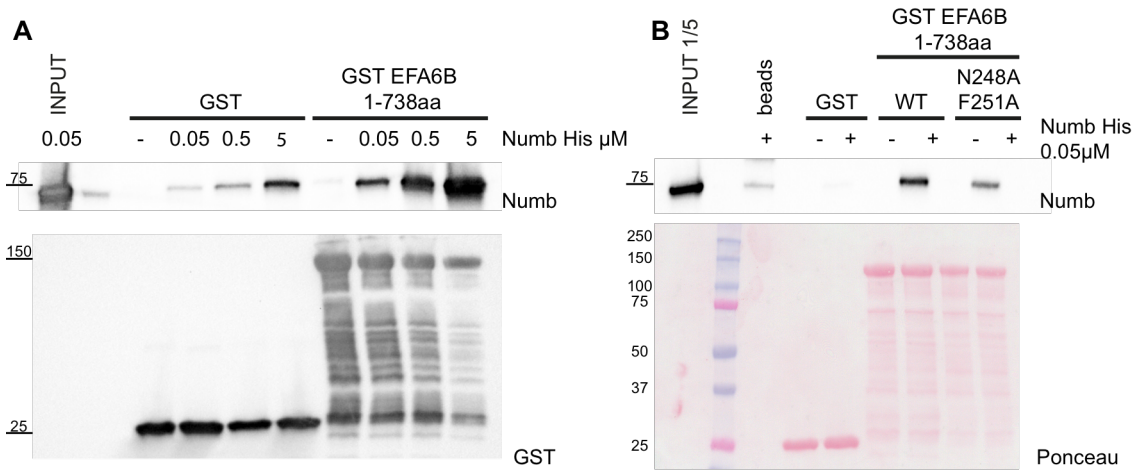

Figure 28. EFA6B binds to NUMB via its NPxF motif.
A. Increasing amounts (0, 0.05, 0.5 and 5 µM) of purified Numb-His were incubated with 0.5 µM GST-EFA6B 1-738 or GST alone (control) immobilized on beads as indicated. Input (0.05 µM) and bound material were analyzed by IB with anti-Numb to visualize NUMB or anti-GST staining to detect GST recombinant protein. MW marker is shown on the left of the blots.
B. Purified Numb-His (0.05 µM) was incubated with 0.5 µM GST-EFA6B 1-739 WT or N248A, F251A mutant or GST alone (control). Input (1/5) and bound material were analyzed by IB with anti-Numb to visualize NUMB or Ponceau staining to detect GST recombinant proteins. MW markers are shown on the left of the blots.

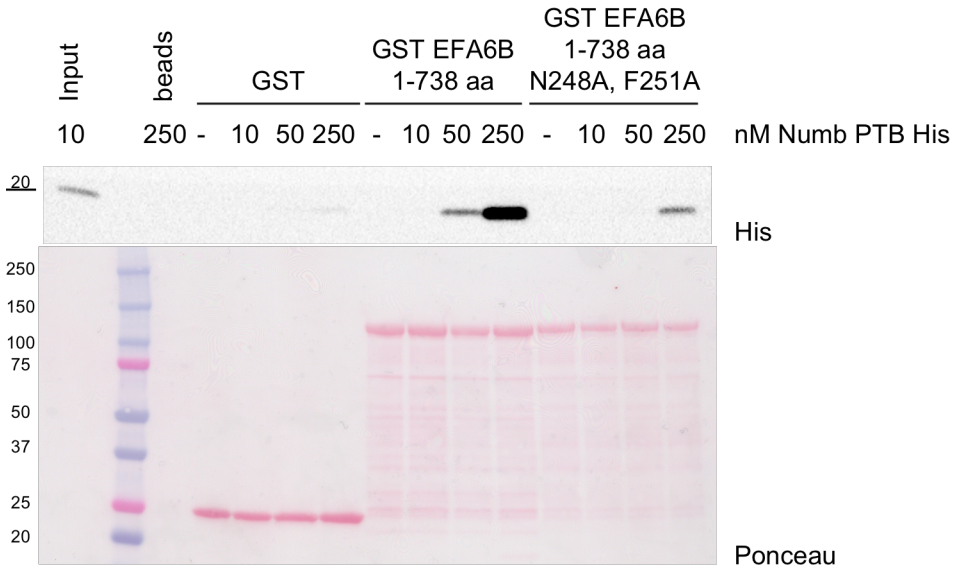

Figure 29. EFA6B binds to NUMB PTB via its NPxF motif.
Increasing amounts of Numb PTB-His (0, 0.01, 0.05, 0.25) were incubated with 0.5 µM GST-EFA6B 1-739 WT, or N248A, F251A mutant or GST alone (control) as indicated. Input (10 nM) and bound material were analyzed by IB with anti-His to visualize NUMB PTB or Ponceau staining to detect GST recombinant protein. M markers are shown on the left of the blots.

To investigate whether the N248A and F251A mutations affect the ability of EFA6B full-length protein to binds NUMB, we performed a pull-down assay to compare the WT EFA6B with the N248A and F251A mutant. We found that the EFA6B N248A and F251A mutant is strongly defective in binding to NUMB and is not able to bind the PTB (Fig. 30). All together, these experiment confirm that the NPxF sequence in the N-terminal of EFA6B mediates the binding with NUMB PTB.

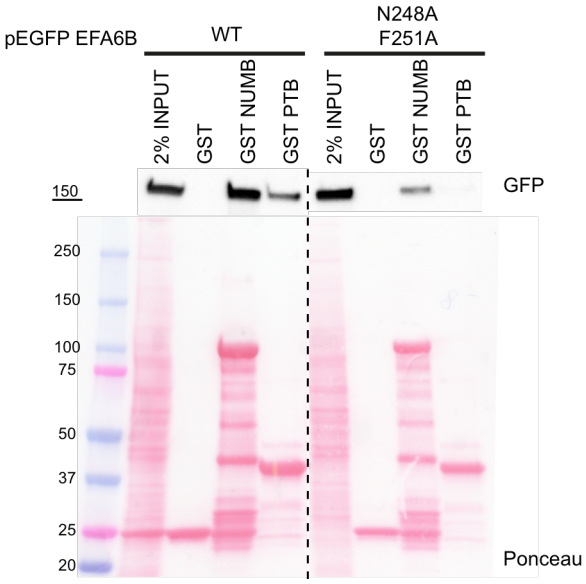

Figure 30. EFA6B carrying the mutation in the NPxF motifs is impaired in its binding to NUMB. Lysates (2 mg) from Phoenix cells transfected with pEGFP-EFA6B WT or pEGFP-EFA6B N248A-F251A were incubated with 0.5 µM GST, GST-NUMB or GST-PTB immobilized on beads as indicated. Input lysates (2% of the total) and bound material were analyzed by IB with anti-GFP to visualize EFA6B or by Ponceau staining to detect the recombinant GST proteins. MW markers are shown on the left of the blot.

4.9 EFA6B localizes in enlarged endosome induced by ARF6 dominant active expression

Since EFA6B is a GEF for ARF6(Donaldson and Jackson 2011b), we analyzed its sub-cellular localization in steady state conditions and in respect to the ARF6 recycling compartment. As previously reported(Derrien et al. 2002), we found that EFA6B is expressed in the cytosol and is enriched at the PM (Fig. 31). The expression of dominant active ARF6 (Q67L) induces the formation of enlarged endosomes, were EFA6B and NUMB re-localize (Fig. 32 and 18B).

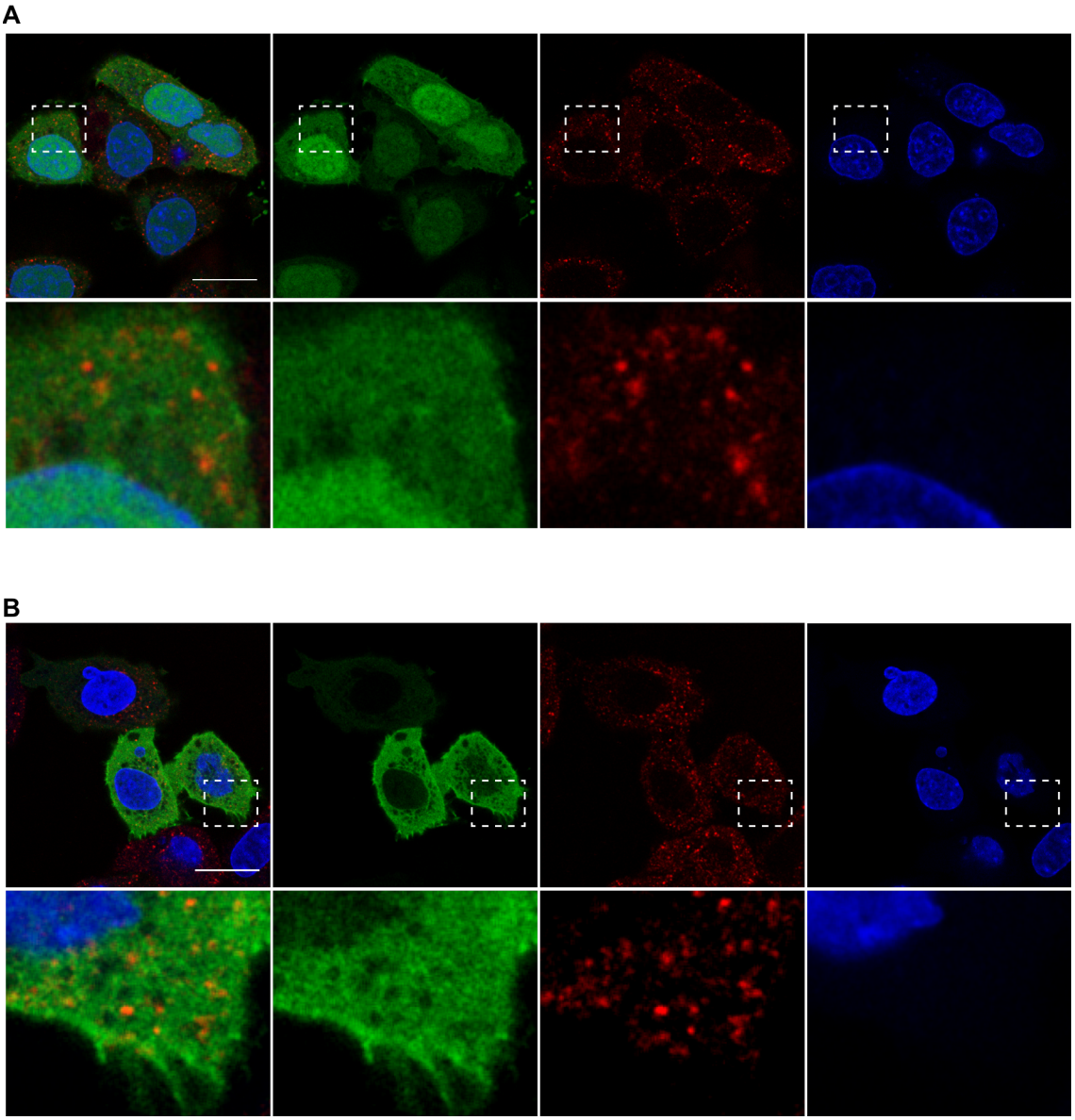

Figure 31. EFA6B is enriched at the PM.
A. Upper panels: confocal analysis of HeLa cells transfected with GFP. 24 hours after transfection, cells were fixed and processed for epifluorescence analysis to visualize GFP (green) or stained with anti EEA1 to visualize the early endosomal compartment (red) and DAPI (blue) to visualize the nuclei. Scale bar: 20 µm.
Lower panels: 5X magnification of the selected area.
B. Upper panels: confocal analysis of HeLa cells transfected with GFP-EFA6B. 24 hours after transfection, cells were fixed and processed for epifluorescence analysis to visualize GFP-EFA6B (green) or stained with anti EEA1 to visualize the early endosomal compartment (red) and DAPI (blue) to visualize the nuclei. Scale bar: 20 µm.
Lower panels: 5X magnification of the selected area.

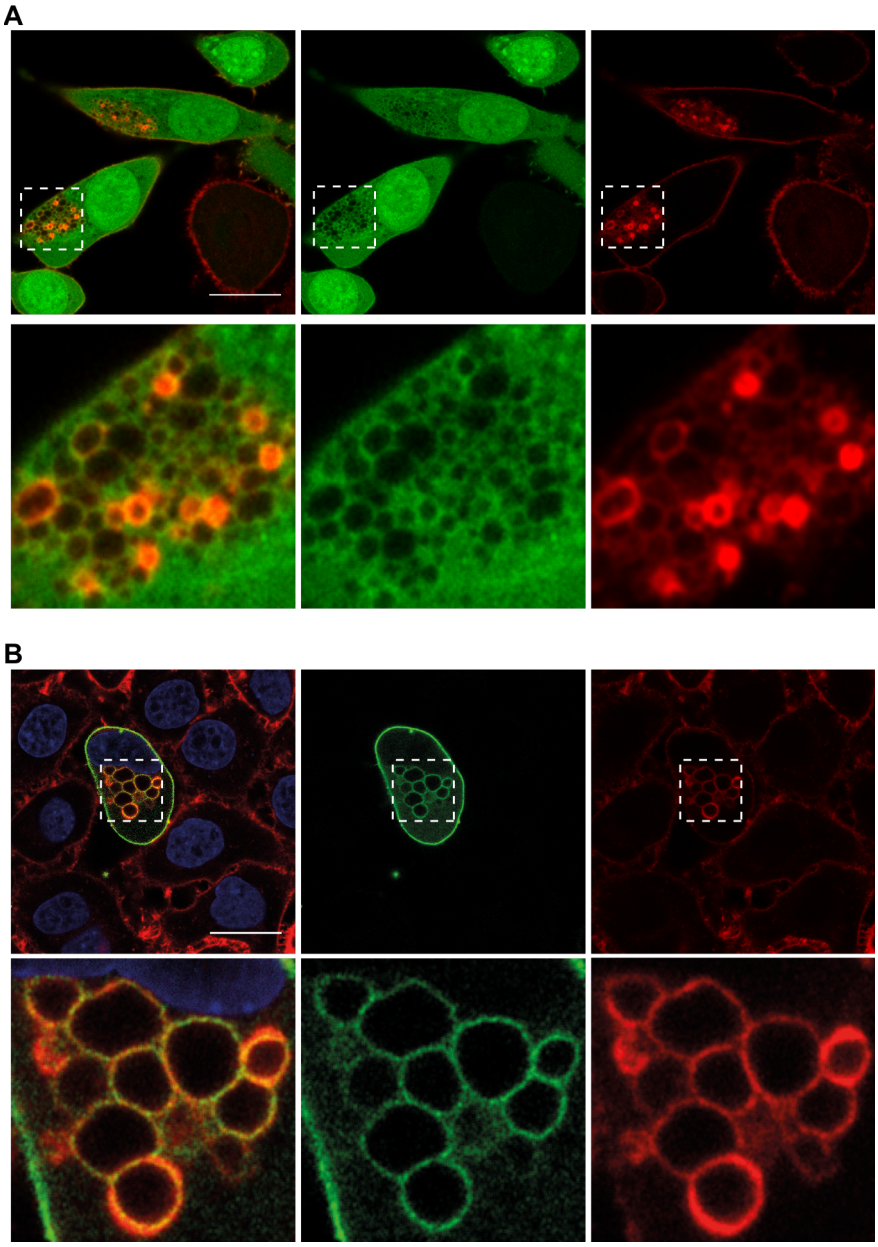

Figure 32. EFA6B stains enlarged endosomes induced by active ARF6.
A. Upper panels: confocal analysis of HeLa cells transfected with GFP and HA-Arf6:Q67L. 24 hours after transfection, cells were fixed and processed for epifluorescence analysis to visualize GFP (green) or stained with rhodamine phalloidin to visualize Arf6:Q67L (red) and DAPI (blue) to visualize the nuclei. Scale bar: 20 μm.
Lower panels: magnification of the selected area.
B. Upper panels: confocal analysis of HeLa cells transfected with GFP-EFA6B and HA-Arf6:Q67L. 24 hours after transfection, cells were fixed and processed for epifluorescence analysis to visualize GFP-EFA6B (green) or stained with rhodamine phalloidin to visualize Arf6:Q67L (red) and DAPI (blue) to visualize the nuclei. Scale bar: 20 μm.
Lower panels: magnification of the selected area.

The enrichment of both NUMB and EFA6B in recycling compartments ARF6 positive prompted us to investigate if the activation of ARF6 favors their interaction. Co-IP experiments were performed on cell lysates transfected with active ARF6. We found that

the expression of ARF6 Q67L enhanced the interaction between NUMB and EFA6B (Fig. 33).

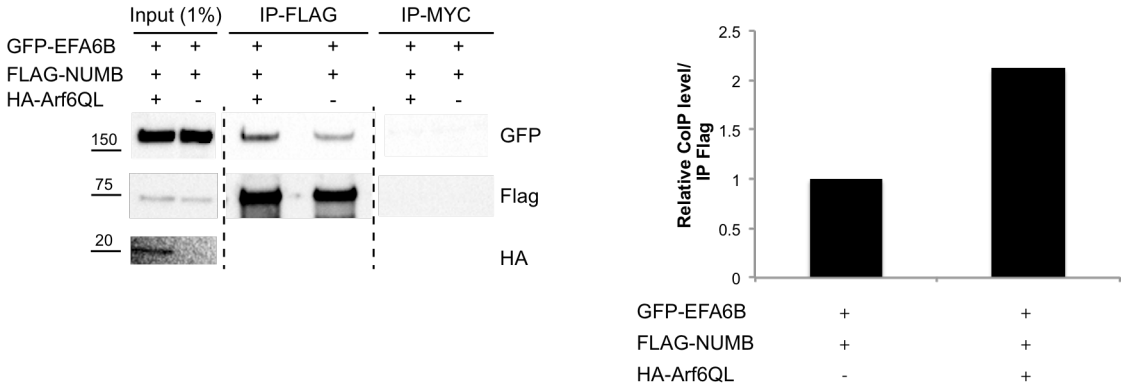

Figure 33. The interaction between NUMB and EFA6B is enhanced in the presence of ARF6.
Left panel**:** NUMB-FLAG was immunoprecipitated with anti-FLAG M2 affinity gel (2 round with 30 µl), using 3.0 mg of total cell lysate from Phoenix cells transfected with GFP-EFA6B and NUMB-FLAG in the presence or not of HA-ARF6 QL. Immunoprecipitates were analyzed by WB analysis with the indicated antibodies. As a control, the same amount of both total cell lysates was immunoprecipited with anti MYC. MW markers are shown on the left of the blots.
Right panel: quantification: relative Co-IP levels over the IP Flag.

4.10 Removal of EFA6B and NUMB restores increased HGF-induced CDR formation induced by NUMB removal.

Our results suggest that NUMB may regulate ARF6-dependent recycling by interacting and possibly by modulating its GEF EFA6B. If this scenario is true, the down-regulation of EFA6B should abrogate the increase of growth factors-induced CDRs due to NUMB ablation. To investigate our hypothesis, we performed EFA6B RNAi experiments in combination with NUMB RNAi. We found that removal of EFA6B by itself does not affect the formation of CDRs, while when combined ablation of EFA6B and NUMB is able to reduce the number of cells forming CDRs to control cell level (Fig. 34). These data suggest that the interaction between NUMB and EFA6B may regulate its GEF activity for ARF6.

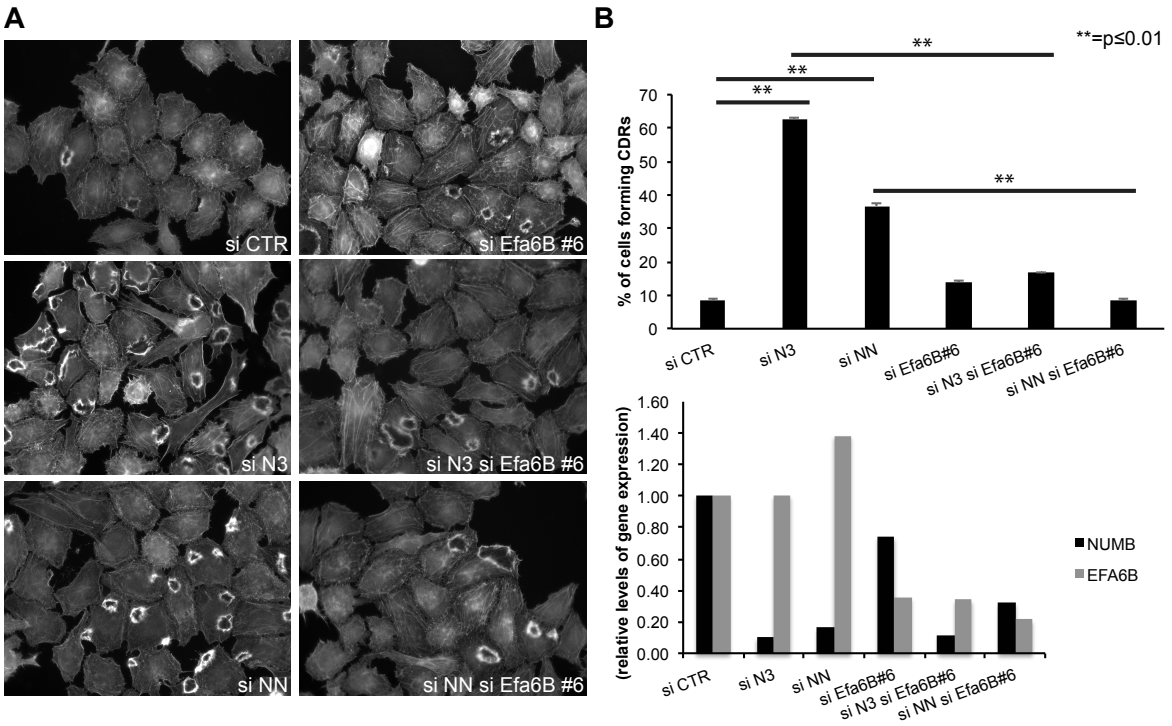

Figure 34. Ablation of EFA6B and NUMB reduces increased HGF-induced CDR formation due to NUMB removal.

A. HeLa cells transfected with siRNA against NUMB (N3, NN) or siRNA against EFA6B (si EFA6B #6) alone or in combination with siRNA against NUMB (si N3 si EFA6B #6 or si NN si EFA6B #6) or scramble oligo (si CTR, control) were seeded on matrigel-coated coverslips. After 48 hours, cells were serum starved (s) for 2 hours and stimulated with 100 ng/ml HGF for 4 minutes, fixed and stained with F-actin antibody. Scale bar 20 μm.

B. Upper pannel. The number of cells forming CDR over the total number of cells per field was counted. At least 20 fields were analyzed in each condition and three independent experiment were performed. The data are presented as the mean ± SEM.

Lower panel: Numb and EFA6B mRNA levels were analyzed by RT-PCR. The data are presented as the relative level of gene expression compared to control cells (si CTR).

5 DISCUSSION

5.1 NUMB is a negative regulator of mesenchymal mode of motility.

Single cells move in a 3D environment by exploiting two different modes of migration: a leucocyte-type ellipsoid “amoeboid” movement and a fibroblast-like spindle-shaped, “mesenchymal” migration(Friedl and Wolf 2003).

The “amoeboid” mode of migration is characterized by less adhesive cell-matrix interaction and displays a diffuse structure of the actin cytoskeleton(Friedl, Borgmann, and Brocker 2001). This mode of migration is used by, for example, leucocytes and tumor cells of hematopoietic origin(Friedl, Borgmann, and Brocker 2001). The “amoeboid” designation is due to the ellipsoid morphology, the rapid cell shape and flexibility, which remind of the single-cell-state of the lower eukaryote *Dictyostelium discoideum* amoeba(Friedl, Borgmann, and Brocker 2001). Like in *Dictyostelium discoideum*, this type of movement does not require Matrix Metallo Proteases (MMPs) and integrins, whereas most cytoskeletal regulatory and adaptor proteins, including small GTPases, PIKs and actin-binding proteins, are necessary(Wolf, Muller, et al. 2003). Lymphomas, leukemia and small cell lung cancer, all of which are fast disseminating tumors, use a fast-gliding, propulsive migration mode independently of integrins, pericellular proteolysis, focal contact formation and stress fibers to rapidly disseminate within different tissues(Wolf, Muller, et al. 2003).

Compared to the amoeboid mode of migration, mesenchymal mode of migration is strictly dependent on integrins and proteases that degrade the ECM(Friedl and Wolf 2003). This mode of migration is marked by tightly regulated focalized adhesion structures, protease activity and cytoskeletal contractility(Wolf, Mazo, et al. 2003; Davies et al. 2005). Thus, to migrate in a mesenchymal fashion, cells have to extend their polarized protrusions driven by a highly dynamic actin cytoskeleton, which is coupled to integrin clusters that serve as a transient clutch to grip onto the substrate, and to further acquire the ability to

proteolytically reorganize the ECM(Davies et al. 2005; Wolf, Mazo, et al. 2003). This mode of migration is typical of cells originating from connective tissue, sarcomas or dedifferentiated carcinomas(Davies et al. 2005; Wolf, Mazo, et al. 2003).

The coordination of the intracellular trafficking of molecules, such as integrins and proteases, the adhesion to the substratum and the remodeling of the actin cytoskeleton to generate the propulsive forces are critical steps during mesenchymal, directed motility. Indeed, the crosstalk between endocytic/recycling compartments and the polarization of protease activity, adhesive molecules and cytoskeleton components is fundamental during mesenchymal migration to ensure spatial restriction of signaling. Thus, in order to study the effect of endocytic/trafficking proteins on the mesenchymal mode of migration, an RNAi screening was set up and CDRs and PRs were used as readout markers.

PRs are actin structures formed at the leading edge of the cells. PRs are active and persistent structures that form immediately upon growth factors stimulation(Suetsugu et al. 2003). CDRs are actin-reach structures that are formed on the dorsal surfaces of motile cells(Suetsugu et al. 2003). These structures are dynamic and transient, and form upon stimulation with growth factors like EGF, HGF and PDGF(Buccione, Orth, and McNiven 2004; Mellstrom, Heldin, and Westermark 1988; Orth and McNiven 2006). CDRs emerge, constrict and close, within 5 to 30 minutes after stimulation(Buccione, Orth, and McNiven 2004). The PI3K and the small GTPase RAC are two major determinants in the signaling events downstream RTKs that drive CDR formation(Lanzetti et al. 2004). CDR formation has been involved in receptor internalization, macropinocytosis and mesenchymal migration(Hoon, Wong, and Koh 2012). As stated above, to migrate in a mesenchymal fashion, cells have to remodel the ECM. The matrix-degrading matrix metalloproteinase-2 (MMP-2), WAVE 1, paxillin and Pyk2, all of which are important components of ECM, localize in CDRs(Buccione, Orth, and McNiven 2004; Suetsugu et al. 2003; Sero et al. 2011).

In our screening, we found that removal of the endocytic adaptor protein NUMB increased

CDR formation without affecting the formation of PR. Since NUMB is one of the main focuses of our research group, and little is known about the negative regulation of CDR formation, we set out to further characterize this novel and unexpected function of NUMB. The results of the screening were validated in two independent cell lines, HeLa and MEFs, stimulated with HGF and PDGF, respectively. Additionally, the expression of human GFP-NUMB isoforms in MEFs interfered for endogenous, murine NUMB rescued the CDR phenotype, further proving that NUMB is a negative regulator of these migratory protrusions.

The loss of NUMB not only increases the capacity of cells to form CDRs, but also enhances growth factor-mediated cell migration and invasion by promoting a mesenchymal mode of locomotion. Our findings are in line with data collected by Wang and colleges in MDCK cells(Wang et al. 2009). In their work, they showed that, during EMT, NUMB functions as an endocytic adaptor protein for E-cadherin and regulates cell migration. They further demonstrated that upon HGF stimulation or Src activation, loss of NUMB caused basal-to-apico-lateral membrane translocation of E-cadherin and mislocalization of the Par-complex. These changes were mirrored by the finding that NUMB removal also promoted wound healing closure and chemotactic invasion: the former phenotype was rescued by re-expression of a siRNA-resistant NUMB version(Wang et al. 2009). NUMB-deficient cells displayed also an increased proliferation, which, however, was shown not to account for the augmented cell migration(Wang et al. 2009). Molecularly, some of the NUMB-dependent changes were ascribed to its ability to modulate E-cadherin junctional stability.

Additionally, NUMB, when phosphorylated by the aPKC polarity complex, has been reported to be required for integrin-dependent directional cell migration in HeLa cells(Nishimura and Kaibuchi 2007). At the leading edge, NUMB localizes to clathrin-coated structures and binds to integrin-ßs, regulating their endocytosis(Nishimura and Kaibuchi 2007). Upon phosphorylation by aPKC, NUMB is released from clathrin-coated

structures and is not able to bind integrins(Nishimura and Kaibuchi 2007). NUMB is also required for GCPs migration(Zhou et al. 2011). In this contest, it binds to activate BDNF receptor TrkB to control receptor endocytosis and recruits aPKC for activation. Active aPKC phosphorylates NUMB, enhancing the interaction between NUMB and TrkB to increase the formation of TrkB-NUMB endosomal complex(Zhou et al. 2011). Thus, the regulated interaction between the endocytic adaptor protein NUMB and the BDNF receptor TrkB is required to link the extracellular signal to the cellular polarity machinery, allowing directed migration in response to a BDNF gradient(Zhou et al. 2011).

In all these studies(Wang et al. 2009; Nishimura and Kaibuchi 2007; Zhou et al. 2011), there is one common mechanism underlying NUMB function in cell migration: NUMB binds to RTKs and functions as a scaffold protein to recruit additional component, such as polarity complex or components of the endocytic machinery. NUMB, for example, could promote endocytosis and relocalization of the receptor to the front of the cells. The NUMB-receptor complex may remain in signaling endosomes within the leading process, and/or be recycled to the front of the cells to promote directional migration in response to receptor activation.

5.2 NUMB is a negative regulator of the recycling compartment

CDR formation has been shown to depend on the small GTPase RAB5(Palamidessi et al. 2008). Indeed, upon motogenic stimuli, RAB5 promotes the accumulation of RAC1 to EE. In these organelles, RAC1 is activated by its GEF TIAM(Palamidessi et al. 2008). From the EE, active RAC1 is recycled back in an ARF6-dependent manner to specific regions of the PM, resulting in spatial restriction of RAC1 activity and the extension of polarized protrusions, such as CDRs(Palamidessi et al. 2008). We found that NUMB localizes in the two main compartments of this pathway: in EE induced by RAB5 expression and in enlarged endosomes induced by ARF6 dominant active expression. NUMB removal, however, does not impact on ARF6-independent recycling of EGFR and TfR (not shown),

but it specifically inhibits recycling of MHC class I and RAC1, which rely on ARF6.

These findings are consistent with a scenario according to which a major functionally conserved role of NUMB is to act as a negative regulator of recycling both in invertebrates and in mammals. For example, in mammals, changes in NUMB expression alter NOTCH1 trafficking(McGill et al. 2009). Indeed, using C2C12 cells, it was shown that NUMB overexpression promotes NOTCH translocation to late endosomes for degradation, whereas NUMB downregulation enhances NOTCH1 recycling(Bric et al. 2009). Although NOTCH recycling is not regulated by ARF6, this work suggests that NUMB is a negative regulator of this transport route(Bric et al. 2009). NUMB exerts negative regulation of the recycling route also in *C. Elegans*(Nilsson et al. 2008; Nilsson, Jonsson, and Tuck 2011) and in *Drosophila*(Cotton, Benhra, and Le Borgne 2013; Couturier, Mazouni, and Schweisguth 2013). In the nematode *C. Elegans*, overexpression of NUM-1A, the nematode NUMB homologue, causes similar defects to those caused by the loss of rme-1, the nematode homologue of EHD. These results indicate that NUM-1A negatively regulates recycling, a finding consistent with the fact that loss of NUM-1A bypasses the requirement for RME(Nilsson et al. 2008). The same groups also proposed that NUM-1A, in the recycling compartment, prevents the ability of TAT-1A to translocate phosphatidylserines across the membranes of recycling endosomes(Nilsson, Jonsson, and Tuck 2011). Two recent studies in *Drosophila* proposed that NUMB inhibits recycling of the Sanpodo-NOTCH complex back to the PM(Cotton, Benhra, and Le Borgne 2013; Couturier, Mazouni, and Schweisguth 2013). The authors suggested that the AP-2 and AP-1-dependent trafficking, regulated by NUMB, is required for Sanpodo localization(Cotton, Benhra, and Le Borgne 2013; Couturier, Mazouni, and Schweisguth 2013). In fish, the OPO protein, a transmembrane protein similar to Sanpodo, antagonizes NUMB in the control of integrin trafficking, once again reinforcing the idea that NUMB negatively regulates post-internalization sorting events(Bogdanovic et al. 2012).

Despite this wealth of concordant evidence, results from early studies in mammalian cells

suggested, instead, a positive role for NUMB in recycling(Smith et al. 2004). NUMB, via its NPF, was shown to interact *in vivo* and *in vitro* with EHD endocytic proteins. Of note, both NUMB and EHD proteins are localized to vesicles containing the small GTPase ARF6(Smith et al. 2004). The authors showed that the removal of NUMB inhibits the recycling of Tac receptors(Smith et al. 2004).

Like the Tac receptor, also the MHC class I is internalized via CME and is recycled back via ARF6(Radhakrishna and Donaldson 1997). Our data support a scenario whereby NUMB removal increases the recycling of two ARF6 cargos, MHC class I and RAC. The differences between our results and those reported by McGlade's laboratory may be due to the use of two different cell systems, to intrinsic limitations in the techniques used to test the recycling pathway, as well as to the reagent used to achieve NUMB removal. Indeed, rather than quantifying the amount of receptor on the PM, the authors monitored the amount of internalized receptor that decrease over time due to of recycling. They did not take into account the possibility that instead of being recycled, the internal pool of the receptor could be reduced due to degradation, especially in the absence of NUMB. The same experiment could be performed in the presence of an inhibitor of degradation to test this possibility.

Nevertheless, other data present in the literature suggest a negative role for NUMB in recycling and support our findings. The underlying mechanisms, however, are still unclear.

5.3 NUMB-EFA6B interaction and its biological implications.

ARF6, like all GTPases, cycles between active and inactive conformation: a process tightly regulated by GEFs and GAPs, respectively(D'Souza-Schorey and Chavrier 2006). Three obvious, but distinct molecular mechanisms that directly impinge on ARF6 activity can be hypothesized to account for how NUMB acts as a negative regulator of the recycling pathway: i) NUMB can inhibit a GEF; or ii) activate a GAP, or iii) modulate the binding or activity of ARF6 downstream effectors.

Since the most common mechanism of regulation of small GTPases relies on GEFs, we initially tested the first hypothesis. We found that among the GEFs for ARF6, EFA6B directly interacts with NUMB via its PTB domain. We have also discovered that the N-terminal region of EFA6B contains an NPxF consensus binding site for the PTB domain of NUMB(Zwahlen et al. 2000), and showed that this motif is required for the interaction with NUMB. Notably, the N-terminal of EFA6B appears to be the major determinant of the interaction with NUMB. However, also the region encompassing the entire PH and C-terminal portion (739-1056) of EFA6B binds to NUMB, albeit weakly.

The expression of EFA6 in cells is able to induce ruffles and microvilli-like protrusions(Derrien et al. 2002; Franco et al. 1999). It has been demonstrated that the conserved C-terminal regions of EFA6A and EFA6B are able to induce morphological changes in the PM due to their ability to bind to F-actin(Derrien et al. 2002; Franco et al. 1999). In our work, we unveiled a novel function for the EFA6B N-terminal portion, whose functional role has long remained ill-defined. We have shown that mutations in the NPxF motif strongly reduce the binding with NUMB and abolish the binding to the PTB domain. Recently, while our study was being carried out, Okada and colleagues found that the N-terminal of EFA6B contains a binding site for dynamin2 that is required for the proper activation of ARF6 by the latter(Okada et al. 2015). Notably, this interaction site is located upstream of the NPxF motif, suggesting the possibility that EFA6B may concomitantly interact with dynamin2 and NUMB and that this complex may serve as a regulatory machinery of the docking site for the recruitment and/or activation of ARF6 at the early stage of internalization. The recent observations that ARF6 is transiently recruited at sites of clathrin coat formation, but that perturbations of its activity do not affect the rate of internalization, support the possibility that this GTPase may indeed be recruited along the endocytic machinery to be functionally operative at later steps of trafficking. Consistently, ARF6 silencing was shown to alter recycling but not internalization of TfR(Montagnac et al. 2011).

Our data are consistent with the possibility that NUMB, by physically interacting with EFA6B, may modulate ARF6 activation. If our hypothesis is correct, NUMB removal should affect the levels of ARF6 activation and its function should strictly depend on EFA6B. The latter possibility is supported by the finding that the increased number of CDRs caused by NUMB silencing is completely abrogated by concomitant loss of EFA6B. Of note, EFA6B by itself does not affect CDR formation induced by growth factors, suggesting that others GEFs, which are not targeted by NUMB, might be involved in this pathway and that only in the absence of NUMB the NUMB-EFA6 axis may become prominent. Further experiments are required to confirm the NUMB-EFA6B genetic interaction. It will be indeed interesting to investigate the effect of the double RNAi on MHC class I or RAC recycling.

Whether by interacting with EFA6B NUMB impacts on its GEF activity and alters ARF6-GTP levels remains still an open issue. We are currently setting up an *in vitro* GEF assay(Derrien et al. 2002; Padovani et al. 2014) using the battery of recombinant purified wild type and mutant proteins described in the result section. We are also setting up pull down assays with GST-GGA3, a protein that recognizes ARF6-GTP specifically, in order to monitor ARF6-GTP levels in cells. We managed to find the proper experimental conditions to detect reliable ARF6-GTP levels in the presence of EFA6B in 293T cell. If NUMB alters EFA6B ARF6-GEF activity, we will also verify whether EFA6B (or its mutant in the NPxF) ectopic expression could rescue the increased capacity of NUMB-depleted cells to form CDRs in conditions in which both endogenous NUMB and EFA6B are knocked down. The same type of experiments will be performed to assess cell migration and invasion.

5.4 NUMB biochemical implications on ARF6 activity.

In our model, we hypothesized that in unperturbed conditions, NUMB binds EFA6B and controls ARF6 activation. Indeed, in the absence of NUMB there is an increase in CDR

formation and in ARF6 recycling, which may be due to the ability of free EFA6B to activate ARF6. If our hypothesis is correct, this should correlate with increased ARF6-GTP levels upon NUMB removal and concomitant stimulation with a growth factor. On the other hand, ectopic expression of NUMB in combination with EFA6B should decrease ARF6-GTP levels.

If, by chance, the experiments will not confirm our model, different molecular mechanisms will be explored to elucidate the NUMB-EFA6B interaction.

5.4.1 Altered localization of key determinants.

Rather than by interfering with the EFA6B GEF activity, NUMB may alter EFA6B and ARF6 localization, ultimately deregulating their function. We have already shown that both EFA6B and NUMB are localized to the PM and in enlarged endosomes induced by ARF6 active mutants, but more localization studies are required to fully address this issue. For example, we will study EFA6B localization in cells that express NUMB or in cells in which the expression of NUMB has been silenced, and look for possible links with the ARF6 compartment.

5.4.2 Impacts on the internalization of selected molecules.

Another possibility is to investigate whether the EFA6B-NUMB interaction alters the internalization step of selected cargos. It has been reported that the expression of EFA6A inhibits TfR uptake and causes redistribution of the TfR to the PM, albeit the mechanisms through which this occurs remains unclear(Franco et al. 1999). The expression of endophilin, a key regulator of CME, was shown to rescue EFA6A-induced inhibition of TfR internalization due to an interaction between the SEC7 domain of EFA6A and the N-BAR domain of endophilin on flat membranes(Boulakirba et al. 2014). Moreover, in the presence of EFA6A, endophilin is redistributed from the cytosol to the PM(Boulakirba et al. 2014). A similar scenario may also be at play in the case of NUMB and EFA6B. We should, however, first prove that, like EFA6A, EFA6B inhibits TfR uptake. Nevertheless,

it will be worth investigating NUMB function in the same context considering the fact that its role regarding TfR trafficking is still not clear(Teckchandani et al. 2009; Sorensen and Conner 2008) and data collected in our laboratory suggest that NUMB is not required for TfR recycling.

A novel mechanism of ARF6 activation has been recently reported. EFA6B, by interacting with dynamin2, was shown to activate ARF6(Okada et al. 2015). The evidence in support of the mechanism of action has been largely obtained through biochemical approaches; indeed, both a GTPase-deficient mutant of dynamin2 and a dominant negative mutant of EFA6B were shown to significantly inhibit dynamin2-induced ARF6 activation(Okada et al. 2015). In addition, the expression of the minimal fragment of EFA6B required for dynamin2 interaction was demonstrated to decreases TfR internalization(Okada et al. 2015). This set of findings suggests the possibility that by interacting with EFA6B, NUMB may impinge on dynamin2-mediated ARF6 activation.

5.4.3 Subversion of trafficking routes.

In the case of the ß2 adrenergic receptor, ARF6 is activated by EFA6A in a ß-arrestin-dependent manner. The activation of ARF6 does not impact on the internalization rate of the receptor but blocks its RAB4-dependent fast recycling. Prolonged activation of ARF6 induces translocation of the ß2 adrenergic receptor in late endosomes, thus leading to desensitization and downregulation of signaling. It can be possible to speculate that upon stimulation of RTKs with their cognate ligands, ARF6 is activated by EFA6B and that in the presence of EFA6B the fast recycling route could be blocked, leading to receptor degradation. If NUMB expression sequesters EFA6B and prevents ARF6-activation, the fast recycling route should be active. Thus, another mechanism by which NUMB could affect endocytic pathways might be the subversion of trafficking routes.

5.5 NUMB-EFA6B-ARF6 axis in cancer and stem cells

Loss of NUMB occurs in 50% of breast cancer(Pece et al. 2004) and in 30% of lung cancer(Westhoff et al. 2009), and correlates with an increased aggressiveness and poor prognosis of these tumors. Although some of the underlying molecular mechanisms have been elucidated(Pece et al. 2004; Colaluca et al. 2008; Westhoff et al. 2009; Pece et al. 2011) (loss of NUMB was shown to lead to decreased p53 levels and increased NOTCH activity), our data highlight a new potential mode of action of NUMB that may also function in the spatial restriction of signaling that controls cell migration and invasion. Our model suggests that NUMB acts downstream of growth factor-activated receptors and may control ARF6-dependent recycling by binding EFA6B. ARF6 and EFA6B have been reported to be involved in breast cancer progression and invasion(Schweitzer, Sedgwick, and D'Souza-Schorey 2011; Zangari et al. 2014; Hashimoto et al. 2016; Hashimoto et al. 2004; Marchesin et al. 2015). Since loss of NUMB correlate with an increased aggressiveness and poor prognosis(Pece et al. 2004) in breast cancer, we will investigate:

1) EFA6B levels and ARF6 GTP status in NUMB positive vs. negative tumors and in breast cancer primary cell lines derived from NUMB-proficient and NUMB-deficient tumors. This approach will allow us to understand if NUMB, EFA6B and ARF6-GTP expression levels correlate with tumor progression and aggressiveness.
2) Cell migration and invasion assays in different NUMB-proficient and NUMB-deficient breast cancer-derived primary cell lines. NUMB levels will be restored in NUMB-deficient cells by inhibition of proteasomal degradation(Pece et al. 2004) or expression of exogenous NUMB. The expression of NUMB will also be knocked-down in primary NUMB-proficient breast cancer cell lines to investigate whether it will affect migration and invasion.

In the contest of the mammary gland, loss of NUMB contributes to tumorigenesis by promoting the expansion of the stem cell pool and driving progenitor maturation through

EMT(Tosoni et al. 2015). These phenotypes depend on the control of NUMB over p53 stability(Tosoni et al. 2015). We are currently characterizing a novel function of NUMB in the regulation of spatial restriction of signaling, which is related to the interaction with the EFA6B-ARF6 pathway. Since little is known about the role of ARF6 and the control of trafficking pathways in stem or progenitor cells of the mammary gland, it would be interesting to investigate whether the removal ARF6 and EFA6 impinge on the tumor suppressor role of NUMB in this setting.

5.6 Concluding remarks

NUMB is an endocytic protein with tumor suppressor functions. As a tumor suppressor, NUMB is downregulated in several types of cancer, such as breast, lung, salivary gland and liver tumors. The mechanism leading to its downregulation in breast and lung tumors is massive ubiquitination and, as a consequence, proteasomal degradation. Loss of NUMB in these tumors correlates with increased p53 degradation and NOTCH hyper-activation.

As an endocytic adaptor, NUMB controls different trafficking routes, such as endocytosis and degradation, and controls different signaling pathways. NUMB regulates also cell migration, cell adhesion and EMT.

In this present study, we have shown that, in cancer cell, NUMB is a negative regulator of spatially defined protrusions, cell migration and invasion.

Molecularly, these phenotypes merge with the nascent scenario in which NUMB is appearing as a negative regulator of recycling pathways even if little is known about the underlying molecular mechanism. Indeed, we found that NUMB is a negative regulator of MHC class I and RAC recycling, both of which depend on ARF6. Data collected in this study suggest that NUMB might regulate ARF6 by modulating its GEF, EFA6B. We have shown that the NUMB PTB domain interacts with the N-terminal region of EFA6B, which contains an NPxF motif. Lastly, we will assess whether NUMB affects ARF6 activation by modulating EFA6B GEF activity.

The novel molecular mechanism that we are characterizing has different potential applications. We will investigate ARF6 and EFA6B status in NUMB-deficient cancer cells in the context of the stem cell niche. These investigations should open new avenues in the development of novel therapies for NUMB-deficient cancers.

6 MATERIALS AND METHODS

6.1 Common laboratory Solutions

6.1.1 Phosphate-buffered saline (PBS)

137 mM NaCl

2.7 mM KCl

10 mM Na_2HPO_4

2 mM KH_2PO_4

The solution is prepared by dissolving 8 g of NaCl, 0.2 g of KCl, 1.44 g of Na_2HPO_4, and 0.24 g of KH_2PO_4 in 800 mL of distilled water. The pH is adjusted to 7.4 with HCl and distilled H_2O is added to 1 litre.

6.1.2 Tris HCl (1 M)

Prepared by dissolving 121.1 g of Tris base in 800 mL distilled H_2O. The pH is adjusted (depending on the case) with HCl, and distilled H_2O is added to 1 litre.

6.1.3 10X Tris EDTA (pH 7.4-8.0)

100 mM Tris HCl (pH 7.4-8.0)

10 mM EDTA (pH 8.0)

6.1.4 50x TAE (Tris-Acetate-EDTA)

242 g/L	Tris base
57.1 mL/L	Acetic acid
20 mL/L	0.5 M EDTA pH 8

The pH is adjusted to 8.5 with HCl and distilled H_2O is added to 1 litre.

6.1.5 Tris-buffered saline (TBS)

It is prepared by dissolving 8 g of NaCl, 0.2 g of KCl, and 3 g of Tris base in 800 mL of distilled H2O. The pH is adjusted to 7.4 with HCl and distilled H_2O is added to 1 litre final volume.

6.1.6 1.4x JS lysis buffer

50 mM HEPES PH 7.5

50 mM NaCl

1% glycerol

1% Triton X-100

1.5 mM $MgCl_2$

5 mM EGTA

To this solution phosphatases and proteases inhibitors were freshly added:

protease inhibitor cocktail (Roche, Basel, Switzerland)

1 mM DTT

20 mM Na pyrophosphate pH 7.5

50 mM NaF

0.5 M Na-vanadate in HEPES pH 7.5

6.1.7 5x (2x) SDS-PAGE Sample Buffer

10% (4%) SDS

500 mM (200mM) Tris pH 6.8

30% (12%) glycerol

0.03% (0.0012%) saturated bromophenol blue

15% (6%) (v/v) β-mercaptoethanol (14M)

Stored at 4°C, protected from light by foil.

6.1.8 10x SDS-PAGE Running Buffer

144 g/L Glycine

30 g/L Tris base

1% SDS

6.1.9 10x Western Transfer Buffer

144 g/L Glycine

30 g/L Tris base

Diluted at 1x concentration in 20% of MeOH.

6.1.10 Ponceau S

0.1% (w/v) Ponceau ($C_{22}H_{12}N_4Na_4O_{13}S_4$) (Sigma)

5% Acetic acid

6.2 Basic cloning techniques

6.2.1 Agarose gel electrophoresis

DNA samples were loaded on 0.8%-2% agarose gels along with DNA markers. Gels were made in TAE buffer containing 0.3 μg/mL ethidium bromide and run at 80V until desired separation was achieved. DNA bands were visualized under a UV lamp.

6.2.2 Minipreps

E.coli Top10 Cells (Invitrogen) picked from individual transformed colonies were used to inoculate 3 mL LB (containing the appropriate antibiotic) and grown overnight at 37°C in 15mL Falcon tubes. Cells were pelleted for 15 minutes at 2500 rpm. Minipreps were performed according to the manual instructions (Promega, Wizard Plus SV Minipreps). The final elution was made in 80μl of milli-Q water. DNA was checked performing an agarose gel electrophoresis using 5μl of the elution.

6.2.3 DNA digestion

Between 0.5 and 2 μg DNA was digested for 2 hours at 37°C with 10 units of restriction enzyme (NEB). For digestion, the volume was readjusted to 10 μl with the appropriate buffer and ddH_2O (20μl in case of double digestions).

6.2.4 Large Scale Plasmid Preparation

E.coli Top10 Cells (Invitrogen) containing the desired DNA vector were expanded into 500 mL cultures overnight with the appropriate antibiotics. Plasmid DNA was isolated from these cells using the Qiagen Maxi-prep kit (Qiagen,Valencia, CA) according to the manufacturer's instructions.

6.2.5 Transformation of competent cells

E.coli Top10 cells (Invitrogen) were used for cloning and large scale DNA preparation, while *E.coli* BL21 Rosetta (DE3) cells (Promega) were used for proteins production. The transformation protocol used was the same for both strains.

50 μl of fresh competent cells, one shot TOP10 (Invitrogen), were thawed on ice for approximately 10 minutes prior to the addition of plasmid DNA. Cells were incubated with DNA on ice for 20 minutes and then subjected to a heat shock for 45 seconds at 42°C. Cells were then returned to ice for 2 minutes. Then, 0.250 mL of LB were added and the cells were left at 37°C for 60 minutes (with 200 rpm shaking) before plating them onto plates with the appropriate antibiotic. 50 μl of the transformed bacterial were usually plated. Plates were incubated overnight at 37°C.

6.2.6 DNA elution from agarose gel

DNA elution from agarose gel was performed using the Wizard SV Gel and PCR Clean-Up System (Promega), following manufacturer's instructions.

6.2.7 PCR (Polymerase Chain Reaction)

Sense and antisense oligos, of 20-30 nucleotides each, were generated, one annealing in 5' (forward) and the other in 3' (reverse) to the target sequence. The primers were designed of similar length and annealing temperature. Melting temperature of the primers was calculated according to the formula: Tm = 81.5+0.41(%GC) - 675\N - % mismatch. These primers were used in a PCR reaction together with the DNA template and the Phusion High-Fidelity DNA Polymerase (NEB).

Reaction mixture	
5x Phusion GC buffer	10 µl
DNA template	10-20 ng
primer forward	0.5 µM
primer reverse	0.5 µM
dNTPs mix	0.2 mM
Pfu (Promega)	1 U
ddH_2O	to a final volume of 50 µl

There are three major steps in a PCR (denaturation, annealing and extension), which were repeated for 25 cycles. This was done on an automated cycler (GeneAmp PCR system 9700, Applied Biosystems), which can heat and cool the tubes with the reaction mixture in a very short time.

Cycling parameters:

Step	Temperature	Time	N° of cycles
A)	denaturation at 98°C	30 seconds	1
B)	denaturation at 98°C	10 seconds	25
	annealing at X°C	30 seconds	
	extension at 72°C	(30 seconds/each kb of target length)	
C)	extension at 72°C	10 minutes	1

6.2.8 Generation of EFA6B deletion constructs

EFA6B deletion constructs were obtained through PCR, using as template the pEGFP_C3 vector containing the cDNA sequence of human EFA6B. To clone the different constructs specific primers were designed flanked by Bgl II and Sal I sites. DNA fragments were then subcloned either in an empty pGEFP_C1 vector after Bgl II-Sal I double digestion, or in an empty pGEX6p1 vector BamH I-Sal I double digestion or in an empty pBAC_His-MBP-TEV vector BamH I-Sal I double digestion and subsequent ligation.

USED PRIMERS:

Constructs	**Primers**	
1-554 aa	Fwd:	5' cgagatctatgggtgactacagactccctg 3' (Tm=59°C)
	Rew:	5' gtcgacttaccaagaagagttcatcggtgt 3' (Tm=56°C)
555-1056 aa	Fwd:	5' cgagatctcttcctgggagccctatg 3' (Tm=57°C)
	Rew:	5' cggtcgactcacagctgattgcggtt 3' (Tm=56°C)
1-738 aa	Fwd:	5' cgagatctatgggtgactacagactccctg 3' (Tm=59°C)
	Rew:	5' gtcgacttagagcttctcgctgcggat 3' (Tm=58°C)
739-1056 aa	Fwd:	5' cgagatctgagtgggccgtggatgaa 3' (Tm=58°C)
	Rew:	5' cggtcgactcacagctgattgcggtt 3' (Tm=56°C)
555-738 aa	Fwd:	5' ggatccgtgatcaatatcacttatgactcc 3' (Tm=58.5°C)
	Rew:	5' cgagatctcttcctgggagccctatg 3' (Tm=57°C)
1-256 aa	Fwd:	5' cgagatctatgggtgactacagactccctg 3' (Tm=59°C)
	Rew:	5'cggtcgacttaaggactcgccaggaagagg3' (Tm=59°C)

256-554 aa	Fwd:	5’ cgagatctccttgctcagagaacagt 3’ (Tm=52°C)
	Rew:	5’ gtcgacttaccaagaagagttcatcggtgt 3’ (Tm=56°C)
EFA6 B	Fwd:	5’ cgagatctatgggtgactacagactccctg 3’ (Tm=59°C)
	Rew:	5’ cggtcgactcacagctgattgcggtt 3’ (Tm=56°C)

6.2.9 Site directed mutagenesis

Site directed mutagenesis was performed using the Quick Change mutagenesis kit (Stratagene), following manufacturer’s instructions. Briefly, a sense and an antisense oligo of about 30-45 nucleotides each, carrying the desired mutation in the middle of the sequence, were generated and used in a PCR reaction using the wild type construct (100-300 ng) as template. PCR was performed using the Phusion High-Fidelity DNA Polymerase (NEB) for 16 cycles.

For the amplification step, 16 PCR cycles were performed with a denaturation step of 30 seconds at 95ºC followed by an annealing step of 1 minute at 55ºC and an extension step at 72ºC of 1 minutes/each kb of plasmid length.

After amplification, 1 µl of DpnI restriction enzyme, which selectively cuts methylated DNA at the GATC sequence, was added to digest the wild-type parental DNA. After one-hour incubation at 37˚C, the PCR product was used to transform competent *E. coli* Top10 cells (Invitrogen) and single colonies were sequenced for the presence of the desired mutation and the absence of other, unwanted, base changes. The presence of the desired DNA amplification was also checked by DNA electrophoresis of 10µl of the product in a 1-2 % agarose gel.

6.2.10 Generation of EFA6B point mutants

The different EFA6 B mutants were generated performing site directed mutagenesis using the Quick Change mutagenesis kit (Stratagene), following manufacturer’s instructions (see also section 7.3.8). Specific primers were designed:

Constructs	Primers	
1-554 aa N248A	Fwd:	5’ atgttcttcagcgccccctcttcc 3’
	Rew:	5’ ggaagaggggggcgctgaagaacat 3’
1-554 aa F251A	Fwd:	5’ atgttcttcagcaacccctcgccctggcgagtcctt 3’
	Rew:	5’ aaggactcgccagggcgaggggttgctgaagaacat 3’

The pGEX EFA6B 1-554 aa N248A, F251A, the pGEX EFA6B 1-739 aa N248A, F251A and the pBAC EFA6B N248A, F251A were generated by GenScript company. Then the EFA6B 1-554 aa N248A, F251A fragment and the EFA6B N248A, F251A were amplified by PCR reaction with primers flanked by Bgl II and Sal I sites. DNA fragments were then subcloned in an empty pGEFP_C1 vector after Bgl II-Sal I double digestion and subsequent ligation.

6.3 Antibodies, plasmid and reagents

The antibodies used were: anti-NUMB (Pece et al. 2004); anti-vinculin (Sigma), anti-GFP (gift from Jan Faix (Hannover)); anti-FLAG (Sigma); anti RAB5A (Santa Cruz Biotechnology); anti HA (Santa Cruz Biotechnology); anti EEA1 (Santa Cruz Biotechnology); anti MHC class I (Santa Cruz Biotechnology).

GFP NUMB isoforms, NUMB FLAG, GST NUMB fusion proteins, NUMB His and NUMB PTB His were a gift from I. Colaluca. pEGFC3 EFA6B, pEGFPC3 EFA6A and pEYFP ARNO were a gift from P. Chavrier. pCMV RAB5A, paGFP-RAC and pCDNA ARF6 QL were described previously in Palamidessi et al, 2008. pBAC_His-MBP-TEV vector was a gift from S. Pasqualato. pEGFPC1 EFA6B deletion mutants and MBP-EFA6B were obtained by PCR reaction.

Recombinant Human HGF (used at 100 ng/mL) was from R&D Systems. Recombinant Human Platelet Derived Growth Factor-BB (PDGF-BB, used at 1 ng/mL) was from

Immunological Sciences.

6.4 Cell culture

6.4.1 Cells culture

HeLa cells were grown in Minimum Essential Medium (MEM Invitrogen) supplemented with 10% South American serum (EuroClone), 1% non essential ammino acids and 1% Sodium Pyruvate. Immortalized mouse embryo fibroblasts [MEFs, (Scita et al., 1999)] were grown in Dulbecco's Modified Eagle Medium (DMEM, Lonza) supplemented with 10% South American serum (EuroClone) and 1% L-Glutamine (EuroClone). Phoenix cells were grown in Dulbecco's modified Eagle's medium (DMEM, Lonza) supplemented with South American serum (EuroClone) and 1% L-Glutamine (EuroClone). Cells were grown at 37°C in 10% CO_2.

6.4.2 Transfection

Transfections were performed using the calcium phosphate method, electroporation or Lipofectamine (Invitrogen).

Phoenix cells were transfected using the calcium phosphate procedure. In this case DNA (20 µg for a 15 cm plate) was diluted in 878 µl of ddH_2O and 122 µl of 2M $CaCl_2$ were added. This solution was added, drop-wise, to 1 mL of HBS 2x. Then, the precipitate was added to the cells (plated on 15 cm dishes) and removed after 12-16 hours.

Electroporation was used to transfect MEF cells for CDR rescue experiment, using the MicroPorator system (Digital Bio Technology) according to manufacturer's instructions. Cells were microporated with one pulse of 20 ms at 1650 V, with a cell density of $5*10^6$ cells.

Lipofectmane (Invitrogen), according to manufacturer's instruction, was used to transfect HeLa cells for IF experiments.

2x HBS pH 7.5

50 mM Hepes pH 7.5

10 mM KCl

12 mM dextrose

280 mM NaCl

1.5 mM Na_2HPO_4

6.4.3 Short interfering RNA (siRNA) experiments

siRNAs (small interfering RNAs) delivery was achieved by mixing from 5 to 50 nM of specific siRNAs with Optimem and Lipofectamine RNAiMAX Transfection Reagent (Life Technologies) by two cycles of transfection according to manufacturer's instruction. For each RNA interference experiment, negative control was performed with the same amount of scrambled siRNAs (si CTR). Knocking down efficiency was controlled by western blot or qRT-PCR.

Four different siRNAs were used for hNUMB KD, three different siRNAs were used for mNUMB KD and two different siRNAs were used for EFA6B KD, with comparable results.

Oligos details as follows:

hNUMB oligo N3: TACACACCTCTTCTAACCATCGGTC (Invitrogen, Inc);

hNUMB oligo NN: GGACCTCATAGTTGACCAGTT (NUMB Nishimura, Thermo);

hNUMB oligo #5: AAATGTAGCTTCCCGGTTA (ON-TARGETplus NUMB siRNA J-015902-05, Dharmacon);

hNUMB oligo #6: TAAGATAGTCGTTGGTTCA (ON-TARGETplus NUMB siRNA J-015902-06, Dharmacon);

mNUMB oligo #2: AGAAAGAAAGACCTTT (Riboox);

mNUMB oligo #3: CGGGAAAGAAAGCAG (Riboox);

mNUMB oligo #4: ATCTGTCATTGTTTC (Riboox);

EFA6B #6: GAACCGCAATCAGCTGTGA (ON-TARGETplus PSD4 siRNA J-019959-06, Thermo);

EFA6B #7: GCAATCATGCTGCTTAACA (ON-TARGETplus PSD4 siRNA J-019959-07, Thermo).

si CTR: TCGAATACGAACATTTATTT (Thermo)

6.4.4 Total RNA extraction and reverse transcription

Total RNA was extracted using RNeasy Mini kit (Qiagen) and quantified by NanoDrop to assess both concentration and quality of the samples. Reverse transcription was performed using SuperScript VILO cDNA Synthesis kit from Invitrogen and gene expression was analyzed using TaqMan Gene expression Assay (Applied Biosystems). GAPDH was used as normalizer.

6.4.5 Quantitative RT-PCR detection of mRNAs

Gene expression was analysed using TaqMan Gene expression Assay (Applied Biosystems). More in details, 0.1 ng cDNA was amplified, in triplicate, in a reaction volume of 25 µl with 10 pMol of each gene-specific primer and the SYBR-green PCR MasterMix (Applied Biosystems). Real-time PCR was performed on the 14 ABI/Prism 7700 Sequence Detector System (PerkinElmer/Applied Biosystems), using a pre-PCR step of 10 min at 95°C, followed by 40 cycles of 15 s at 95°C and 60 s at 60°C. Specificity of the amplified products was confirmed by melting curve analysis (Dissociation Curve TM; PerkinElmer/Applied Biosystems) and by 6% PAGE. Samples were amplified with primers for each gene (listed in the table below) The Ct values were normalized to the GAPDH curve. Results were quantified using the $2^{-\Delta\Delta CT}$ method. PCR experiments were performed in triplicate.

Gene name	**Primer assay ID**
GADPH	Hs99999905_m1 Mm99999915_g1

EFA6A	Hs00160539_m1 Mm01194193_m1
EFA6C	Hs00260268_m1 Mm01158081_m1
EFA6D	Hs00209633_m1 Mm01351099_m1
EFA6B	Hs00202892_m1 Mm00617130_m1
Cytohesin 1	Hs00245092_m1 Mm01248760_m1
Cytohesin 2	Hs00244669_m1 Mm01194052_g1
Cytohesin 3	Hs01028931_m1 Mm01201634_m1

6.4.6 Cell lysis

After washing with PBS 1x, cells were lysed in JS buffer directly on the plates using a cell-scraper. About 200 µl of JS buffer/10 cm plates were used. Lysates were incubated on ice for 10 minutes and spun at 13200 rpm for 10 min at 4ºC. The surnatant was transferred into a new eppendorf and protein concentration was measured by the Bradford assay (Biorad), following manufactur's instructions.

6.5 Imaging techniques

6.5.1 Immunofluorescence

Cells were plated on glass coverslips (pre-incubated with 0.5% gelatin in PBS at 37˚C for 30 minutes in the case of MEFs). After 24 h, cells were processed for epifluorescence or indirect immunofluorescence microscopy. Cells were fixed in 4% paraformaldehyde for 10', washed with PBS and permeabilized in PBS 0,1% Triton X-100 for 10 minutes at room temperature (RT). To prevent non-specific binding of the antibodies, cells were then incubated with PBS in the presence of 1 % BSA for 10 minutes.

The coverslips were then gently deposited, face down, on 50 µl of primary antibody diluted in PBS 1% BSA, spotted on Parafilm. After 40 minutes of incubation at RT, coverslips were transferred into 12 well plates and washed three times with PBS. Cells were then incubated for 40 minutes at RT with the appropriate secondary antibody. F-actin

was detected by staining with Alexa 488 or Alexa 594-conjugated phalloidin (Molecular Probes) at a concentration of 6.7 U/mL.

After three washes in PBS, coverslips were transferred into 12 well plates and incubated in PBS containing DAPI (1:3000) for 5 minutes at RT. Coverslips were washed three times in PBS coverslips and mounted in mowiol (20% Mowiol (Sigma), 5% Glycerol, 2.5% DABCO (Molecular Probes), 0.02% NaN3 in PBS) and examined by fluorescent optical microscopy or in a 90% glycerol solution containing diazabicyclo-(2.2.2)octane antifade (Sigma) and examined under a Biorad MRC 1024 confocal microscope equipped with a 20 mW Kr-Ar laser for colocalization analysis. Confocal image acquisition was performed in sequential mode to limit channel cross-talk and corrected for residual fluorescence bleed through. Green fluorescence was collected through a 520±35 nm band-pass filter, while the red channel filter was a 605±20 nm band-pass. Images were further processed with the Image J software (Adobe).

For two-photon fluorescence microscopy, a Chameleon-XR (Coherent) Ti:sapphire laser source was directly coupled to the scanning head of a Leica TCS SP5 AOBS confocal microscope using an infrared port. Two-photon activation was performed by irradiating a specific vesicle at λ = 790 nm with a pixel dwell time of 4.9 μs and an activation average power $< p > = 10$ mW. The targeted region was subjected to pulses of high-energy-density infrared light (λ = 790 nm) to induce photoactivation. Each pulse had a 1 s duration, and a time interval of 20 s between pulses was set to avoid photobleaching of the activated molecules. Imaging of the activated proteins was obtained using the 488 nm line of a 20 mW Argon ion laser using a 100× oil N.A. = 1.4 objective HCX PL APO (Leica Microsystems). The spectral window used for collecting fluorescence was 500–600 nm

6.5.2 Si RNA- based screening

A candidate siRNA-based screening was performed to identify endocytic molecules specifically required for the formation of HGF- induced circular dorsal ruffles (CDRs) or

peripheral ruffles**.** HeLa cells were transfected with scrambled control (si CTR) or the indicated specific siRNA and stimulated with HGF (100 ng/mL) and/or EGF (100 ng/mL) for 10 min before fixing and staining with phalloidin. The identification of F-actin–positive apical CDRs and Peripheral ruffles was facilitated by 3D reconstruction of confocal serial z sections**.** The fraction of siRNA-treated HeLa cells forming CDR or PR structures relative to that of control, HGF-stimulated cells was calculated. Three independent experiments were performed and 40 cells/experiment were analyzed.

6.5.3 CDR formation assay

To evaluate CDR formation HeLa cells were seed on matrigel coated coverslips. To perform the coating, matrigel was diluted at 0.5 mg/mL in cold 50% DMEM/F12 (without serum) on ice. Then a refrigerated 6-well plate with coverslips placed was putted on ice and 1mL of solution was added and homogeneously distributed. Then the plate was incubated 1h at RT. After two washes with PBS, 75.000-100.000 HeLa cells were seed for 48h until to perform the serum starvation and the HGF stimulation.

6.5.4 Single cell migration assay

Single cells migration was monitored as followed. Briefly, si CTR and si NUMB HeLa cells, upon 24h of interference, were seeded sparsely in a 6-well plate ($2*10^4$ cells/well) in complete medium. After 24h cells were serum starved for 2h and stimulated with 100 ng/mL HGF. Random cell motility was monitored over a 19 hours period. Pictures were taken every 5 minutes from 10 positions/condition, using a motorized Olympus Scan^R inverted microscope with 40X objective. All the experiments were performed using an environmental microscope incubator set to 37°C and 5% CO_2 perfusion. Single cells were manually tracked using Manual Tracking Tool ImageJ software plugin. Elongation Index was calculated as the ratio between the major and the minor axis. Distance and velocity were obtained by Chemotaxis and Migration Tool ImageJ software plugin.

6.5.5 Invasion assay

Cell invasion assays were performed using a BD BioCoat GFR Matrigel Invasion Chamber (BD Biosciences) composed of a polycarbonate membrane, containing 8 μm pores, covered with a thin layer of GFR Matrigel Basement Membrane Matrix. Equal number of cells ($2.5*10^4$) were seeded into the upper chamber of the transwell and allowed to migrate for 72 h. The lower chamber additionally contained HGF (100 ng/mL). Cells were fixed with 4% paraformaldehyde for 10 min, washed with PBS and stained with TRITC phalloidin. Cells were analyzed by serial confocal Z sections, taken from the top of the matrigel to the bottom of the supporting plastic porous filter. The number of cells was counted in four randomly chosen fields. Data are expressed as the mean +/- s.e.m. of three independent experiments.

6.5.6 MHC class I recycling

si CTR and si NUMB HeLa cells, upon 48h of interference, were washed twice with PBS, and incubated at 16°C for 3h in, CO_2-independent, L-15 medium Leibovitz (Gibco), supplemented with 10% FBS, containing 10 μg/mL of mouse MHC I antibody (sc-32235). Under these conditions, recycling is blocked, whereas internalization proceeds, albeit at a reduced rate(Punnonen, Ryhanen, and Marjomaki 1998). The cells were washed twice with ice-cold PBS, three times with acid wash buffer (0.5M NaCl, 0.5 M acetic acid, pH 2.5), followed by successive rinses with PBS to remove surface antibody and complete medium was added. The cells were then transferred to 37°C to allow recycling of internalized MHC I. At various time points, cells were harvested on ice in PBS 10 mM EDTA, transferred in a clean tube and washed once in PBS 1% BSA. Pellet was incubated with secondary antibody resuspended in PBS 1% BSA. Cells were washed three times with PBS 1% BSA. Cells were fixed in 2% formaldeahyde for 20' on ice. Cells were washed once in PBS 1% BSA, resuspendend in PBS and kepped at 4C until FACS analysis. The amount of MHC

class I recycled at different time points was calculated as percentage of total MHC class I internalized at time 0 (t0).

6.5.7 In situ proximity ligation assay (PLA)

We detected the association in situ between NUMB-FLAG and GFP-EFA6B with a Duolink II detection kit (Olink Bioscience), according to the manufacturer's instructions. Upon fixation in 4%PFA, cells were incubated 10' with blocking solution (PBS, 0.1 % Tween 20, 1% BSA). Primary antibodies against FLAG and GFP were incubated in the presence of blocking solution (PBS, 0.05 Tween 20, 1% BSA). This was followed by incubation with secondary antibodies conjugated to oligonucleotides that are ligated to form a closed circle in the presence of Duolink Ligation Solution(Soderberg et al. 2006). In the final step, we added DNA polymerase in order to amplify ligated oligos, which were detected using complementary, fluorescently labeled oligonucleotides.

6.6 Biochemical procedures

6.6.1 SDS polyacrylamide gel electrophoresis (SDS PAGE)

Gels for resolution of proteins were made from a 30%, 37.5:1 mix of acrylamide:bisacrylamide (Sigma). As polymerisation catalysts, 10% ammonium persulphate (APS) and TEMED (Fluka) were used.

6.6.2 Western blot

Desired amounts of proteins were loaded onto 0.75-1.5 mm thick polyacrylamide gels for electrophoresis (Biorad). Proteins were transferred in Western transfer tanks (Biorad) to nitrocellulose (Schleicher and Schuell) in Western Transfer buffer 1x (diluted in 20% methanol) at constant Voltage (100V for 1 hour or 30V overnight). PonceauS colouring was used to reveal roughly the amount of proteins transferred on the filters. Filters were blocked 1 hour (or overnight) in 5% milk or 5% BSA in TBS 0.1% Tween (TBS-T).

After blocking, filters were incubated with the primary antibody, diluted in TBS-T 5% milk, for one hour at room temperature, or overnight at 4˚C, followed by three washes of five minutes each in TBS-T and then incubated with the appropriate peroxidase-conjugated secondary antibody diluted in TBS-T for 1 hour. After the incubation with the secondary antibody, the filter was washed three times in TBS-T and the bound secondary antibody was revealed using the ECL (Enhanced Chemiluminescence) method (Amersham).

6.6.3 Co-immunoprecipitation assay

Lysates prepared in JS buffer were incubated in the presence the anti FLAG M2 affinity gel (a purified murine IgG1 monoclonal antibody covalently attached to agarose, Sigma Aldrich) for two cycles of 1 h each at 4°C with rocking.

Immunoprecipitates were then washed 3 times in JS buffer. After washing, beads were resuspended in 1:1 volume of 2x SDS-PAGE Sample Buffer, boiled for 10 min at 95°C, centrifuged for 1 minute and then loaded onto polyacrylamide gels.

6.6.4 Pull-down assay

Lysates prepared in JS buffer were incubated in the presence of 0.5 μM of GST tagged purified proteins immobilized on beads for 1 h at 4°C under mild agitation.

Beads were then washed 3 times in JS buffer. After washing, beads were resuspended in 1:1 volume of 2x SDS-PAGE Sample Buffer, boiled for 10 min at 95°C, centrifuged for 1 minute and then loaded onto polyacrylamide gels.

6.6.5 *In vitro* binding assay

0.5 μM of purified proteins immobilized on beads were incubated with indicated amount of purified protein in JS buffer for 1h at 4°C under mild agitation.

Beads were then washed 3 times in JS buffer. After washing, beads were resuspended in 1:1 volume of 2x SDS-PAGE Sample Buffer, boiled for 10 min at 95°C, centrifuged for 1 minute and then loaded onto polyacrylamide gels.

6.6.6 GST-fusion and His-fusion proteins production

All the GST and His fusion proteins used were product in bacteria using *E. coli* BL21 Rosetta (DE3) competent cells transformed with the pGEX6P1 or pET30 vector in which the desired construct had been cloned.

6.6.6.1 Bacterial culture

E. coli BL21 Rosetta (DE3) cells picked from individual colonies, transformed with the indicated GST-fusion or His-fusion constructs, were used to inoculate 200 mL of LB medium (containing ampicillin at 50 μg/mL) and were grown overnight at 37°C. Between 10 and 100 mL of the overnight culture was diluted in 1 litre of LB and was grown at 37°C (240 rpm shaking) till it reached approximately OD=0.4-0.6.

Then IPTG was used to induce the protein production using different conditions depending on the protein:

Construct	**IPTG concentration**	**Time**	**Temperature**
GST NUMB FL, PTB, PRR1, PRR2	0.3mM	6-8 h	18°C
GST EFA6B 1-738 aa	0.2mM	o/n	18°C
GST PTB EPS8	0.3mM	3h	37°C
GST	1mM	3h	37°C
His NUMB FL and PTB	0.1 mM	3h	30°C

After the induction cells were pelleted down at 6000 rpm for 15 minutes at 4°C and pellets were used immediately or conserved at -80°C after washing in PBS 1X.

6.6.6.2 Protein production

Pellets were suspended in GST-lysis buffer or His-lysis buffer based on the tag (15mL for 1L culture). Samples were sonicated 3 times for 30 seconds/each on ice and were pelleted down at 13200 rpm for 30 minutes at 4°C using a JA 20 Beckman rotor or at 40000 rpm for 45 minutes at 4°C using a 55.2 Ti Beckman rotor. 1 mL of glutathione-sepharose beads

(Amersham) or 5 mL of Ni-NTA (Qiagen), previously washed 3 times with GST-lysis buffer or His lysis buffer respectively, was added to the surnatant and samples were incubated 1-2 hour at 4°C while rocking. Beads were then washed 3 times (with 5 minutes of incubation at 4°C each) in the GST or His lysis solution. GST-proteins were resuspendend 50% slurry in the GST-lysis solution. The quantification was achieved in an SDS PAGE gel using a titration curve with BSA.

GST-lysis buffer

2x TBS

0.5 mM EDTA

10% Glycerol

protease inhibitor cocktail (Roche, Basel, Switzerland) (freshly added)

1 mM DTT (freshly added)

His-lysis buffer

2x TBS

2 mM ß-mercaptoehanol

10% Glycerol

protease inhibitor cocktail (Roche, Basel, Switzerland) (freshly added)

20 mM Imidazole

6.6.6.3 Numb His-fusion protein elution

Beads were washed once in the washing solution and than subjected to six cycles of elution in the elution buffer in Poly-Prep Chromatography columns (Biorad). Eluted proteins were collected in clean tubes containing 1mM EDTA and 1 mM DTT. The best fraction identified in SDS-PAGE gel were collected together and dialyzed overnight in dialysis buffer. After dialysis, precipitates were removed by centrifugation and the surnatant was diluted to have finally 40 mM NaCl and purified through ion exchange chromatography using a Resource Q column (GE Healthcare Life Science), on an AKTA purifier system

(Amersham Bioscience). The fractions in the area under the curve were collected together, concentrated with Vivaspin concentrators (Vivaspin 20 MWCO 100000, Sartorius Stedim Biotech), flesh frozen using liquid Nitrogen and stored at -80˚C.

Washing buffer

1X TBS

50 mM Imidazole

10% Glycerol

Elution buffer

1X TBS

200 mM Imidazole

10% Glycerol

Dialysis and storage buffer

20 mM Tris pH 7.1

10% Glycerol

0.5 mM EDTA

1mM DTT

160 mM NaCl

6.6.6.4 Numb PTB His-fusion protein elution

Beads were washed once in the washing solution and than subjected to six cycles of elution in the elution buffer in Poly-Prep Chromatography columns (Biorad). Eluted proteins were collected in clean tubes containing 1mM EDTA and 1 mM DTT. The best fraction identified in SDS-PAGE gel were collected together and dialyzed overnight in dialysis buffer. After dialysis, precipitates were removed by centrifugation and the surnatant was concentrated in Vivaspin concentrators (Vivaspin 20 MWCO 3000, GE Healthcare Life Science) and purified through gel filtration using a Superdex 200 10\30 column (GE Healthcare Life Science), equilibrated with storage buffer, on an AKTA purifier system

(Amersham Bioscience). Proteins were loaded in 500 µl volume using a Hamilton syringe. Typical flow rate was 0.5 mL\min. Finally, the fractions in the area under the curve were collected together, concentrated with Vivaspin concentrators (Vivaspin 20 MWCO 100000, Sartorius Stedim Biotech), flesh frozen using liquid Nitrogen and stored at -80˚C.

Washing buffer

1X TBS

50 mM Imidazole

Elution buffer

1X TBS

200 mM Imidazole

Dialysis buffer

1X TBS

0.5 mM EDTA

1mM DTT

Storage buffer

20 mM Tris pH 7.6

5% Glycerol

10 mM NaCl

0.5 mM EDTA

1 mM DTT

6.6.7 MBP EFA6B protein production

The MBP EFA6B protein used was produced in Baculovirus system. EFA6B was cloned in pBAC_His-MBP-TEV vector.

6.6.7.1 Transposition

Transposition was made using DH10MultiBac-YFP electro competent cells (a gift from A. Musacchio) that were electroporeted in presence of 1 µl of DNA from average yeld miniprep.

Selection of the recombinant bacteria was made after plating on LB plates containing 50 µg/mL kanamycin, 7 µg/mL gentamycin, 10 µg/mL tetracycline, 200 µg/mL X-gal, 40 µg/mL IPTG at least 48 hours.

White recombinant proteins were selected and bacmid DNA was isolate using the Promega, Wizard Plus SV Minipreps kit with a slight protocol modification. Because the bacmid DNA is to big to be eluted the kit columns, DNA was extracted using isopropanol precipitation.

6.6.7.2 Virus production

The DNA was used then to transfect Sf21 insect cells (Invitrogen) in order to produce the virus. Sf21 cells were plated at $0.5*10^6$/mL in a six well plate and transfected using Insectogene reagent (Biontex Laboratories), according to manufacturer's instruction. Cells transfection was monitored looking at the appearance of YFP positive cells. After 72 hours the surnatant was collected (this was the V0, primary stock virus production). The virus was amplified in H5 cells (Invitrogen). 25 mL of H5 cells at $0.5*10^6$/mL were infected using 1.5 mL of the V0 virus. Cells infection was monitored looking at appearance if YFP positive cells and at the cells growth arrest that is caused by the viral infection. After 72 hours from the cell growth arrest the surnatant was collected (this is the V1 generation). The virus was amplified a second time using 200 mL of H5 cells infected with 2.5 mL of the V1 virus, following the same protocol.

6.6.7.3 Protein production

Protein production was finally made following the same protocol but starting from 500 mL of H5 cells at $0.5*10^6$ cells/mL infected with 12.5 mL of V2 virus.

For protein purification the cells were harvested three days after infection. After 15 minutes centrifugation at 1200 rpm Pellets were suspended in lysis buffer (25mL for 1L culture) or conserved at -80 °C after washing in PBS1X. Samples were sonicated 3 times for 30 seconds/each on ice and were pelleted down at 45000 rpm for 1 hour at 4°C using a 55.2 Ti Beckman rotor. 1 mL of amylose beads (NEB), previously washed 3 times with lysis buffer, was added to the surnatant and samples were incubated 1-2 hour at 4°C while rocking. Beads were then washed 3 times (with 5 minutes of incubation at 4°C each) lysis solution.

Lysis solution

2x TBS

0.5 mM EDTA

10% Glycerol

protease inhibitor cocktail (Roche, Basel, Switzerland) (freshly added)

1 mM DTT (freshly added)

6.6.7.4 MBP EFA6B protein elution

Beads were washed once in the lysis solution and than subjected to six cycles of elution in the elution buffer in Poly-Prep Chromatography columns (Biorad). Eluted proteins were collected in clean tubes. The best fraction identified in SDS-PAGE gel were collected together and dialyzed overnight in dialysis buffer. After dialysis precipitates were removed by centrifugation and the surnatant was concentrated in Vivaspin concentrator (Vivaspin 20 MWCO 100000, Sartorius Stedim Biotech), flesh frozen using liquid Nitrogen and stored at –80˚C.

Elution buffer

2X TBS

10% Glycerol

10 mM Amylose

0.5 mM EDTA

1 mM DTT (freshly added)

Dialysis and storage buffer

1X TBS

10% Glycerol

0.5 mM EDTA

1mM DTT

6.7 Statistical analysis

In the CDR formation assay 20 fields were analyzed for each sample and the percentage of cells forming CDRs (number of cells with CDRs/total number of cells in the field) was scored. In case of re-infection with GFP constructs, only GFP-positive cells were considered for the analysis. All data are presented as the mean±standard errors of mean (s.e.m.) from at least three independent experiments.

A Student's t-test was used to calculate the P-values.

REFERENCES

Al-Awar, O., H. Radhakrishna, N. N. Powell, and J. G. Donaldson. 2000. 'Separation of membrane trafficking and actin remodeling functions of ARF6 with an effector domain mutant', *Mol Cell Biol*, 20: 5998-6007.

Albertinazzi, C., L. Za, S. Paris, and I. de Curtis. 2003. 'ADP-ribosylation factor 6 and a functional PIX/p95-APP1 complex are required for Rac1B-mediated neurite outgrowth', *Mol Biol Cell*, 14: 1295-307.

Amor, J. C., D. H. Harrison, R. A. Kahn, and D. Ringe. 1994. 'Structure of the human ADP-ribosylation factor 1 complexed with GDP', *Nature*, 372: 704-8.

Amson, R., S. Pece, A. Lespagnol, R. Vyas, G. Mazzarol, D. Tosoni, I. Colaluca, G. Viale, S. Rodrigues-Ferreira, J. Wynendaele, O. Chaloin, J. Hoebeke, J. C. Marine, P. P. Di Fiore, and A. Telerman. 2012. 'Reciprocal repression between P53 and TCTP', *Nat Med*, 18: 91-9.

Aranda, V., M. E. Nolan, and S. K. Muthuswamy. 2008. 'Par complex in cancer: a regulator of normal cell polarity joins the dark side', *Oncogene*, 27: 6878-87.

Arcuri, F., S. Papa, A. Carducci, R. Romagnoli, S. Liberatori, M. G. Riparbelli, J. C. Sanchez, P. Tosi, and M. T. del Vecchio. 2004. 'Translationally controlled tumor protein (TCTP) in the human prostate and prostate cancer cells: expression, distribution, and calcium binding activity', *Prostate*, 60: 130-40.

Baass, P. C., G. M. Di Guglielmo, F. Authier, B. I. Posner, and J. J. Bergeron. 1995. 'Compartmentalized signal transduction by receptor tyrosine kinases', *Trends in cell biology*, 5: 465-70.

Balana, M. E., F. Niedergang, A. Subtil, A. Alcover, P. Chavrier, and A. Dautry-Varsat. 2005. 'ARF6 GTPase controls bacterial invasion by actin remodelling', *J Cell Sci*, 118: 2201-10.

Balasubramanian, N., D. W. Scott, J. D. Castle, J. E. Casanova, and M. A. Schwartz. 2007. 'Arf6 and microtubules in adhesion-dependent trafficking of lipid rafts', *Nat Cell Biol*, 9: 1381-91.

Bartek, J., J. Bartkova, B. Vojtesek, Z. Staskova, A. Rejthar, J. Kovarik, and D. P. Lane. 1990. 'Patterns of expression of the p53 tumour suppressor in human breast tissues and tumours in situ and in vitro', *Int J Cancer*, 46: 839-44.

Bartek, J., R. Iggo, J. Gannon, and D. P. Lane. 1990. 'Genetic and immunochemical analysis of mutant p53 in human breast cancer cell lines', *Oncogene*, 5: 893-9.

Bellusci, S., Y. Furuta, M. G. Rush, R. Henderson, G. Winnier, and B. L. Hogan. 1997. 'Involvement of Sonic hedgehog (Shh) in mouse embryonic lung growth and morphogenesis', *Development*, 124: 53-63.

Berdnik, D., T. Torok, M. Gonzalez-Gaitan, and J. A. Knoblich. 2002. 'The endocytic protein alpha-Adaptin is required for numb-mediated asymmetric cell division in Drosophila', *Dev Cell*, 3: 221-31.

Beronja, S., P. Laprise, O. Papoulas, M. Pellikka, J. Sisson, and U. Tepass. 2005. 'Essential function of Drosophila Sec6 in apical exocytosis of epithelial photoreceptor cells', *J Cell Biol*, 169: 635-46.

Blankenship, J. T., M. T. Fuller, and J. A. Zallen. 2007. 'The Drosophila homolog of the Exo84 exocyst subunit promotes apical epithelial identity', *J Cell Sci*, 120: 3099-110.

Bogdanovic, O., M. Delfino-Machin, M. Nicolas-Perez, M. P. Gavilan, I. Gago-Rodrigues, A. Fernandez-Minan, C. Lillo, R. M. Rios, J. Wittbrodt, and J. R. Martinez-Morales. 2012. 'Numb/Numbl-Opo antagonism controls retinal epithelium morphogenesis by regulating integrin endocytosis', *Dev Cell*, 23: 782-95.

Bonifacino, J. S., and B. S. Glick. 2004. 'The mechanisms of vesicle budding and fusion', *Cell*, 116: 153-66.

Bork, P., and B. Margolis. 1995. 'A phosphotyrosine interaction domain', *Cell*, 80: 693-4.
Boshans, R. L., S. Szanto, L. van Aelst, and C. D'Souza-Schorey. 2000. 'ADP-ribosylation factor 6 regulates actin cytoskeleton remodeling in coordination with Rac1 and RhoA', *Mol Cell Biol*, 20: 3685-94.
Boulakirba, S., E. Macia, M. Partisani, S. Lacas-Gervais, F. Brau, F. Luton, and M. Franco. 2014. 'Arf6 exchange factor EFA6 and endophilin directly interact at the plasma membrane to control clathrin-mediated endocytosis', *Proc Natl Acad Sci U S A*, 111: 9473-8.
Bretscher, M. S. 1983. 'Distribution of receptors for transferrin and low density lipoprotein on the surface of giant HeLa cells', *Proc Natl Acad Sci U S A*, 80: 454-8.
Bretscher, M. S., and C. Aguado-Velasco. 1998a. 'EGF induces recycling membrane to form ruffles', *Curr Biol*, 8: 721-4.
———. 1998b. 'Membrane traffic during cell locomotion', *Curr Opin Cell Biol*, 10: 537-41.
Bretscher MS, Aguado-Velasco C. 1998. 'Membrane traffic during cell locomotion', *Curr Opin Cell Biol*.
Bric, A., C. Miething, C. U. Bialucha, C. Scuoppo, L. Zender, A. Krasnitz, Z. Xuan, J. Zuber, M. Wigler, J. Hicks, R. W. McCombie, M. T. Hemann, G. J. Hannon, S. Powers, and S. W. Lowe. 2009. 'Functional identification of tumor-suppressor genes through an in vivo RNA interference screen in a mouse lymphoma model', *Cancer Cell*, 16: 324-35.
Brown, H. A., S. Gutowski, C. R. Moomaw, C. Slaughter, and P. C. Sternweis. 1993. 'ADP-ribosylation factor, a small GTP-dependent regulatory protein, stimulates phospholipase D activity', *Cell*, 75: 1137-44.
Buccione, R., J. D. Orth, and M. A. McNiven. 2004. 'Foot and mouth: podosomes, invadopodia and circular dorsal ruffles', *Nat Rev Mol Cell Biol*, 5: 647-57.
Cans, C., B. J. Passer, V. Shalak, V. Nancy-Portebois, V. Crible, N. Amzallag, D. Allanic, R. Tufino, M. Argentini, D. Moras, G. Fiucci, B. Goud, M. Mirande, R. Amson, and A. Telerman. 2003. 'Translationally controlled tumor protein acts as a guanine nucleotide dissociation inhibitor on the translation elongation factor eEF1A', *Proc Natl Acad Sci U S A*, 100: 13892-7.
Casanova, J. E. 2007a. 'PARtitioning numb', *EMBO Rep*, 8: 233-5.
———. 2007b. 'Regulation of Arf activation: the Sec7 family of guanine nucleotide exchange factors', *Traffic*, 8: 1476-85.
Caswell, P. T., H. J. Spence, M. Parsons, D. P. White, K. Clark, K. W. Cheng, G. B. Mills, M. J. Humphries, A. J. Messent, K. I. Anderson, M. W. McCaffrey, B. W. Ozanne, and J. C. Norman. 2007. 'Rab25 associates with alpha5beta1 integrin to promote invasive migration in 3D microenvironments', *Dev Cell*, 13: 496-510.
Chardin, P., S. Paris, B. Antonny, S. Robineau, S. Beraud-Dufour, C. L. Jackson, and M. Chabre. 1996. 'A human exchange factor for ARF contains Sec7- and pleckstrin-homology domains', *Nature*, 384: 481-4.
Chen SH1, Wu PS, Chou CH, Yan YT, Liu H, Weng SY, Yang-Yen HF. 2007. 'A knockout mouse approach reveals that TCTP functions as an essential factor for cell proliferation and survival in a tissue- or cell type-specific manner', *Mol Biol Cell*.
Claing, A., W. Chen, W. E. Miller, N. Vitale, J. Moss, R. T. Premont, and R. J. Lefkowitz. 2001. 'beta-Arrestin-mediated ADP-ribosylation factor 6 activation and beta 2-adrenergic receptor endocytosis', *J Biol Chem*, 276: 42509-13.
Cockcroft, S., G. M. Thomas, A. Fensome, B. Geny, E. Cunningham, I. Gout, I. Hiles, N. F. Totty, O. Truong, and J. J. Hsuan. 1994. 'Phospholipase D: a downstream effector of ARF in granulocytes', *Science*, 263: 523-6.
Coda, L., A. E. Salcini, S. Confalonieri, G. Pelicci, T. Sorkina, A. Sorkin, P. G. Pelicci, and P. P. Di Fiore. 1998. 'Eps15R is a tyrosine kinase substrate with characteristics

of a docking protein possibly involved in coated pits-mediated internalization', *J Biol Chem*, 273: 3003-12.
Colaluca, I. N., D. Tosoni, P. Nuciforo, F. Senic-Matuglia, V. Galimberti, G. Viale, S. Pece, and P. P. Di Fiore. 2008. 'NUMB controls p53 tumour suppressor activity', *Nature*, 451: 76-80.
Confalonieri, S., and P. P. Di Fiore. 2002. 'The Eps15 homology (EH) domain', *FEBS Lett*, 513: 24-9.
Confalonieri, S., A. E. Salcini, C. Puri, C. Tacchetti, and P. P. Di Fiore. 2000. 'Tyrosine phosphorylation of Eps15 is required for ligand-regulated, but not constitutive, endocytosis', *J Cell Biol*, 150: 905-12.
Conner SD, Schmid SL. 2003. 'Regulated portals of entry into the cell', *Nature*.
Cotton, M., N. Benhra, and R. Le Borgne. 2013. 'Numb inhibits the recycling of Sanpodo in Drosophila sensory organ precursor', *Curr Biol*, 23: 581-7.
Coumailleau, F., and M. Gonzalez-Gaitan. 2008. 'From endocytosis to tumors through asymmetric cell division of stem cells', *Curr Opin Cell Biol*, 20: 462-9.
Couturier, L., K. Mazouni, and F. Schweisguth. 2013. 'Numb Localizes at Endosomes and Controls the Endosomal Sorting of Notch after Asymmetric Division in Drosophila', *Current Biology*, 23: 588-93.
D'Souza-Schorey, C. 2005. 'Disassembling adherens junctions: breaking up is hard to do', *Trends Cell Biol*, 15: 19-26.
D'Souza-Schorey, C., R. L. Boshans, M. McDonough, P. D. Stahl, and L. Van Aelst. 1997. 'A role for POR1, a Rac1-interacting protein, in ARF6-mediated cytoskeletal rearrangements', *EMBO J*, 16: 5445-54.
D'Souza-Schorey, C., and P. Chavrier. 2006. 'ARF proteins: roles in membrane traffic and beyond', *Nat Rev Mol Cell Biol*, 7: 347-58.
D'Souza-Schorey, C., G. Li, M. I. Colombo, and P. D. Stahl. 1995. 'A regulatory role for ARF6 in receptor-mediated endocytosis', *Science*, 267: 1175-8.
Dai, P., H. Akimaru, Y. Tanaka, T. Maekawa, M. Nakafuku, and S. Ishii. 1999. 'Sonic Hedgehog-induced activation of the Gli1 promoter is mediated by GLI3', *J Biol Chem*, 274: 8143-52.
Davies, M., M. Robinson, E. Smith, S. Huntley, S. Prime, and I. Paterson. 2005. 'Induction of an epithelial to mesenchymal transition in human immortal and malignant keratinocytes by TGF-beta1 involves MAPK, Smad and AP-1 signalling pathways', *J Cell Biochem*, 95: 918-31.
De Donatis, A., G. Comito, F. Buricchi, M. C. Vinci, A. Parenti, A. Caselli, G. Camici, G. Manao, G. Ramponi, and P. Cirri. 2008. 'Proliferation versus migration in platelet-derived growth factor signaling: the key role of endocytosis', *J Biol Chem*, 283: 19948-56.
De Strooper, B., W. Annaert, P. Cupers, P. Saftig, K. Craessaerts, J. S. Mumm, E. H. Schroeter, V. Schrijvers, M. S. Wolfe, W. J. Ray, A. Goate, and R. Kopan. 1999. 'A presenilin-1-dependent gamma-secretase-like protease mediates release of Notch intracellular domain', *Nature*, 398: 518-22.
Decressac, S., M. Franco, S. Bendahhou, R. Warth, S. Knauer, J. Barhanin, M. Lazdunski, and F. Lesage. 2004. 'ARF6-dependent interaction of the TWIK1 K+ channel with EFA6, a GDP/GTP exchange factor for ARF6', *EMBO Rep*, 5: 1171-5.
del Pozo, M. A., N. B. Alderson, W. B. Kiosses, H. H. Chiang, R. G. Anderson, and M. A. Schwartz. 2004. 'Integrins regulate Rac targeting by internalization of membrane domains', *Science*, 303: 839-42.
del Pozo, M. A., N. Balasubramanian, N. B. Alderson, W. B. Kiosses, A. Grande-Garcia, R. G. Anderson, and M. A. Schwartz. 2005. 'Phospho-caveolin-1 mediates integrin-regulated membrane domain internalization', *Nat Cell Biol*, 7: 901-8.
Derrien, V., C. Couillault, M. Franco, S. Martineau, P. Montcourrier, R. Houlgatte, and P. Chavrier. 2002. 'A conserved C-terminal domain of EFA6-family ARF6-guanine

nucleotide exchange factors induces lengthening of microvilli-like membrane protrusions', *J Cell Sci*, 115: 2867-79.
Dho, S. E., M. B. French, S. A. Woods, and C. J. McGlade. 1999. 'Characterization of four mammalian numb protein isoforms. Identification of cytoplasmic and membrane-associated variants of the phosphotyrosine binding domain', *J Biol Chem*, 274: 33097-104.
Di Fiore, P. P., P. G. Pelicci, and A. Sorkin. 1997. 'EH: a novel protein-protein interaction domain potentially involved in intracellular sorting', *Trends Biochem Sci*, 22: 411-3.
Di Guglielmo, G. M., C. Le Roy, A. F. Goodfellow, and J. L. Wrana. 2003. 'Distinct endocytic pathways regulate TGF-beta receptor signalling and turnover', *Nat Cell Biol*, 5: 410-21.
Di Marcotullio, L., E. Ferretti, A. Greco, E. De Smaele, A. Po, M. A. Sico, M. Alimandi, G. Giannini, M. Maroder, I. Screpanti, and A. Gulino. 2006. 'Numb is a suppressor of Hedgehog signalling and targets Gli1 for Itch-dependent ubiquitination', *Nat Cell Biol*, 8: 1415-23.
Disanza, A., E. Frittoli, A. Palamidessi, and G. Scita. 2009. 'Endocytosis and spatial restriction of cell signaling', *Mol Oncol*, 3: 280-96.
Doherty, G. J., and H. T. McMahon. 2009. 'Mechanisms of endocytosis', *Annu Rev Biochem*, 78: 857-902.
Donaldson, J. G. 2003. 'Multiple roles for Arf6: sorting, structuring, and signaling at the plasma membrane', *J Biol Chem*, 278: 41573-6.
Donaldson, J. G., D. Finazzi, and R. D. Klausner. 1992. 'Brefeldin A inhibits Golgi membrane-catalysed exchange of guanine nucleotide onto ARF protein', *Nature*, 360: 350-2.
Donaldson, J. G., and A. Honda. 2005. 'Localization and function of Arf family GTPases', *Biochem Soc Trans*, 33: 639-42.
Donaldson, J. G., and C. L. Jackson. 2011a. 'ARF family G proteins and their regulators: roles in membrane transport, development and disease', *Nat Rev Mol Cell Biol*, 12: 362-75.
Donaldson, JG., and CL. Jackson. 2011b. 'ARF family G proteins and their regulators: roles in membrane transport, development and disease', *Nat Rev Mol Cell Biol.*, 12: 362-75.
Echelard, Y., D. J. Epstein, B. St-Jacques, L. Shen, J. Mohler, J. A. McMahon, and A. P. McMahon. 1993. 'Sonic hedgehog, a member of a family of putative signaling molecules, is implicated in the regulation of CNS polarity', *Cell*, 75: 1417-30.
el-Deiry, W. S., S. E. Kern, J. A. Pietenpol, K. W. Kinzler, and B. Vogelstein. 1992. 'Definition of a consensus binding site for p53', *Nat Genet*, 1: 45-9.
Farmer, G., J. Bargonetti, H. Zhu, P. Friedman, R. Prywes, and C. Prives. 1992. 'Wild-type p53 activates transcription in vitro', *Nature*, 358: 83-6.
Fazioli, F., L. Minichiello, B. Matoskova, W. T. Wong, and P. P. Di Fiore. 1993. 'eps15, a novel tyrosine kinase substrate, exhibits transforming activity', *Mol Cell Biol*, 13: 5814-28.
Franco, M., P. J. Peters, J. Boretto, E. van Donselaar, A. Neri, C. D'Souza-Schorey, and P. Chavrier. 1999. 'EFA6, a sec7 domain-containing exchange factor for ARF6, coordinates membrane recycling and actin cytoskeleton organization', *EMBO J*, 18: 1480-91.
Friedl, P., S. Borgmann, and E. B. Brocker. 2001. 'Amoeboid leukocyte crawling through extracellular matrix: lessons from the Dictyostelium paradigm of cell movement', *J Leukoc Biol*, 70: 491-509.
Friedl, P., and K. Wolf. 2003. 'Tumour-cell invasion and migration: diversity and escape mechanisms', *Nat Rev Cancer*, 3: 362-74.

Frittoli, E., A. Palamidessi, P. Marighetti, S. Confalonieri, F. Bianchi, C. Malinverno, G. Mazzarol, G. Viale, I. Martin-Padura, M. Garre, D. Parazzoli, V. Mattei, S. Cortellino, G. Bertalot, P. P. Di Fiore, and G. Scita. 2014. 'A RAB5/RAB4 recycling circuitry induces a proteolytic invasive program and promotes tumor dissemination', *J Cell Biol*, 206: 307-28.

Furthauer, M., and M. Gonzalez-Gaitan. 2009. 'Endocytosis, asymmetric cell division, stem cells and cancer: unus pro omnibus, omnes pro uno', *Mol Oncol*, 3: 339-53.

Gillingham, A. K., and S. Munro. 2007. 'The small G proteins of the Arf family and their regulators', *Annu Rev Cell Dev Biol*, 23: 579-611.

Goldberg, J. 1998. 'Structural basis for activation of ARF GTPase: mechanisms of guanine nucleotide exchange and GTP-myristoyl switching', *Cell*, 95: 237-48.

Goldstein, B., and I. G. Macara. 2007. 'The PAR proteins: fundamental players in animal cell polarization', *Dev Cell*, 13: 609-22.

Gonczy, P. 2008. 'Mechanisms of asymmetric cell division: flies and worms pave the way', *Nat Rev Mol Cell Biol*, 9: 355-66.

Goodrich, L. V., R. L. Johnson, L. Milenkovic, J. A. McMahon, and M. P. Scott. 1996. 'Conservation of the hedgehog/patched signaling pathway from flies to mice: induction of a mouse patched gene by Hedgehog', *Genes Dev*, 10: 301-12.

Guo, M., L. Y. Jan, and Y. N. Jan. 1996. 'Control of daughter cell fates during asymmetric division: interaction of Numb and Notch', *Neuron*, 17: 27-41.

Gupta, R., P. Vyas, and T. Enver. 2009. 'Molecular targeting of cancer stem cells', *Cell Stem Cell*, 5: 125-6.

H, Stenmark. 2009. 'Rab GTPases as coordinators of vesicle traffic', *Nat Rev Mol Cell Biol.*

Hanyaloglu, A. C., and M. von Zastrow. 2008. 'Regulation of GPCRs by endocytic membrane trafficking and its potential implications', *Annu Rev Pharmacol Toxicol*, 48: 537-68.

Hashimoto, S., S. Mikami, H. Sugino, A. Yoshikawa, A. Hashimoto, Y. Onodera, S. Furukawa, H. Handa, T. Oikawa, Y. Okada, M. Oya, and H. Sabe. 2016. 'Lysophosphatidic acid activates Arf6 to promote the mesenchymal malignancy of renal cancer', *Nat Commun*, 7: 10656.

Hashimoto, S., Y. Onodera, A. Hashimoto, M. Tanaka, M. Hamaguchi, A. Yamada, and H. Sabe. 2004. 'Requirement for Arf6 in breast cancer invasive activities', *Proc Natl Acad Sci U S A*, 101: 6647-52.

Haupt, Y., R. Maya, A. Kazaz, and M. Oren. 1997. 'Mdm2 promotes the rapid degradation of p53', *Nature*, 387: 296-9.

Hernandez-Deviez, D. J., M. G. Roth, J. E. Casanova, and J. M. Wilson. 2004. 'ARNO and ARF6 regulate axonal elongation and branching through downstream activation of phosphatidylinositol 4-phosphate 5-kinase alpha', *Mol Biol Cell*, 15: 111-20.

Honda, A., M. Nogami, T. Yokozeki, M. Yamazaki, H. Nakamura, H. Watanabe, K. Kawamoto, K. Nakayama, A. J. Morris, M. A. Frohman, and Y. Kanaho. 1999. 'Phosphatidylinositol 4-phosphate 5-kinase alpha is a downstream effector of the small G protein ARF6 in membrane ruffle formation', *Cell*, 99: 521-32.

Hongu, T., Y. Funakoshi, S. Fukuhara, T. Suzuki, S. Sakimoto, N. Takakura, M. Ema, S. Takahashi, S. Itoh, M. Kato, H. Hasegawa, N. Mochizuki, and Y. Kanaho. 2015. 'Arf6 regulates tumour angiogenesis and growth through HGF-induced endothelial beta1 integrin recycling', *Nat Commun*, 6: 7925.

Hoon, J. L., W. K. Wong, and C. G. Koh. 2012. 'Functions and regulation of circular dorsal ruffles', *Mol Cell Biol*, 32: 4246-57.

Howe, C. L., and W. C. Mobley. 2005. 'Long-distance retrograde neurotrophic signaling', *Current opinion in neurobiology*, 15: 40-8.

Hurley, J. H. 2008. 'ESCRT complexes and the biogenesis of multivesicular bodies', *Current opinion in cell biology*, 20: 4-11.

Hutterer, A., and J. A. Knoblich. 2005. 'Numb and alpha-Adaptin regulate Sanpodo endocytosis to specify cell fate in Drosophila external sensory organs', *EMBO Rep*, 6: 836-42.

Iggo, R., K. Gatter, J. Bartek, D. Lane, and A. L. Harris. 1990. 'Increased expression of mutant forms of p53 oncogene in primary lung cancer', *Lancet*, 335: 675-9.

Jarriault, S., C. Brou, F. Logeat, E. H. Schroeter, R. Kopan, and A. Israel. 1995. 'Signalling downstream of activated mammalian Notch', *Nature*, 377: 355-8.

Jekely, G., H. H. Sung, C. M. Luque, and P. Rorth. 2005. 'Regulators of endocytosis maintain localized receptor tyrosine kinase signaling in guided migration', *Dev Cell*, 9: 197-207.

JG, Donaldson. 2005. 'Arfs, phosphoinositides and membrane traffic', *Biochem Soc Trans*.

Jiang, J., and C. C. Hui. 2008. 'Hedgehog signaling in development and cancer', *Dev Cell*, 15: 801-12.

Jiang, X., and A. Sorkin. 2002. 'Coordinated traffic of Grb2 and Ras during epidermal growth factor receptor endocytosis visualized in living cells', *Molecular biology of the cell*, 13: 1522-35.

Jung, J., M. Kim, M. J. Kim, J. Kim, J. Moon, J. S. Lim, M. Kim, and K. Lee. 2004. 'Translationally controlled tumor protein interacts with the third cytoplasmic domain of Na,K-ATPase alpha subunit and inhibits the pump activity in HeLa cells', *J Biol Chem*, 279: 49868-75.

Karaczyn, A., M. Bani-Yaghoub, R. Tremblay, C. Kubu, R. Cowling, T. L. Adams, I. Prudovsky, D. Spicer, R. Friesel, C. Vary, and J. M. Verdi. 2010. 'Two novel human NUMB isoforms provide a potential link between development and cancer', *Neural Dev*, 5: 31.

Kastan, M. B., O. Onyekwere, D. Sidransky, B. Vogelstein, and R. W. Craig. 1991. 'Participation of p53 protein in the cellular response to DNA damage', *Cancer Res*, 51: 6304-11.

Kawasaki, M., K. Nakayama, and S. Wakatsuki. 2005. 'Membrane recruitment of effector proteins by Arf and Rab GTPases', *Curr Opin Struct Biol*, 15: 681-9.

Kermorgant, S., and P. J. Parker. 2008. 'Receptor trafficking controls weak signal delivery: a strategy used by c-Met for STAT3 nuclear accumulation', *The Journal of cell biology*, 182: 855-63.

Kikuchi, A., H. Yamamoto, and S. Kishida. 2007. 'Multiplicity of the interactions of Wnt proteins and their receptors', *Cell Signal*, 19: 659-71.

Klein, S., M. Partisani, M. Franco, and F. Luton. 2008. 'EFA6 facilitates the assembly of the tight junction by coordinating an Arf6-dependent and -independent pathway', *J Biol Chem*, 283: 30129-38.

Knoblich, J. A., L. Y. Jan, and Y. N. Jan. 1995. 'Asymmetric segregation of Numb and Prospero during cell division', *Nature*, 377: 624-7.

Krauss, M., M. Kinuta, M. R. Wenk, P. De Camilli, K. Takei, and V. Haucke. 2003. 'ARF6 stimulates clathrin/AP-2 recruitment to synaptic membranes by activating phosphatidylinositol phosphate kinase type Igamma', *J Cell Biol*, 162: 113-24.

Krueger, E. W., J. D. Orth, H. Cao, and M. A. McNiven. 2003. 'A dynamin-cortactin-Arp2/3 complex mediates actin reorganization in growth factor-stimulated cells', *Mol Biol Cell*, 14: 1085-96.

Kubbutat, M. H., S. N. Jones, and K. H. Vousden. 1997. 'Regulation of p53 stability by Mdm2', *Nature*, 387: 299-303.

Kyriazis, G. A., Z. Wei, M. Vandermey, D. G. Jo, O. Xin, M. P. Mattson, and S. L. Chan. 2008. 'Numb endocytic adapter proteins regulate the transport and processing of the amyloid precursor protein in an isoform-dependent manner: implications for Alzheimer disease pathogenesis', *J Biol Chem*, 283: 25492-502.

Lane, D. P. 1992. 'Cancer. p53, guardian of the genome', *Nature*, 358: 15-6.

Langevin, J., M. J. Morgan, J. B. Sibarita, S. Aresta, M. Murthy, T. Schwarz, J. Camonis, and Y. Bellaiche. 2005. 'Drosophila exocyst components Sec5, Sec6, and Sec15 regulate DE-Cadherin trafficking from recycling endosomes to the plasma membrane', *Dev Cell*, 9: 365-76.

Lanzetti, L., and P. P. Di Fiore. 2008. 'Endocytosis and cancer: an 'insider' network with dangerous liaisons', *Traffic*, 9: 2011-21.

Lanzetti, L., A. Palamidessi, L. Areces, G. Scita, and P. P. Di Fiore. 2004. 'Rab5 is a signalling GTPase involved in actin remodelling by receptor tyrosine kinases', *Nature*, 429: 309-14.

Le Roy, C., and J. L. Wrana. 2005. 'Clathrin- and non-clathrin-mediated endocytic regulation of cell signalling', *Nat Rev Mol Cell Biol*, 6: 112-26.

Lecuit T, Pilot F. 2003. 'Developmental control of cell morphogenesis: a focus on membrane growth.', *Nat Cell Biol*.

Liu, H., S. Urbe, and M. J. Clague. 2012. 'Selective protein degradation in cell signalling', *Semin Cell Dev Biol*, 23: 509-14.

Luton, F., S. Klein, J. P. Chauvin, A. Le Bivic, S. Bourgoin, M. Franco, and P. Chardin. 2004. 'EFA6, exchange factor for ARF6, regulates the actin cytoskeleton and associated tight junction in response to E-cadherin engagement', *Mol Biol Cell*, 15: 1134-45.

Macia, E., M. Partisani, C. Favard, E. Mortier, P. Zimmermann, M. F. Carlier, P. Gounon, F. Luton, and M. Franco. 2008. 'The pleckstrin homology domain of the Arf6-specific exchange factor EFA6 localizes to the plasma membrane by interacting with phosphatidylinositol 4,5-bisphosphate and F-actin', *J Biol Chem*, 283: 19836-44.

Macia, E., M. Partisani, O. Paleotti, F. Luton, and M. Franco. 2012. 'Arf6 negatively controls the rapid recycling of the beta2 adrenergic receptor', *J Cell Sci*, 125: 4026-35.

Maiorano, E., G. Favia, S. Pece, L. Resta, P. Maisonneuve, P. P. Di Fiore, S. Capodiferro, U. Urbani, and G. Viale. 2007. 'Prognostic implications of NUMB immunoreactivity in salivary gland carcinomas', *Int J Immunopathol Pharmacol*, 20: 779-89.

Maltzman, W., and L. Czyzyk. 1984. 'UV irradiation stimulates levels of p53 cellular tumor antigen in nontransformed mouse cells', *Mol Cell Biol*, 4: 1689-94.

Marchesin, V., A. Castro-Castro, C. Lodillinsky, A. Castagnino, J. Cyrta, H. Bonsang-Kitzis, L. Fuhrmann, M. Irondelle, E. Infante, G. Montagnac, F. Reyal, A. Vincent-Salomon, and P. Chavrier. 2015. 'ARF6-JIP3/4 regulate endosomal tubules for MT1-MMP exocytosis in cancer invasion', *J Cell Biol*, 211: 339-58.

Marco E, Wedlich-Soldner R, Li R, Altschuler SJ, Wu LF. 2007. 'Endocytosis optimizes the dynamic localization of membrane proteins that regulate cortical polarity', *Cell*.

Marigo, V., R. A. Davey, Y. Zuo, J. M. Cunningham, and C. J. Tabin. 1996. 'Biochemical evidence that patched is the Hedgehog receptor', *Nature*, 384: 176-9.

Matsuya, S., H. Sakagami, A. Tohgo, Y. Owada, H. W. Shin, H. Takeshima, K. Nakayama, S. Kokubun, and H. Kondo. 2005. 'Cellular and subcellular localization of EFA6C, a third member of the EFA6 family, in adult mouse Purkinje cells', *J Neurochem*, 93: 674-85.

Matveev, S. V., and E. J. Smart. 2002. 'Heterologous desensitization of EGF receptors and PDGF receptors by sequestration in caveolae', *Am J Physiol Cell Physiol*, 282: C935-46.

Maxfield, F. R., and T. E. McGraw. 2004. 'Endocytic recycling', *Nat Rev Mol Cell Biol*, 5: 121-32.

Mayor, S., and R. E. Pagano. 2007. 'Pathways of clathrin-independent endocytosis', *Nat Rev Mol Cell Biol*, 8: 603-12.

McDonald, J. A., E. M. Pinheiro, L. Kadlec, T. Schupbach, and D. J. Montell. 2006. 'Multiple EGFR ligands participate in guiding migrating border cells', *Dev Biol*, 296: 94-103.

McGill, M. A., S. E. Dho, G. Weinmaster, and C. J. McGlade. 2009. 'Numb regulates post-endocytic trafficking and degradation of Notch1', *J Biol Chem*, 284: 26427-38.

McGill, M. A., and C. J. McGlade. 2003. 'Mammalian numb proteins promote Notch1 receptor ubiquitination and degradation of the Notch1 intracellular domain', *J Biol Chem*, 278: 23196-203.

Mellstrom, K., C. H. Heldin, and B. Westermark. 1988. 'Induction of circular membrane ruffling on human fibroblasts by platelet-derived growth factor', *Exp Cell Res*, 177: 347-59.

Merdes, G., P. Soba, A. Loewer, M. V. Bilic, K. Beyreuther, and R. Paro. 2004. 'Interference of human and Drosophila APP and APP-like proteins with PNS development in Drosophila', *EMBO J*, 23: 4082-95.

Miaczynska, M., S. Christoforidis, A. Giner, A. Shevchenko, S. Uttenweiler-Joseph, B. Habermann, M. Wilm, R. G. Parton, and M. Zerial. 2004. 'APPL proteins link Rab5 to nuclear signal transduction via an endosomal compartment', *Cell*, 116: 445-56.

Mishra, S. K., P. A. Keyel, M. J. Hawryluk, N. R. Agostinelli, S. C. Watkins, and L. M. Traub. 2002. 'Disabled-2 exhibits the properties of a cargo-selective endocytic clathrin adaptor', *EMBO J*, 21: 4915-26.

Mishra, S. K., S. C. Watkins, and L. M. Traub. 2002. 'The autosomal recessive hypercholesterolemia (ARH) protein interfaces directly with the clathrin-coat machinery', *Proc Natl Acad Sci U S A*, 99: 16099-104.

Misumi, Y., Y. Misumi, K. Miki, A. Takatsuki, G. Tamura, and Y. Ikehara. 1986. 'Novel blockade by brefeldin A of intracellular transport of secretory proteins in cultured rat hepatocytes', *J Biol Chem*, 261: 11398-403.

Montagnac, G., H. de Forges, E. Smythe, C. Gueudry, M. Romao, J. Salamero, and P. Chavrier. 2011. 'Decoupling of activation and effector binding underlies ARF6 priming of fast endocytic recycling', *Curr Biol*, 21: 574-9.

Mossessova, E., R. A. Corpina, and J. Goldberg. 2003. 'Crystal structure of ARF1*Sec7 complexed with Brefeldin A and its implications for the guanine nucleotide exchange mechanism', *Mol Cell*, 12: 1403-11.

Mullor, J. L., P. Sanchez, and A. Ruiz i Altaba. 2002. 'Pathways and consequences: Hedgehog signaling in human disease', *Trends Cell Biol*, 12: 562-9.

Mumm, J. S., E. H. Schroeter, M. T. Saxena, A. Griesemer, X. Tian, D. J. Pan, W. J. Ray, and R. Kopan. 2000. 'A ligand-induced extracellular cleavage regulates gamma-secretase-like proteolytic activation of Notch1', *Mol Cell*, 5: 197-206.

Naslavsky, N., R. Weigert, and J. G. Donaldson. 2003. 'Convergence of non-clathrin- and clathrin-derived endosomes involves Arf6 inactivation and changes in phosphoinositides', *Mol Biol Cell*, 14: 417-31.

Niedergang, F., E. Colucci-Guyon, T. Dubois, G. Raposo, and P. Chavrier. 2003. 'ADP ribosylation factor 6 is activated and controls membrane delivery during phagocytosis in macrophages', *J Cell Biol*, 161: 1143-50.

Nilsson, L., B. Conradt, A. F. Ruaud, C. C. Chen, J. Hatzold, J. L. Bessereau, B. D. Grant, and S. Tuck. 2008. 'Caenorhabditis elegans num-1 negatively regulates endocytic recycling', *Genetics*, 179: 375-87.

Nilsson, L., E. Jonsson, and S. Tuck. 2011. 'Caenorhabditis elegans numb inhibits endocytic recycling by binding TAT-1 aminophospholipid translocase', *Traffic*, 12: 1839-49.

Nishimura, T., Y. Fukata, K. Kato, T. Yamaguchi, Y. Matsuura, H. Kamiguchi, and K. Kaibuchi. 2003. 'CRMP-2 regulates polarized Numb-mediated endocytosis for axon growth', *Nat Cell Biol*, 5: 819-26.

Nishimura, T., and K. Kaibuchi. 2007. 'Numb controls integrin endocytosis for directional cell migration with aPKC and PAR-3', *Dev Cell*, 13: 15-28.

Nusslein-Volhard, C., and E. Wieschaus. 1980. 'Mutations affecting segment number and polarity in Drosophila', *Nature*, 287: 795-801.

Okada, R., Y. Yamauchi, T. Hongu, Y. Funakoshi, N. Ohbayashi, H. Hasegawa, and Y. Kanaho. 2015. 'Activation of the Small G Protein Arf6 by Dynamin2 through Guanine Nucleotide Exchange Factors in Endocytosis', *Sci Rep*, 5: 14919.

Oneyama, C., T. Hikita, K. Enya, M. W. Dobenecker, K. Saito, S. Nada, A. Tarakhovsky, and M. Okada. 2008. 'The lipid raft-anchored adaptor protein Cbp controls the oncogenic potential of c-Src', *Mol Cell*, 30: 426-36.

Orth, J. D., and M. A. McNiven. 2003. 'Dynamin at the actin-membrane interface', *Curr Opin Cell Biol*, 15: 31-9.

———. 2006. 'Get off my back! Rapid receptor internalization through circular dorsal ruffles', *Cancer Res*, 66: 11094-6.

Padovani, D., M. Folly-Klan, A. Labarde, S. Boulakirba, V. Campanacci, M. Franco, M. Zeghouf, and J. Cherfils. 2014. 'EFA6 controls Arf1 and Arf6 activation through a negative feedback loop', *Proc Natl Acad Sci U S A*, 111: 12378-83.

Palacios, F., L. Price, J. Schweitzer, J. G. Collard, and C. D'Souza-Schorey. 2001. 'An essential role for ARF6-regulated membrane traffic in adherens junction turnover and epithelial cell migration', *EMBO J*, 20: 4973-86.

Palacios, F., J. K. Schweitzer, R. L. Boshans, and C. D'Souza-Schorey. 2002. 'ARF6-GTP recruits Nm23-H1 to facilitate dynamin-mediated endocytosis during adherens junctions disassembly', *Nat Cell Biol*, 4: 929-36.

Palamidessi, A., E. Frittoli, M. Garre, M. Faretta, M. Mione, I. Testa, A. Diaspro, L. Lanzetti, G. Scita, and P. P. Di Fiore. 2008. 'Endocytic trafficking of Rac is required for its activation and for the spatial restriction of signaling in cell migration', *Cell*, 134: 135-47.

Paleotti, O., E. Macia, F. Luton, S. Klein, M. Partisani, P. Chardin, T. Kirchhausen, and M. Franco. 2005. 'The small G-protein Arf6GTP recruits the AP-2 adaptor complex to membranes', *J Biol Chem*, 280: 21661-6.

Paoluzi, S., L. Castagnoli, I. Lauro, A. E. Salcini, L. Coda, S. Fre, S. Confalonieri, P. G. Pelicci, P. P. Di Fiore, and G. Cesareni. 1998. 'Recognition specificity of individual EH domains of mammals and yeast', *EMBO J*, 17: 6541-50.

Pasqualato, S., J. Menetrey, M. Franco, and J. Cherfils. 2001. 'The structural GDP/GTP cycle of human Arf6', *EMBO Rep*, 2: 234-8.

Paterson, A. D., R. G. Parton, C. Ferguson, J. L. Stow, and A. S. Yap. 2003. 'Characterization of E-cadherin endocytosis in isolated MCF-7 and chinese hamster ovary cells: the initial fate of unbound E-cadherin', *J Biol Chem*, 278: 21050-7.

Pece, S., S. Confalonieri, R. Romano P, and P. P. Di Fiore. 2011. 'NUMB-ing down cancer by more than just a NOTCH', *Biochim Biophys Acta*, 1815: 26-43.

Pece, S., M. Serresi, E. Santolini, M. Capra, E. Hulleman, V. Galimberti, S. Zurrida, P. Maisonneuve, G. Viale, and PP. Di Fiore. 2004. 'Loss of negative regulation by Numb over Notch is relevant to human breast carcinogenesis.', *J Cell Biol.*, 167: 215-21.

Pece, S., D. Tosoni, S. Confalonieri, G. Mazzarol, M. Vecchi, S. Ronzoni, L. Bernard, G. Viale, P. G. Pelicci, and P. P. Di Fiore. 2010. 'Biological and molecular heterogeneity of breast cancers correlates with their cancer stem cell content', *Cell*, 140: 62-73.

Peters, P. J., V. W. Hsu, C. E. Ooi, D. Finazzi, S. B. Teal, V. Oorschot, J. G. Donaldson, and R. D. Klausner. 1995. 'Overexpression of wild-type and mutant ARF1 and ARF6: distinct perturbations of nonoverlapping membrane compartments', *J Cell Biol*, 128: 1003-17.

Peyroche, A., B. Antonny, S. Robineau, J. Acker, J. Cherfils, and C. L. Jackson. 1999. 'Brefeldin A acts to stabilize an abortive ARF-GDP-Sec7 domain protein complex: involvement of specific residues of the Sec7 domain', *Mol Cell*, 3: 275-85.

Pollard, T. D., and G. G. Borisy. 2003. 'Cellular motility driven by assembly and disassembly of actin filaments', *Cell*, 112: 453-65.

Polo, S., S. Pece, and P. P. Di Fiore. 2004. 'Endocytosis and cancer', *Curr Opin Cell Biol*, 16: 156-61.

Porter, J. A., S. C. Ekker, W. J. Park, D. P. von Kessler, K. E. Young, C. H. Chen, Y. Ma, A. S. Woods, R. J. Cotter, E. V. Koonin, and P. A. Beachy. 1996. 'Hedgehog patterning activity: role of a lipophilic modification mediated by the carboxy-terminal autoprocessing domain', *Cell*, 86: 21-34.

Porter, J. A., D. P. von Kessler, S. C. Ekker, K. E. Young, J. J. Lee, K. Moses, and P. A. Beachy. 1995. 'The product of hedgehog autoproteolytic cleavage active in local and long-range signalling', *Nature*, 374: 363-6.

Poupart, M. E., D. Fessart, M. Cotton, S. A. Laporte, and A. Claing. 2007. 'ARF6 regulates angiotensin II type 1 receptor endocytosis by controlling the recruitment of AP-2 and clathrin', *Cell Signal*, 19: 2370-8.

Powelka, A. M., J. Sun, J. Li, M. Gao, L. M. Shaw, A. Sonnenberg, and V. W. Hsu. 2004. 'Stimulation-dependent recycling of integrin beta1 regulated by ARF6 and Rab11', *Traffic*, 5: 20-36.

Prigozhina, N. L., and C. M. Waterman-Storer. 2006. 'Decreased polarity and increased random motility in PtK1 epithelial cells correlate with inhibition of endosomal recycling', *J Cell Sci*, 119: 3571-82.

Punnonen, E. L., K. Ryhanen, and V. S. Marjomaki. 1998. 'At reduced temperature, endocytic membrane traffic is blocked in multivesicular carrier endosomes in rat cardiac myocytes', *Eur J Cell Biol*, 75: 344-52.

Qin, H., A. Percival-Smith, C. Li, C. Y. Jia, G. Gloor, and S. S. Li. 2004. 'A novel transmembrane protein recruits numb to the plasma membrane during asymmetric cell division', *J Biol Chem*, 279: 11304-12.

Qiu, L., C. Joazeiro, N. Fang, H. Y. Wang, C. Elly, Y. Altman, D. Fang, T. Hunter, and Y. C. Liu. 2000. 'Recognition and ubiquitination of Notch by Itch, a hect-type E3 ubiquitin ligase', *J Biol Chem*, 275: 35734-7.

Radhakrishna, H., O. Al-Awar, Z. Khachikian, and J. G. Donaldson. 1999. 'ARF6 requirement for Rac ruffling suggests a role for membrane trafficking in cortical actin rearrangements', *J Cell Sci*, 112 (Pt 6): 855-66.

Radhakrishna, H., and J. G. Donaldson. 1997. 'ADP-ribosylation factor 6 regulates a novel plasma membrane recycling pathway', *J Cell Biol*, 139: 49-61.

Radhakrishna, H., R. D. Klausner, and J. G. Donaldson. 1996. 'Aluminum fluoride stimulates surface protrusions in cells overexpressing the ARF6 GTPase', *J Cell Biol*, 134: 935-47.

Ramsay, A. G., J. F. Marshall, and I. R. Hart. 2007. 'Integrin trafficking and its role in cancer metastasis', *Cancer Metastasis Rev*, 26: 567-78.

Rasin, M. R., V. R. Gazula, J. J. Breunig, K. Y. Kwan, M. B. Johnson, S. Liu-Chen, H. S. Li, L. Y. Jan, Y. N. Jan, P. Rakic, and N. Sestan. 2007. 'Numb and Numbl are required for maintenance of cadherin-based adhesion and polarity of neural progenitors', *Nat Neurosci*, 10: 819-27.

Raz, E. 2004. 'Guidance of primordial germ cell migration', *Curr Opin Cell Biol*, 16: 169-73.

Renault, L., B. Guibert, and J. Cherfils. 2003. 'Structural snapshots of the mechanism and inhibition of a guanine nucleotide exchange factor', *Nature*, 426: 525-30.

Rennstam, K., N. McMichael, P. Berglund, G. Honeth, C. Hegardt, L. Ryden, L. Luts, P. O. Bendahl, and I. Hedenfalk. 2010. 'Numb protein expression correlates with a

basal-like phenotype and cancer stem cell markers in primary breast cancer', *Breast Cancer Res Treat*, 122: 315-24.

Reya, T., S. J. Morrison, M. F. Clarke, and I. L. Weissman. 2001. 'Stem cells, cancer, and cancer stem cells', *Nature*, 414: 105-11.

Rhyu, M. S., L. Y. Jan, and Y. N. Jan. 1994. 'Asymmetric distribution of numb protein during division of the sensory organ precursor cell confers distinct fates to daughter cells', *Cell*, 76: 477-91.

Riley, K. N., A. E. Maldonado, P. Tellier, C. D'Souza-Schorey, and I. M. Herman. 2003. 'Betacap73-ARF6 interactions modulate cell shape and motility after injury in vitro', *Mol Biol Cell*, 14: 4155-61.

Robert, C. H., J. Cherfils, L. Mouawad, and D. Perahia. 2004. 'Integrating three views of Arf1 activation dynamics', *J Mol Biol*, 337: 969-83.

Roegiers, F., L. Y. Jan, and Y. N. Jan. 2005. 'Regulation of membrane localization of Sanpodo by lethal giant larvae and neuralized in asymmetrically dividing cells of Drosophila sensory organs', *Mol Biol Cell*, 16: 3480-7.

Roncarati, R., N. Sestan, M. H. Scheinfeld, B. E. Berechid, P. A. Lopez, O. Meucci, J. C. McGlade, P. Rakic, and L. D'Adamio. 2002. 'The gamma-secretase-generated intracellular domain of beta-amyloid precursor protein binds Numb and inhibits Notch signaling', *Proc Natl Acad Sci U S A*, 99: 7102-7.

Sadowski, L., I. Pilecka, and M. Miaczynska. 2009. 'Signaling from endosomes: location makes a difference', *Exp Cell Res*, 315: 1601-9.

Sakagami, H., H. Suzuki, A. Kamata, Y. Owada, K. Fukunaga, H. Mayanagi, and H. Kondo. 2006. 'Distinct spatiotemporal expression of EFA6D, a guanine nucleotide exchange factor for ARF6, among the EFA6 family in mouse brain', *Brain Res*, 1093: 1-11.

Salcini, A. E., S. Confalonieri, M. Doria, E. Santolini, E. Tassi, O. Minenkova, G. Cesareni, P. G. Pelicci, and P. P. Di Fiore. 1997. 'Binding specificity and in vivo targets of the EH domain, a novel protein-protein interaction module', *Genes Dev*, 11: 2239-49.

Sancho, E., E. Batlle, and H. Clevers. 2004. 'Signaling pathways in intestinal development and cancer', *Annu Rev Cell Dev Biol*, 20: 695-723.

Sandvig K, Torgersen ML, Raa HA, van Deurs B. 2008. 'Clathrin-independent endocytosis: from nonexisting to an extreme degree of complexity.', *Histochem Cell Biol*.

Santolini, E., C. Puri, A. E. Salcini, M. C. Gagliani, P. G. Pelicci, C. Tacchetti, and P. P. Di Fiore. 2000. 'Numb is an endocytic protein', *J Cell Biol*, 151: 1345-52.

Santolini, E., A. E. Salcini, B. K. Kay, M. Yamabhai, and P. P. Di Fiore. 1999. 'The EH network', *Exp Cell Res*, 253: 186-209.

Santy, L. C., and J. E. Casanova. 2001. 'Activation of ARF6 by ARNO stimulates epithelial cell migration through downstream activation of both Rac1 and phospholipase D', *J Cell Biol*, 154: 599-610.

Sanz-Moreno, V., G. Gadea, J. Ahn, H. Paterson, P. Marra, S. Pinner, E. Sahai, and C. J. Marshall. 2008. 'Rac activation and inactivation control plasticity of tumor cell movement', *Cell*, 135: 510-23.

Sasaki, H., Y. Nishizaki, C. Hui, M. Nakafuku, and H. Kondoh. 1999. 'Regulation of Gli2 and Gli3 activities by an amino-terminal repression domain: implication of Gli2 and Gli3 as primary mediators of Shh signaling', *Development*, 126: 3915-24.

Schweitzer, J. K., A. E. Sedgwick, and C. D'Souza-Schorey. 2011. 'ARF6-mediated endocytic recycling impacts cell movement, cell division and lipid homeostasis', *Semin Cell Dev Biol*, 22: 39-47.

Scita G, Di Fiore PP. 2010. 'The endocytic matrix.', *Nature*.

Sero, J. E., C. K. Thodeti, A. Mammoto, C. Bakal, S. Thomas, and D. E. Ingber. 2011. 'Paxillin mediates sensing of physical cues and regulates directional cell motility by controlling lamellipodia positioning', *PLoS One*, 6: e28303.

Shaw, P., R. Bovey, S. Tardy, R. Sahli, B. Sordat, and J. Costa. 1992. 'Induction of apoptosis by wild-type p53 in a human colon tumor-derived cell line', *Proc Natl Acad Sci U S A*, 89: 4495-9.

Shin, O. H., A. D. Couvillon, and J. H. Exton. 2001. 'Arfophilin is a common target of both class II and class III ADP-ribosylation factors', *Biochemistry*, 40: 10846-52.

Shin, O. H., and J. H. Exton. 2001. 'Differential binding of arfaptin 2/POR1 to ADP-ribosylation factors and Rac1', *Biochem Biophys Res Commun*, 285: 1267-73.

Sigismund, S., E. Argenzio, D. Tosoni, E. Cavallaro, S. Polo, and P. P. Di Fiore. 2008. 'Clathrin-mediated internalization is essential for sustained EGFR signaling but dispensable for degradation', *Dev Cell*, 15: 209-19.

Sigismund, S., T. Woelk, C. Puri, E. Maspero, C. Tacchetti, P. Transidico, P. P. Di Fiore, and S. Polo. 2005. 'Clathrin-independent endocytosis of ubiquitinated cargos', *Proc Natl Acad Sci U S A*, 102: 2760-5.

Sima, J., B. Zhang, Y. Yu, X. Sima, and Y. Mao. 2015. 'Overexpression of Numb suppresses growth, migration, and invasion of human clear cell renal cell carcinoma cells', *Tumour Biol*, 36: 2885-92.

Simons, K., and E. Ikonen. 1997. 'Functional rafts in cell membranes', *Nature*, 387: 569-72.

Singh, A., and J. Settleman. 2010. 'EMT, cancer stem cells and drug resistance: an emerging axis of evil in the war on cancer', *Oncogene*, 29: 4741-51.

Sironi, C., T. Teesalu, A. Muggia, G. Fontana, F. Marino, S. Savaresi, and D. Talarico. 2009. 'EFA6A encodes two isoforms with distinct biological activities in neuronal cells', *J Cell Sci*, 122: 2108-18.

Skeath, J. B., and C. Q. Doe. 1998. 'Sanpodo and Notch act in opposition to Numb to distinguish sibling neuron fates in the Drosophila CNS', *Development*, 125: 1857-65.

Smith, C. A., S. E. Dho, J. Donaldson, U. Tepass, and C. J. McGlade. 2004. 'The cell fate determinant numb interacts with EHD/Rme-1 family proteins and has a role in endocytic recycling', *Mol Biol Cell*, 15: 3698-708.

Smith, C. A., K. M. Lau, Z. Rahmani, S. E. Dho, G. Brothers, Y. M. She, D. M. Berry, E. Bonneil, P. Thibault, F. Schweisguth, R. Le Borgne, and C. J. McGlade. 2007. 'aPKC-mediated phosphorylation regulates asymmetric membrane localization of the cell fate determinant Numb', *EMBO J*, 26: 468-80.

Soderberg, O., M. Gullberg, M. Jarvius, K. Ridderstrale, K. J. Leuchowius, J. Jarvius, K. Wester, P. Hydbring, F. Bahram, L. G. Larsson, and U. Landegren. 2006. 'Direct observation of individual endogenous protein complexes in situ by proximity ligation', *Nat Methods*, 3: 995-1000.

Sorensen, E. B., and S. D. Conner. 2008. 'AAK1 regulates Numb function at an early step in clathrin-mediated endocytosis', *Traffic*, 9: 1791-800.

Sorkin A, Goh LK. 2009. 'Endocytosis and intracellular trafficking of ErbBs'.

Spana, E. P., and C. Q. Doe. 1996. 'Numb antagonizes Notch signaling to specify sibling neuron cell fates', *Neuron*, 17: 21-6.

Spana, E. P., C. Kopczynski, C. S. Goodman, and C. Q. Doe. 1995. 'Asymmetric localization of numb autonomously determines sibling neuron identity in the Drosophila CNS', *Development*, 121: 3489-94.

St-Jacques, B., H. R. Dassule, I. Karavanova, V. A. Botchkarev, J. Li, P. S. Danielian, J. A. McMahon, P. M. Lewis, R. Paus, and A. P. McMahon. 1998. 'Sonic hedgehog signaling is essential for hair development', *Curr Biol*, 8: 1058-68.

Stearns, T., M. C. Willingham, D. Botstein, and R. A. Kahn. 1990. 'ADP-ribosylation factor is functionally and physically associated with the Golgi complex', *Proc Natl Acad Sci U S A*, 87: 1238-42.

Stone, D. M., M. Hynes, M. Armanini, T. A. Swanson, Q. Gu, R. L. Johnson, M. P. Scott, D. Pennica, A. Goddard, H. Phillips, M. Noll, J. E. Hooper, F. de Sauvage, and A. Rosenthal. 1996. 'The tumour-suppressor gene patched encodes a candidate receptor for Sonic hedgehog', *Nature*, 384: 129-34.

Struhl, G., and I. Greenwald. 1999. 'Presenilin is required for activity and nuclear access of Notch in Drosophila', *Nature*, 398: 522-5.

Suetsugu, S., D. Yamazaki, S. Kurisu, and T. Takenawa. 2003. 'Differential roles of WAVE1 and WAVE2 in dorsal and peripheral ruffle formation for fibroblast cell migration', *Dev Cell*, 5: 595-609.

Tague, S. E., V. Muralidharan, and C. D'Souza-Schorey. 2004. 'ADP-ribosylation factor 6 regulates tumor cell invasion through the activation of the MEK/ERK signaling pathway', *Proc Natl Acad Sci U S A*, 101: 9671-6.

Teckchandani, A., N. Toida, J. Goodchild, C. Henderson, J. Watts, B. Wollscheid, and J. A. Cooper. 2009. 'Quantitative proteomics identifies a Dab2/integrin module regulating cell migration', *J Cell Biol*, 186: 99-111.

Teglund, S., and R. Toftgard. 2010. 'Hedgehog beyond medulloblastoma and basal cell carcinoma', *Biochim Biophys Acta*, 1805: 181-208.

Teis, D., W. Wunderlich, and L. A. Huber. 2002. 'Localization of the MP1-MAPK scaffold complex to endosomes is mediated by p14 and required for signal transduction', *Developmental cell*, 3: 803-14.

Theard, D., F. Labarrade, M. Partisani, J. Milanini, H. Sakagami, E. A. Fon, S. A. Wood, M. Franco, and F. Luton. 2010. 'USP9x-mediated deubiquitination of EFA6 regulates de novo tight junction assembly', *EMBO J*, 29: 1499-509.

Thiery, J. P., H. Acloque, R. Y. Huang, and M. A. Nieto. 2009. 'Epithelial-mesenchymal transitions in development and disease', *Cell*, 139: 871-90.

Thiery, J. P., and J. P. Sleeman. 2006. 'Complex networks orchestrate epithelial-mesenchymal transitions', *Nat Rev Mol Cell Biol*, 7: 131-42.

Thomas, G., G. Thomas, and H. Luther. 1981. 'Transcriptional and translational control of cytoplasmic proteins after serum stimulation of quiescent Swiss 3T3 cells', *Proc Natl Acad Sci U S A*, 78: 5712-6.

Tosoni, D., S. Zecchini, M. Coazzoli, I. Colaluca, G. Mazzarol, A. Rubio, M. Caccia, E. Villa, O. Zilian, P. P. Di Fiore, and S. Pece. 2015. 'The Numb/p53 circuitry couples replicative self-renewal and tumor suppression in mammary epithelial cells', *J Cell Biol*, 211: 845-62.

Tushir, J. S., and C. D'Souza-Schorey. 2007. 'ARF6-dependent activation of ERK and Rac1 modulates epithelial tubule development', *EMBO J*, 26: 1806-19.

Tuynder, M., G. Fiucci, S. Prieur, A. Lespagnol, A. Geant, S. Beaucourt, D. Duflaut, S. Besse, L. Susini, J. Cavarelli, D. Moras, R. Amson, and A. Telerman. 2004. 'Translationally controlled tumor protein is a target of tumor reversion', *Proc Natl Acad Sci U S A*, 101: 15364-9.

Tuynder, M., L. Susini, S. Prieur, S. Besse, G. Fiucci, R. Amson, and A. Telerman. 2002. 'Biological models and genes of tumor reversion: cellular reprogramming through tpt1/TCTP and SIAH-1', *Proc Natl Acad Sci U S A*, 99: 14976-81.

Uemura, T., S. Shepherd, L. Ackerman, L. Y. Jan, and Y. N. Jan. 1989. 'numb, a gene required in determination of cell fate during sensory organ formation in Drosophila embryos', *Cell*, 58: 349-60.

Varjosalo, M., and J. Taipale. 2008. 'Hedgehog: functions and mechanisms', *Genes Dev*, 22: 2454-72.

Veracini, L., V. Simon, V. Richard, B. Schraven, V. Horejsi, S. Roche, and C. Benistant. 2008. 'The Csk-binding protein PAG regulates PDGF-induced Src mitogenic signaling via GM1', *J Cell Biol*, 182: 603-14.

Verdi, J. M., A. Bashirullah, D. E. Goldhawk, C. J. Kubu, M. Jamali, S. O. Meakin, and H. D. Lipshitz. 1999. 'Distinct human NUMB isoforms regulate differentiation vs. proliferation in the neuronal lineage', *Proc Natl Acad Sci U S A*, 96: 10472-6.

Verdi, J. M., R. Schmandt, A. Bashirullah, S. Jacob, R. Salvino, C. G. Craig, A. E. Program, H. D. Lipshitz, and C. J. McGlade. 1996. 'Mammalian NUMB is an evolutionarily conserved signaling adapter protein that specifies cell fate', *Curr Biol*, 6: 1134-45.

Vogelstein, B., D. Lane, and A. J. Levine. 2000. 'Surfing the p53 network', *Nature*, 408: 307-10.

Wakamatsu, Y., T. M. Maynard, S. U. Jones, and J. A. Weston. 1999. 'NUMB localizes in the basal cortex of mitotic avian neuroepithelial cells and modulates neuronal differentiation by binding to NOTCH-1', *Neuron*, 23: 71-81.

Wang, C., T. Cui, W. Feng, H. Li, and L. Hu. 2015. 'Role of Numb expression and nuclear translocation in endometrial cancer', *Oncol Lett*, 9: 1531-36.

Wang, Z., S. Sandiford, C. Wu, and S. S. Li. 2009. 'Numb regulates cell-cell adhesion and polarity in response to tyrosine kinase signalling', *EMBO J*, 28: 2360-73.

Westhoff, B., I. N. Colaluca, G. D'Ario, M. Donzelli, D. Tosoni, S. Volorio, G. Pelosi, L. Spaggiari, G. Mazzarol, G. Viale, S. Pece, and P. P. Di Fiore. 2009. 'Alterations of the Notch pathway in lung cancer', *Proc Natl Acad Sci U S A*, 106: 22293-8.

Wolf, K., I. Mazo, H. Leung, K. Engelke, U. H. von Andrian, E. I. Deryugina, A. Y. Strongin, E. B. Brocker, and P. Friedl. 2003. 'Compensation mechanism in tumor cell migration: mesenchymal-amoeboid transition after blocking of pericellular proteolysis', *J Cell Biol*, 160: 267-77.

Wolf, K., R. Muller, S. Borgmann, E. B. Brocker, and P. Friedl. 2003. 'Amoeboid shape change and contact guidance: T-lymphocyte crawling through fibrillar collagen is independent of matrix remodeling by MMPs and other proteases', *Blood*, 102: 3262-9.

Wong, K. W., and R. R. Isberg. 2003. 'Arf6 and phosphoinositol-4-phosphate-5-kinase activities permit bypass of the Rac1 requirement for beta1 integrin-mediated bacterial uptake', *J Exp Med*, 198: 603-14.

Wu, J., S. L. Shen, B. Chen, J. Nie, and B. G. Peng. 2014. 'Numb promotes cell proliferation and correlates with poor prognosis in hepatocellular carcinoma', *PLoS One*, 9: e95849.

Wu, S., S. Q. Mehta, F. Pichaud, H. J. Bellen, and F. A. Quiocho. 2005. 'Sec15 interacts with Rab11 via a novel domain and affects Rab11 localization in vivo', *Nat Struct Mol Biol*, 12: 879-85.

Wu, X., J. H. Bayle, D. Olson, and A. J. Levine. 1993. 'The p53-mdm-2 autoregulatory feedback loop', *Genes Dev*, 7: 1126-32.

Xie, C., Z. Lu, G. Liu, Y. Fang, J. Liu, Z. Huang, F. Wang, X. Wu, X. Lei, X. Li, Y. Zhang, Z. Hu, K. Qian, J. Hu, S. Huang, D. Zhong, and X. Xu. 2015. 'Numb downregulation suppresses cell growth and is associated with a poor prognosis of human hepatocellular carcinoma', *Int J Mol Med*, 36: 653-60.

Yamamoto, H., H. Sakane, H. Yamamoto, T. Michiue, and A. Kikuchi. 2008. 'Wnt3a and Dkk1 regulate distinct internalization pathways of LRP6 to tune the activation of beta-catenin signaling', *Dev Cell*, 15: 37-48.

Yap, A. S., M. S. Crampton, and J. Hardin. 2007. 'Making and breaking contacts: the cellular biology of cadherin regulation', *Curr Opin Cell Biol*, 19: 508-14.

Yenofsky, R., I. Bergmann, and G. Brawerman. 1982. 'Messenger RNA species partially in a repressed state in mouse sarcoma ascites cells', *Proc Natl Acad Sci U S A*, 79: 5876-80.

Yonish-Rouach, E., D. Resnitzky, J. Lotem, L. Sachs, A. Kimchi, and M. Oren. 1991. 'Wild-type p53 induces apoptosis of myeloid leukaemic cells that is inhibited by interleukin-6', *Nature*, 352: 345-7.

Yoon, T., J. Jung, M. Kim, K. M. Lee, E. C. Choi, and K. Lee. 2000. 'Identification of the self-interaction of rat TCTP/IgE-dependent histamine-releasing factor using yeast two-hybrid system', *Arch Biochem Biophys*, 384: 379-82.

Zangari, J., M. Partisani, F. Bertucci, J. Milanini, G. Bidaut, C. Berruyer-Pouyet, P. Finetti, E. Long, F. Brau, O. Cabaud, B. Chetaille, D. Birnbaum, M. Lopez, P. Hofman, M. Franco, and F. Luton. 2014. 'EFA6B antagonizes breast cancer', *Cancer Res*, 74: 5493-506.

Zerial, M., and H. McBride. 2001. 'Rab proteins as membrane organizers', *Nature reviews. Molecular cell biology*, 2: 107-17.

Zhang, Q., D. Cox, C. C. Tseng, J. G. Donaldson, and S. Greenberg. 1998. 'A requirement for ARF6 in Fcgamma receptor-mediated phagocytosis in macrophages', *J Biol Chem*, 273: 19977-81.

Zhong, W., J. N. Feder, M. M. Jiang, L. Y. Jan, and Y. N. Jan. 1996. 'Asymmetric localization of a mammalian numb homolog during mouse cortical neurogenesis', *Neuron*, 17: 43-53.

Zhong, W., M. M. Jiang, M. D. Schonemann, J. J. Meneses, R. A. Pedersen, L. Y. Jan, and Y. N. Jan. 2000. 'Mouse numb is an essential gene involved in cortical neurogenesis', *Proc Natl Acad Sci U S A*, 97: 6844-9.

Zhong, W., M. M. Jiang, G. Weinmaster, L. Y. Jan, and Y. N. Jan. 1997. 'Differential expression of mammalian Numb, Numblike and Notch1 suggests distinct roles during mouse cortical neurogenesis', *Development*, 124: 1887-97.

Zhou, P., J. Alfaro, E. H. Chang, X. Zhao, M. Porcionatto, and R. A. Segal. 2011. 'Numb links extracellular cues to intracellular polarity machinery to promote chemotaxis', *Dev Cell*, 20: 610-22.

Zimmermann, P., Z. Zhang, G. Degeest, E. Mortier, I. Leenaerts, C. Coomans, J. Schulz, F. N'Kuli, P. J. Courtoy, and G. David. 2005. 'Syndecan recycling [corrected] is controlled by syntenin-PIP2 interaction and Arf6', *Dev Cell*, 9: 377-88.

Zwahlen, C., S. C. Li, L. E. Kay, T. Pawson, and J. D. Forman-Kay. 2000. 'Multiple modes of peptide recognition by the PTB domain of the cell fate determinant Numb', *EMBO J*, 19: 1505-15.

ACKNOLEDGMENTS

First of all, I am sincerely grateful to my PhD supervisor Prof. Pier Paolo Di Fiore for giving me the opportunity to work in his group and for being my guide during the years of my PhD.

A special thanks goes to Prof. Giorgio Scita for being my internal advisor, for his support during these years, for his constant discussion and for transmit me his passion for science.

I thank also Philippe Chavrier, from Curie Institute in Paris, for his continuous supervision during my PhD project and for all the scientific advices.

I want to express my gratitude to Dr. Andrea Disanza because all I know from a scientific point of view is thanks to his teaching. I thank him for having believed in me during this year and for having taught me that science is passion and sacrifices to reach the success. I thank him for his support during the difficult moments and for his friendship.

I thank Francesca Senic Matuglia who started this project.

I would also like to thank my external examiner Dr. Chiara Zurzolo, from in Institute Pasteur in Paris, and my internal examiner Dr. Nils Gauthier, from IFOM in Milan, for having accepted to be my examination committee.

I thank all the past and present members of Scita's group who constantly supported and encouraged me during the course of my PhD. I am thankful to them for everyday life in the lab and outside the lab.

I thank all the people from Pier Paolo Di Fiore's Lab for their friendship and scientific discussions, all the IFOM-IEO Campus Facilities, the SEMM Graduate Office and all my friends at IFOM-IEO Campus, which shared with me the hard and the good moments.

I thank Dr. Wessen Maruwge for critically reviewing this thesis.

Lastly, I'm grateful to my beloved family who never stopped to believe in me. Them constant support and encouragement was extremely helpful during these years.